PROSTHETIC CONFIGURATION AFFECTS THE BIOMECHANICS AND METABOLIC COST OF TRANSPORT OF ATHLETES WITH TRANSTIBIAL AMPUTATIONS DURING RUNNING

by

Owen Nathaniel Beck

B.S. Humboldt State University, 2013

A thesis submitted to the Faculty of the Graduate School of the

University of Colorado in partial fulfillment

of the requirement for the degree of

Doctor of Philosophy

Department of Integrative Physiology

Fall 2017

This thesis entitled:
Prosthetic configuration affects the biomechanics and metabolic cost of transport of athletes with transtibial amputations

Written by Owen Nathaniel Beck
has been approved for the Department of Integrative Physiology

_____
Alena M. Grabowski Ph.D.

_____
Rodger Kram Ph.D.

Date_____

The final copy of this thesis has been examined by the signatories, and we find that both the content and the form meet acceptable presentation standards of scholarly work in the above-mentioned discipline.

IRB protocol # __13-0559__

Beck, Owen Nathaniel (Ph.D., Integrative Physiology)

Prosthetic configuration affects the biomechanics and metabolic cost of transport of athletes with transtibial amputations during running

Thesis directed by Assistant Professor Alena M. Grabowski

Athletes with unilateral and bilateral transtibial amputations use carbon-fiber running-specific prostheses (RSPs) to run. These devices consist of different model, stiffness, and height combinations. Since nearly all prior research has measured biomechanical and physiological effects of athletes with transtibial amputations using their own RSP(s), it is unknown how RSP characteristics affect the biomechanics and metabolic cost of transport of athletes with transtibial amputations during running.

Accordingly, the first aim of my dissertation was to quantify how prosthetic model, stiffness, and height affect the metabolic cost of transport of athletes with transtibial amputations during running. To accomplish this goal, I quantified RSP stiffness spanning multiple configurations of prosthetic model, height, and sagittal-plane angle. Then, athletes with unilateral and bilateral transtibial amputations ran 15 trials, each trial with a different RSP model, stiffness, and height configuration. These investigations demonstrated that prosthetic model, but not height, affects the metabolic cost of transport during running for athletes with unilateral and bilateral transtibial amputations. In addition, prosthetic stiffness affects the metabolic cost of running for athletes with bilateral, but not unilateral, transtibial amputations. Subsequently, I found that metabolic cost of transport is similar between athletes with transtibial amputations and non-amputees during running.

The second aim of my dissertation was to uncover how running biomechanics change across speeds for athletes with transtibial amputations. Initially, I assessed the influence of

prosthetic stiffness and height on biomechanics across running speeds for athletes with bilateral transtibial amputations. I found that the influence of prosthetic stiffness on running biomechanics was mitigated at faster running speeds, whereas the influence of prosthetic height on biomechanics remained constant across running speeds. Next, I characterized the running biomechanics of the fastest athlete with a unilateral transtibial amputation across running speeds. In this study, I found that the fastest athlete with a unilateral transtibial amputation elicits running biomechanics that differ from athletes with bilateral transtibial amputations and non-amputees.

Overall, my dissertation indicates the importance of RSP configuration on distance running performance and sprinting biomechanics for athletes with transtibial amputations.

ACKNOWLEDGEMENTS

Thank you, Aria Turney for your love and support throughout my graduate studies. Thank you, Alena Grabowski for guiding me through this journey and for displaying confidence in me. Thank you, Rodger Kram for selflessly providing assistance throughout my studies and for sharing many nuggets of wisdom along the way. Thank you, Paolo Taboga, Wouter Hoogkamer, and the rest of the Applied Biomechanics Lab, Locomotion Lab, and Neuromechanics lab members for teaching me many lessons, in life and research. Thank you, mom for your willingness to provide feedback throughout my education. Finally, thank you, Polly for your patience, play time is coming soon.

TABLE OF CONTENTS

1 INTRODUCTION 1

2 CHAPTER 1: CHARACTERIZING THE MECHANICAL PROPERTIES OF RUNNING-SPECIFIC PROSTHESES 6

2.1 ABSTRACT 6
2.2 INTRODUCTION 7
2.3 METHODS 10
2.4 RESULTS 17
2.5 DISCUSSION 22
2.6 CONCLUSIONS 26

3 CHAPTER 2: REDUCED PROSTHETIC STIFFNESS LOWERS THE METABOLIC COST OF RUNNING FOR ATHLETES WITH BILATERAL TRANSTIBIAL AMPUTATIONS 33

3.1 ABSTRACT 33
3.2 INTRODUCTION 34
3.3 METHODS 38
3.4 RESULTS 45
3.5 DISCUSSION 50
3.6 CONCLUSION 57

4 CHAPTER 3: PROSTHETIC MODEL, BUT NOT STIFFNESS OR HEIGHT, AFFECTS THE METABOLIC COST OF RUNNING FOR ATHLETES WITH UNILATERAL TRANSTIBIAL AMPUTATIONS 58

4.1 ABSTRACT 58
4.2 INTRODUCTION 59
4.3 METHODS 64
4.4 RESULTS 72
4.5 DISCUSSION 80
4.6 CONCLUSION 85

5 CHAPTER 4: RUNNING ECONOMY IS SIMILAR BETWEEN ATHLETES WITH AND WITHOUT TRANSTIBIAL AMPUTATIONS 87

5.1 ABSTRACT 87
5.2 INTRODUCTION 87
5.3 RUNNING ECONOMY FOR ATHLETES WITH TRANSTIBIAL AMPUTATIONS 90
5.4 RUNNING ECONOMY COMPARISONS 91
5.5 LOWER LEG ARCHITECTURE AND ELICITED BIOMECHANICS OF ATHLETES WITH VERSUS WITHOUT TRANSTIBIAL AMPUTATIONS: IMPLICATIONS FOR RUNNING ECONOMY 96
5.6 LIMITATIONS 98
5.7 FUTURE DIRECTIONS 98
5.8 CONCLUSIONS 99

6 CHAPTER 5: HOW DO PROSTHETIC STIFFNESS, HEIGHT, AND RUNNING SPEED AFFECT THE BIOMECHANICS OF ATHLETES WITH BILATERAL TRANSTIBIAL AMPUTATIONS? 100

6.1 ABSTRACT 100
6.2 INTRODUCTION 101

6.3 METHODS 104
6.4 RESULTS 111
6.5 DISCUSSION 117
6.6 CONCLUSION 123
7 CHAPTER 6: THE BIOMECHANICS OF THE FASTEST ATHLETE WITH A UNILATERAL TRANSTIBIAL AMPUTATION 125
7.1 ABSTRACT 125
7.2 INTRODUCTION 126
7.3 METHODS 127
7.4 RESULTS 130
7.5 DISCUSSION 134
7.6 CONCLUSIONS 137
8 CONCLUSIONS 138
REFERENCES 141

TABLES

Table 2.1. The tested running-specific prostheses with the recommended user body mass for each stiffness category. …….....14

Table 2.2. The manufacturer recommended prosthetic stiffness across models ……21

Table 2.3. The stiffness and hysteresis characteristics for Freedom Innovations Catapult FX6 prostheses at each testing condition.……..28

Table 2.4. The stiffness and hysteresis characteristics for Össur Flex-Run prostheses at each testing condition …….....…...29

Table 2.5. The stiffness and hysteresis characteristics for Össur Cheetah Xtend prostheses at each testing condition ……...….30

Table 2.6. The stiffness and hysteresis characteristics for Ottobock 1E90 Sprinter prostheses at each testing condition.....32

Table 3.1. Participant characteristics.....38

Table 3.2. Gross metabolic cost of transport for athletes with bilateral transtibial amputations.……..…….56

Table 4.1. Mean anthropometric measurements and standing metabolic rates.....65

Table 4.2. Participants for each prosthetic configuration.....72

Table 4.3. The biomechanical variables that influenced net CoT at each stiffness category…....77

Table 4.4. The biomechanical variables that influenced net CoT at each prosthetic height……..78

Table 5.1. Running economy of athletes with transitbial amputation……...90

Table 6.1. Participant characteristics……...104

Table 6.2. Prosthetic stiffness values……...113

Table 7.1. Affected and unaffected leg ground reaction forces and leg stiffness across running speeds……...133

FIGURES

Figure 1.1. Spring-mass model for athletes with and without leg amputations …….....1

Figure 2.1. Depiction of the running specific-prostheses' vertical axis relative to the peak ground reaction force vector….....12

Figure 2.2. Material testing setup with each running specific-prosthetic model. ……...13

Figure 2.3. Representative force-displacement profiles for running-specific prosthetic models at each testing angle.……..……19

Figure 2.4. Prescribed prosthetic stiffness.…….20

Figure 3.1. Spring-mass model for athletes with and without leg amputations……...35

Figure 3.2. Running-specific prostheses. ……...35

Figure 3.3. Net metabolic cost of transport versus prosthetic stiffness category and stiffness values…….46

Figure 3.4. Net metabolic cost of transport versus prosthetic height ……46

Figure 3.5. The net metabolic cost of transport as a function of running-specific prosthesis mechanical energy return……...48

Figure 3.6. Overall leg stiffness and residual limb stiffness versus running-specific prosthesis stiffness.…….49

Figure 4.1. Spring-mass model for athletes with and without leg amputations.....59

Figure 4.2. Running-specific prostheses. …….....66

Figure 4.3. The average net cost of transport across prosthetic stiffness categories and heights……74

Figure 4.4. Residual limb stiffness and affected leg stiffness versus running-specific prosthetic stiffness 75

Figure 4.5. Net cost of transport plotted as a function of absolute peak vertical ground reaction force asymmetry. ……...77

Figure 4.6. Representative vertical and horizontal ground reaction forces across prosthetic models and stiffness categories ……..79

Figure 4.7. Representative vertical and horizontal ground reaction forces across prosthetic models and heights.....80

Figure 5.1. Prostheses …….....90

Figure 5.2. Running economy of athletes with and without transtibial amputations ……93

Figure 6.1 Spring-mass model for athletes with and without leg amputations ……101

Figure 6.2. Running-specific prostheses……...106

Figure 6.3. Overall leg, running-specific prostheses, and residual limb stiffness across running speeds……...113

Figure 6.4. Contact length, contact time, stance average vertical ground reaction force, and step frequency per prosthetic stiffness category and running speed……114

Figure 6.5. Theta, peak leg spring compression and peak vertical ground reaction force per prosthetic stiffness category and running speed……115

Figure 6.6. Representative vertical ground reaction forces and center of mass trajectories at with different stiffness categories and running speeds……..119

Figure 6.7. Stride lengths and stride frequency across running speeds…….....…….122

Figure 7.1. Contact time and aerial time across running speeds ……..…….131

Figure 7.2. Step length and step time across running speeds …….……...132

Figure 7.3. Vertical ground reaction forces across running speeds……...133

1 INTRODUCTION

During running, the vertical position of an athlete's center of mass (CoM) reaches its lowest position at mid-stance and its highest position at the middle of the aerial phase. This fundamental cyclic movement is due to the spring-like behavior of the stance leg and is well-described by a spring-mass model [1-5]. The spring-mass model simplifies the leg's complex musculoskeletal system to a simple massless linear leg spring supporting a point mass that represents the athlete's CoM during running [1-5]. Throughout the first half of ground contact, elastic potential energy is stored as the leg spring is compressed. Subsequently, the stored mechanical energy is released during the second half of ground contact as the leg spring recoils, thereby accelerating the CoM forward and upward into the aerial phase [6]. The magnitude of the stored and returned mechanical energy is inversely related to leg stiffness and is thought to influence running performance by altering muscular mechanics [6-8].

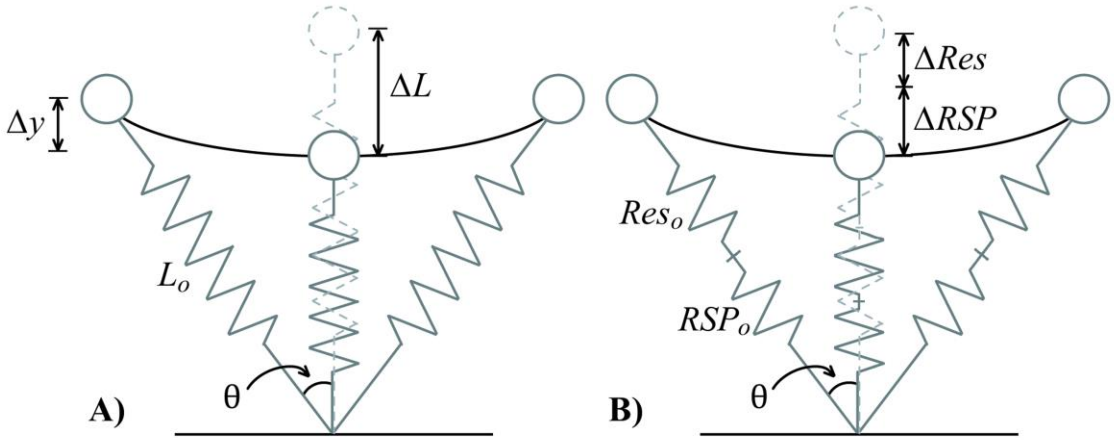

Figure 1.1. Illustration of a spring-mass model of running (A), and a spring-mass model of running with an in-series running-specific prosthesis (RSP) (B). Body mass is represented as a point mass (circle) and the touch-down angle is indicated by theta (θ). The stance leg is represented by a massless linear spring for non-amputees (A), or two in-series massless linear springs for the affected leg of athletes with transtibial amputations (B). The initial leg length (L_0) shortens (ΔL), as does its vertical height (Δy) during the stance phase of running. Modeled

residual limb length (Res_0) and prosthetic height (RSP_0) compress and extend (ΔRes and ΔRSP) during the first and second half of the stance phase of running, respectively.

Fundamentally, the spring-mass model characterizes running biomechanics for athletes with [5, 9-11] and without transtibial amputations [1-5]; however, the product of step length and step frequency ultimately dictates running speed. Step length can be calculated from the product of the horizontal distance traveled by the CoM during ground contact (contact length) and the stance average vertical ground reaction force magnitude normalized to body weight [12, 13]. Step frequency can be calculated from the reciprocal of the sum of ground contact time and aerial time [12, 13]. Together, the spring-mass model describes the biomechanics of running while kinematic and kinetic parameters dictate running speed.

Distance running performance is governed by three physiological parameters: aerobic capacity, running economy, and lactate threshold [14, 15]. Aerobic capacity refers to the maximum rate of oxygen uptake ($\dot{V}O_2$ max) relative to body mass [16-18]. Running economy refers to the submaximal $\dot{V}O_2$ or aerobic energy expenditure while running at a given speed [16, 18]. By assessing running economy at multiple speeds, along with aerobic capacity measures, scientists can predict an athlete's relative aerobic intensity as a percentage of their aerobic capacity [19], also known as fractional utilization [20]. Subsequently, while controlling for lactate threshold, athletes who can run a given speed at a lower relative aerobic intensity often outperform their competitors through their ability to run farther at the given speed and faster at a given relative aerobic intensity [16, 21-23].

Running biomechanics relate to running economy [24-26]. That is because altered running biomechanics change muscular demands [24-26], and consequently the metabolic energy required to sustain the new muscle mechanics. For example, while considering

covariates, improving the stance leg's effective mechanical advantage during running mitigates the required active muscle volume [26, 27], thereby improving running economy. Therefore, scientists often study running biomechanics due to their implications on running economy, and in turn distance-running performance.

Athletes with transtibial amputations primarily use passive-elastic carbon-fiber running-specific prostheses (RSPs) to run [28]. These devices attach in-series to carbon-fiber sockets that encompass the residual limbs and facilitate the fundamental spring-like behavior of level-ground running [5, 9, 29]. Unlike biological lower legs, RSPs cannot generate mechanical power *de novo* or adjust stiffness neurally during running [30]. Further, RSP mass is considerably less than the corresponding biological leg segment mass [31]. Despite differences between purely biological and RSP incorporated lower legs, RSPs have enabled many athletes with leg amputations to compete with non-amputees in track races ranging from regional competitions to the Olympic Games [31].

Athlete with transtibial amputations using RSPs exhibit running biomechanics that vary in magnitude compared to those of non-amputees [5, 31-33]. For example, athletes with bilateral transtibial amputations exhibit lower vertical and anterior-posterior ground reaction forces, faster stride frequencies, and longer ground contact lengths than non-amputees [31]. In addition, athletes with unilateral transtibial amputations exhibit more asymmetric stride kinematics and kinetics between their legs than non-amputees during running [5, 32-34]. Notably, Grabowski et al. [33] reported that athletes with unilateral transtibial amputations exhibit ~9% lower stance average vertical ground reaction forces with their affected legs compared to their unaffected legs across running speeds. Additionally, RSP incorporated legs for athletes with bilateral and unilateral transtibial amputations exhibit leg stiffness that is inversely related to running speed

[5], whereas biological leg stiffness is independent of running speed [2, 35]. Collectively, these studies indicate that RSPs do not fully restore the function of biological lower legs.

Nearly all the preceding running studies on athletes with transtibial amputations had their participants use their own RSP(s), making it difficult to tell how much of the exhibited biomechanics are influenced by the RSP(s) versus the cohort's characteristics. Athletes can acquire RSPs that vary in model, stiffness, and height. A preliminary investigation by Wilson et al. [34] indicated that prosthetic stiffness may affect biomechanical symmetry for athletes with unilateral transtibial amputations. Thus, prosthetic configuration likely affects running biomechanics for athletes with unilateral and bilateral transtibial amputations.

The central goal of my dissertation was to determine how prosthetic model, stiffness, and height affect running biomechanics and metabolic cost of transport of athletes with unilateral and bilateral transtibial amputations. In my first study (chapter two), published in *PLoS One*, I characterized the mechanical properties of RSPs. In my second study (chapter three), published in the *Journal of Applied Physiology*, I quantified how prosthetic configuration affects running biomechanics and metabolic cost of transport at 2.5 and 3.0 m/s of athletes with bilateral transtibial amputations. In my third study (chapter four), published in the *Journal of Applied Physiology*, I quantified how prosthetic configuration affects running mechanics and metabolic cost of transport at 2.5 and 3.0 m/s of athletes with unilateral transtibial amputations. In my fourth study (chapter five), under review in *Exercise Science and Sports Reviews*, I compared metabolic cost of transport values across athletes with unilateral, bilateral, and without transtibial amputations. In my fifth study (chapter six), published in the *Journal of the Royal Society Interface*, I studied how prosthetic configuration affects running mechanics for athletes with bilateral transtibial amputations across running speeds. In my sixth study (chapter seven),

published in the *Journal of Applied Physiology*, I studied the biomechanics of the fastest athlete with a unilateral transtibial amputation across running speeds from 2.87 – 11.55 m/s. Overall, these six studies highlight the influence of prosthetic configuration on distance running performance and sprinting biomechanics for athletes with unilateral and bilateral transtibial amputations.

2 Chapter 1: Characterizing the mechanical properties of running-specific prostheses

2.1 Abstract

The mechanical stiffness of running-specific prostheses likely affects the functional abilities of athletes with leg amputations. However, each prosthetic manufacturer recommends prostheses based on subjective stiffness categories rather than performance based metrics. The actual mechanical stiffness values of running-specific prostheses (e.g. kN/m) are unknown. Consequently, we sought to characterize and disseminate the stiffness values of running-specific prostheses so that researchers, clinicians, and athletes can objectively evaluate prosthetic function. We characterized the stiffness values of 55 running-specific prostheses across various models, stiffness categories, and heights using forces and angles representative of those measured from athletes with transtibial amputations during running. Characterizing prosthetic force-displacement profiles with a 2^{nd} degree polynomial explained 4.4% more of the variance than a linear function ($p<0.001$). The prosthetic stiffness values of manufacturer-recommended stiffness categories varied between prosthetic models ($p<0.001$). Also, prosthetic stiffness was 10% to 39% less at angles typical of running 3 m/s and 6 m/s (10°-25°) compared to neutral (0°) ($p<0.001$). Furthermore, prosthetic stiffness was inversely related to height in J-shaped ($p<0.001$), but not C-shaped prostheses. Running-specific prostheses should be tested under the demands of the respective activity to derive relevant characterizations of stiffness and function. In all, our results indicate that when athletes with leg amputations alter prosthetic model, height, and/or sagittal plane alignment, their prosthetic stiffness profiles also change; therefore, variations in comfort, performance, etc. may be indirectly due to altered stiffness.

2.2 Introduction

Running is a bouncing gait that is well-characterized by a spring-mass model [1-3]. The spring-mass model portrays the stance leg as a mass-less linear spring supporting a point mass representing the runner's center of mass. Upon ground contact, the leg spring compresses and stores elastic energy until mid-stance, and then returns mechanical energy from mid-stance through the end of ground contact [6]. In this model, the leg spring is completely elastic, however the structures of a biological leg are viscoelastic and therefore only a portion of the stored potential elastic energy is returned (due to hysteresis). The spring-like action of the leg conserves a portion of the runner's mechanical energy, theoretically mitigating the mechanical energy input necessary to maintain running speed [6, 8]. The magnitude of the stored and returned mechanical energy is inversely related to leg stiffness (resistance to compression), and is influenced by the magnitude and orientation of the external force vector acting on the leg [1]. Simply modeled as a linear spring, leg stiffness (k_{leg}) equals the quotient of the peak applied force (F) and the change in leg length (Δl) from touchdown to mid-stance [2]:

$$k_{leg} = \frac{F}{\Delta l} \tag{2.1}$$

Inspired by the spring-like nature of running, passive-elastic running-specific prostheses (RSPs) were developed to enable athletes with lower-limb amputations to run. These carbon-fiber devices are attached to the sockets that encompass the residual limbs, are in-series with the residual limbs, and mimic the mechanical energy storage and return of tendons during ground contact. Unlike biological ankles, RSPs cannot generate mechanical power anew and only return 63% to 95% of the stored elastic energy during running [28, 31, 36]. For context, biological ankles generate mechanical power through use of elastic structures as well as muscles, and thus appear to "return" 241% of the energy stored while running at 2.8 m/s [36].

Athletes with leg amputations may adapt similar leg spring mechanics as non-amputees by using RSPs that emulate biological lower leg stiffness. Individually, non-amputees adopt a constant [2, 35], metabolically optimal leg stiffness during running [4, 37, 38]. Non-amputee runners maintain leg stiffness across speeds by exhibiting constant ankle joint stiffness (sagittal plane torsional stiffness) [39, 40]. It has been assumed that prosthetic stiffness is also constant across speeds [31, 32], which if true, RSPs would act like biological ankles [39, 40]. Yet, McGowan et al. [5] reported that the affected leg stiffness of athletes with transtibial amputations decreases as speed increases from 3.0 m/s to top speed (the range of top speeds achieved were 7.0 m/s to 10.8 m/s), indicating that prosthetic stiffness and/or affected leg knee stiffness may be inversely related with speed. Moreover, Dyer et al. [41] mechanically tested two Elite Blade RSPs (Chas A Blatchford & Sons Ltd. Basingstoke, UK) in a materials testing machine and reported that the RSPs have curvilinear force-displacement profiles, suggesting that prosthetic stiffness is non-constant and force dependent. Due to conflicting evidence in the literature, coupled with insufficient information provided by manufacturers regarding prosthetic stiffness profiles, it is unknown whether the force-displacement profiles of RSPs are linear, or curvilinear, which would indicate that stiffness is contingent upon the applied force magnitude.

Prosthetic manufacturers do not report the stiffness values of RSPs (e.g. in kN/m). Instead, they classify RSPs into predetermined stiffness categories (e.g. categories 1 to 7), which are recommended to users based on body mass and intended activity (slow or fast running) [42-44]. Larger/heavier athletes with amputations are generally prescribed RSPs with numerically greater stiffness categories, which are presumably stiffer than numerically lower stiffness categories. Additionally, some prosthetic models are recommend at greater stiffness categories for fast running than for slow running [42, 43], whereas other models are recommended at the

same stiffness category irrespective of intended running speed [45, 46]. These inconsistencies in prosthetic stiffness recommendations persist despite the potential influence of stiffness on running mechanics and performance. Therefore, it is imperative to quantify and disseminate stiffness values to further understand prosthetic function.

To accurately quantify prosthetic stiffness, it seems obvious to evaluate RSPs using forces and angles indicative of those produced during the respective activity. When athletes with transtibial amputations run, they generate peak vertical ground reaction forces (GRFs) with their affected legs that are 2.1 to 3.3 times body weight at speeds of 2.5 m/s to 10.8 m/s [11, 31, 33]. During running, peak resultant GRFs typically occur around mid-stance and are oriented vertically. At the same instant, the proximal end of the stance leg's RSP is rotated forward in the sagittal plane relative to the peak resultant GRF vector. Therefore, the proximal bending moment acting on shorter RSPs may be less than that on taller RSPs for a given applied force, due to a reduced moment arm length. A smaller moment (torque) associated with shorter RSPs may reduce vertical displacement, and in turn increase prosthetic stiffness. Nonetheless, the peak resultant GRF magnitudes and sagittal plane orientations relative to RSPs are unknown, as is the influence of prosthetic height on stiffness.

Since prosthetic stiffness and hysteresis likely affect running performance, we aimed to 1) characterize the force-displacement profiles of RSPs, 2) quantify and compare prosthetic stiffness and 3) hysteresis values across prosthetic models, stiffness categories, and heights using angles and forces that replicate those exhibited during running, and 4) determine whether prosthetic height affects stiffness. Such information will enable accurate and objective comparisons between RSPs, subsequently allowing for potential improvements in prosthetic design, prescription, and athletic performance. Based on the predominant assumption that

prosthetic stiffness is constant during running [31, 32]; we hypothesized that the force-displacement profiles of RSPs would be linear. We hypothesized that for a given body mass and running speed, manufacturer recommended prosthetic stiffness would be similar between models. We also hypothesized that the magnitude of prosthetic hysteresis would not differ across testing conditions. Lastly, we hypothesized that shorter RSPs would be stiffer than taller RSPs.

2.3 Methods

2.3.1 Testing Procedure

We measured GRFs and sagittal plane angles of RSPs relative to the peak resultant GRF vectors from 11 athletes (5 males and 6 females; mean ± SD; age: 27.8 ± 5.7; standing height: 1.74 ± 0.08 m; body mass: 68.9 ± 15.3 kg) with unilateral transtibial amputations while they ran at 3 m/s and 6 m/s on a force-measuring treadmill. Each athlete used their own personal RSP. 3 m/s represents a typical distance running speed [47-49] and 6 m/s represents the fastest speed that all of our participants could achieve. The Intermountain Healthcare IRB, Colorado Multiple IRB, and the USAMRMC Office of Research Protection, Human Research Protection Office approved this study. Prior to participating, nine athletes provided informed written consent in accordance with the Intermountain Healthcare IRB and two participants provided informed written consent in accordance with the Colorado Multiple IRB and USAMRMC Office of Research Protection, Human Research Protection Office. Data collection took place in two separate labs.

We placed reflective markers on the lateral proximal and distal ends of each RSP's longitudinal axis and measured segment motion during each trial using a motion capture system (Motion Analysis Corporation, Santa Rosa, CA, USA, or Vicon Nexus, Oxford, UK) at 240 Hz

(lab 1) or 200 Hz (lab 2) and implemented a 4th order low-pass Butterworth filter with a cutoff frequency of 6 Hz (Visual 3D, C-motion, Inc., Germantown, MD, USA) (Fig. 2.1). The longitudinal axis was defined by a line through the center of the pylon connecting each socket to the corresponding C-shaped RSP, and along the center of the proximal, longitudinal section of each J-shaped RSP (Fig. 2.1). Four athletes used a C-shaped RSP, and seven used a J-shaped RSP. We recorded GRFs via force-measuring treadmills (Treadmetrix, Park City, UT, USA) at 2400 Hz (lab 1) or 1000 Hz (lab 2) and applied a 4th order low-pass Butterworth filter with a cutoff frequency of 30 Hz using a custom MATLAB script (MathWorks Inc, Natick, MA, USA). Our data were comparable because each participant ran both speeds at one lab, and due to the implementation of the same filtering process.

We determined the peak GRF magnitude, as well as the average sagittal plane angle of the longitudinal axis for each athlete's RSP relative to the peak resultant GRF vector from 10 consecutive ground contacts with the affected leg. We assessed the average angles for trials performed with C-shaped RSPs at 3 m/s (α_3) and 6 m/s (α_6), and with J-shaped RSPs at 3 m/s (β_3) and 6 m/s (β_6). When the RSP's longitudinal axis is parallel to the peak resultant GRF vector, the RSP is at 0°. Positive angles indicate that the proximal longitudinal axis was rotated forward in the sagittal plane relative to the peak resultant GRF vector (Fig. 2.1). Sequentially, we implemented the measured angles (α_3, α_6, β_3, and β_6) and peak resultant GRF magnitudes into our prosthetic testing procedure.

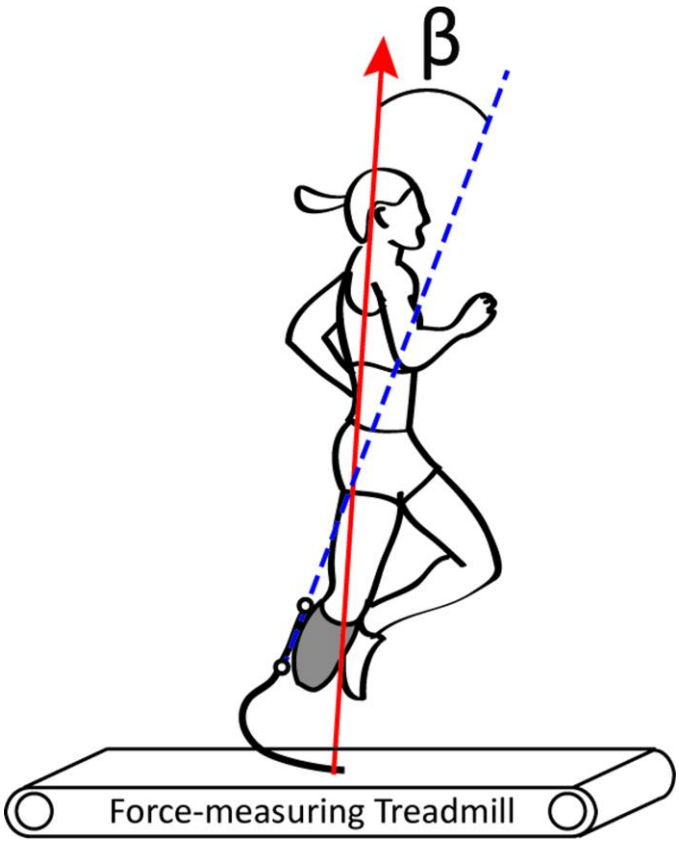

Figure 2.1. Illustration of the calculated angle (β) between the longitudinal axis of the running-specific prosthesis (dashed blue line) and the peak resultant GRF vector (solid red arrow).

2.3.2 Running-Specific Prostheses

Three prosthetic manufacturers, Össur (Reykjavik, Iceland), Freedom Innovations (Irvine, CA, USA), and Ottobock (Duderstadt, Germany) donated a combined total of 55 RSPs for use in our study. We characterized prosthetic stiffness profiles and hysteresis magnitudes from 14 C-shaped Össur Flex-Run prostheses (stiffness categories 3 low – 7 high), 12 C-shaped Freedom Innovations Catapult FX6 prostheses (stiffness categories 2 – 7), 14 J-shaped Ottobock 1E90 Sprinter prostheses (stiffness categories 1 – 5), and 15 J-shaped Össur Cheetah Xtend prostheses (stiffness categories 2 – 7) (Fig. 2.2) (Table 2.1). The unique design of the Catapult prosthesis allows for stiffness modifications via interchangeable carbon-fiber supports

(PowerSprings) that are designed to supplement overall stiffness [42] (Fig. 2.2). PowerSprings have designated stiffness categories based on the manufacturer's categorization. We tested each Catapult with the PowerSpring of the matching stiffness category (e.g. a category 2 Catapult with a category 2 PowerSpring).

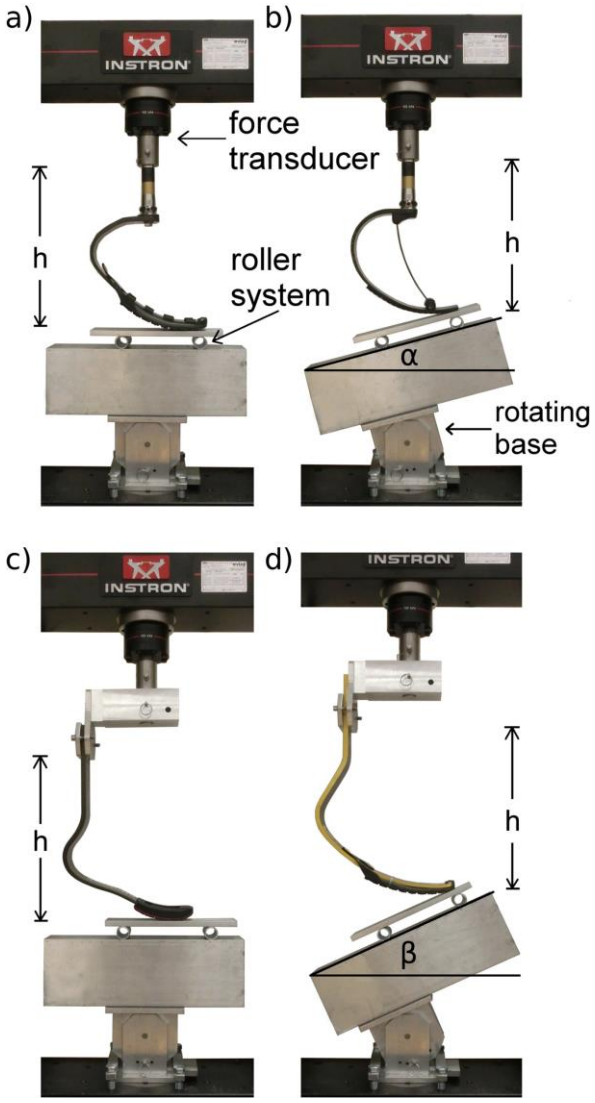

Figure 2.2. Material testing setup with each running specific-prosthetic model.
Each running specific-prosthesis (RSP) was tested with the respective manufacturer's rubber sole (Össur Cheetah Xtend prosthesis was equipped with an Össur Flex-Run's sole), using our rotating base, and low-friction roller system. a) An Össur Flex-Run prosthesis (C-shaped) tested at 0°. b) A Freedom Innovations Catapult prosthesis (C-shaped) tested at α° (3 m/s). c) An Ottobock 1E90 Sprinter prosthesis (J-shaped) tested at neutral (0°). d) An Össur Cheetah Xtend prosthesis (J-shaped) tested at β° (6 m/s). h indicates prosthetic height.

RSP Model	Stiffness Category	Body Mass (kg)		Quantity of RSPs
		Distance Running	Sprinting	
Össur Flex-Run	3 Low	53-56	N/A	1
	3 High	56-59		1
	4 Low	60-64.5		1
	4 High	64.5-68		2
	5 Low	69-73		1
	5 High	73-77		2
	6 Low	78-83		1
	6 High	83-88		2
	7 Low	89-94.5		1
	7 High	94.5-100		2
Freedom Innovations Catapult FX6	2	53-59	N/A	2
	3	60-68		2
	4	69-77		2
	5	78-88		2
	6	89-100		2
	7	101-116		2
Ottobock 1E90 Sprinter	1	40-59	40-52	3
	2	60-70	53-63	3
	3	71-86	64-79	3
	4	87-102	80-95	3
	5	103-118	96-111	3
Össur Cheetah Xtend	2	53-59	53-59	2
	3	60-68	60-68	2
	4	69-77	69-77	3
	5	78-88	78-88	3
	6	89-100	89-100	3
	7	101-116	101-116	2

Table 2.1 The manufacturer recommended running-specific prosthesis (RSP) stiffness categories with the corresponding body mass for distance running and sprinting, plus the quantity of RSPs tested.

2.3.3 Stiffness Testing

To assess prosthetic stiffness and hysteresis at conditions that matched those of our analyzed running data, we fabricated an aluminum attachment to secure each RSP on to the force transducer of our materials testing machine (Instron Series 5859, Norwood, MA) (Fig. 2.2). We also constructed an aluminum rotating base and fixed it under each C-shaped RSP at 0°, α_3, and

α_6, as well as under each J-shaped RSP at 0°, β_3, and β_6 (Fig. 2.2). We applied three successive loading and unloading cycles at 100 N/s on each RSP for each condition. This loading rate was relatively fast and ensured that our materials testing machine operated within the safe speed range, even with our most compliant RSPs. Three compressive loading and unloading cycles matched the number of cycles from Brüggeman et al. [31].

To determine the peak GRF magnitude applied on each RSP, we considered the heaviest manufacturer recommended body weight for each prosthetic stiffness category, then multiplied it by 3.0 to replicate the upper limit of peak GRFs typically produced by affected legs while running at 3 m/s [5], and by 3.5 to replicate the upper limit of peak GRFs produced by affected legs while running at 6 m/s [5]. We compared the effects of testing angle and prosthetic height on stiffness and hysteresis by evaluating prosthetic compression with an applied peak resultant GRF of 3.0 times the largest recommended body weight for each RSP. We minimized shearing forces by using a low-friction roller-system beneath each RSP that allowed anterior and posterior translation while maintaining the angle of the applied force relative to the longitudinal axis (Fig. 2.2) [50]. We set the threshold for force detection at 10 N. We recorded applied force magnitudes and prosthetic displacement measurements at 10 Hz, which, when combined with the loading rate (100 N/s), allowed the measurement of force-displacement data from every 10 N of applied force; ~150 to 400 data points per loading cycle.

To determine the effect of prosthetic height on the stiffness of C-shaped RSPs, we tested the Catapult and Flex-Run prostheses at 38.2 cm and 69.7 cm by altering the aluminum pylon height. To determine the effect of height on the stiffness of J-shaped RSPs, we tested the 1E90 Sprinter prostheses at 25.0, 31.5, and 38.0 cm, and the Cheetah Xtend prostheses at 31.5, 38.0, and 41.5 cm. Prosthetic height was measured vertically from the ground to the base of our height

adjustment attachment in an unloaded state (Fig. 2.2). We chose to test C-shaped RSPs across the largest possible height range given our components. We tested J-shaped RSPs at heights that spanned the largest possible range while allowing matched height comparisons (31.5 cm and 38.0 cm) between different models.

2.3.4 Analyses

To characterize prosthetic stiffness, we calculated the average coefficients of determination (R^2) for linear and curvilinear characterizations of the applied force relative to the vertical displacement for each 3-cycle trial. Next, we averaged R^2 values within and across trials for a given prosthetic model, stiffness category, height, and testing angle combination. Furthermore, we calculated average prosthetic stiffness for each model across stiffness categories using the force-displacement function during simulated running conditions.

For every cycle, we calculated hysteresis as the ratio of energy lost during recoil relative to the energy stored during compression, then expressed it as a percentage:

$$Hysteresis = \frac{\int_o^H F(h)dh - \int_H^o F(h)dh}{\int_o^H F(h)dh} \times 100 \quad (2.2)$$

where F is the applied force as a function of the change in prosthetic height (h) and peak change in prosthetic height (H) of the corresponding cycle. Hysteresis was averaged for each 3-cycle trial, and averaged across trials of the same prosthetic model, stiffness category, height, and testing angle. We measured prosthetic stiffness and hysteresis with the respective manufacturers supplied rubber sole. We also measured the stiffness and hysteresis of the highest stiffness category from each model at 0° without the rubber sole.

2.3.5 Statistical Analyses

We used paired two-tailed t-tests to compare average R^2 values from linear and curvilinear force-displacement functions across prosthetic models and to compare the

manufacturer recommended stiffness across prosthetic models for athletes at body masses of 55 kg to 100 kg in 5 kg increments using the average angles and peak applied force magnitudes produced at 3 m/s (α_3 and β_3) from the C- and J-shaped RSPs, respectively. We also used paired two-tailed t-tests to compare the prescribed stiffness of different prosthetic models for athletes at body masses of 55 kg to 100 kg in 5 kg increments using the average angles and peak applied force magnitudes produced at 6 m/s (α_6 and β_6) from the C- and J-shaped RSPs, respectively. The recommended stiffness values for J-shaped RSPs were calculated using the tallest mutual height (38 cm).

Moreover, for C-shaped RSPs, we used linear mixed models to compare 1) prosthetic stiffness and 2) hysteresis for each prosthetic model across stiffness categories, testing angles, and interaction effects. For the J-shaped RSPs we included prosthetic height as an independent variable and used two linear mixed models to compare 1) prosthetic stiffness and 2) hysteresis for each prosthetic model across stiffness categories, testing angles, and heights, in addition to their interactions. We performed paired two-tailed t-tests to assess the influence of the prosthetic sole on stiffness and hysteresis. We carried out our statistical analyses using R-studio (Boston, MA, USA) software. Significance was set at $p<0.05$. When applicable, we implemented the Bonferroni correction to account for multiple comparisons.

2.4 Results

2.4.1 Subject Data

When participants used C-shaped RSPs to run 3 m/s, the average angle of their RSP's longitudinal axis relative to the peak resultant GRF was 15.1° ± 4.8° and the mean peak resultant GRF was 2.5 ± 0.3 times body weight. At 6 m/s the average angle was 10.0° ± 4.2° and the peak

resultant GRF was 2.7 ± 0.3 times body weight. When participants used a J-shaped RSP to run 3 m/s, the average angle of their RSP's longitudinal axis relative to the peak resultant GRF was 20.9° ± 8.9° while the average peak resultant GRF was 2.6 ± 0.3 times body weight. At 6 m/s, the average angle was 24.2° ± 9.3° and the average peak resultant GRF magnitude was 2.8 ± 0.3 times body weight. Since our custom base was constructed to rotate in incremental steps, we used the following values for RSP testing: $\alpha_3 = 15.0°$, $\alpha_6 = 10.0°$, $\beta_3 = 20.0°$ and $\beta_6 = 25.0°$.

2.4.2 Prosthetic force-displacement characteristics

Overall, characterizing the slope of the force-displacement curves with a 2nd degree polynomial explained 4.4% more of the variance than a linear function using angles indicative of 3 m/s and 6 m/s ($p<0.001$) (Fig. 2.3). At a testing angle of 0°, a 2nd degree polynomial explained 5.0% more of the variance than using a linear function ($p<0.001$). We did not explore functions beyond a 2nd degree polynomial due to its impeccable fit (average $R^2 = 0.998$).

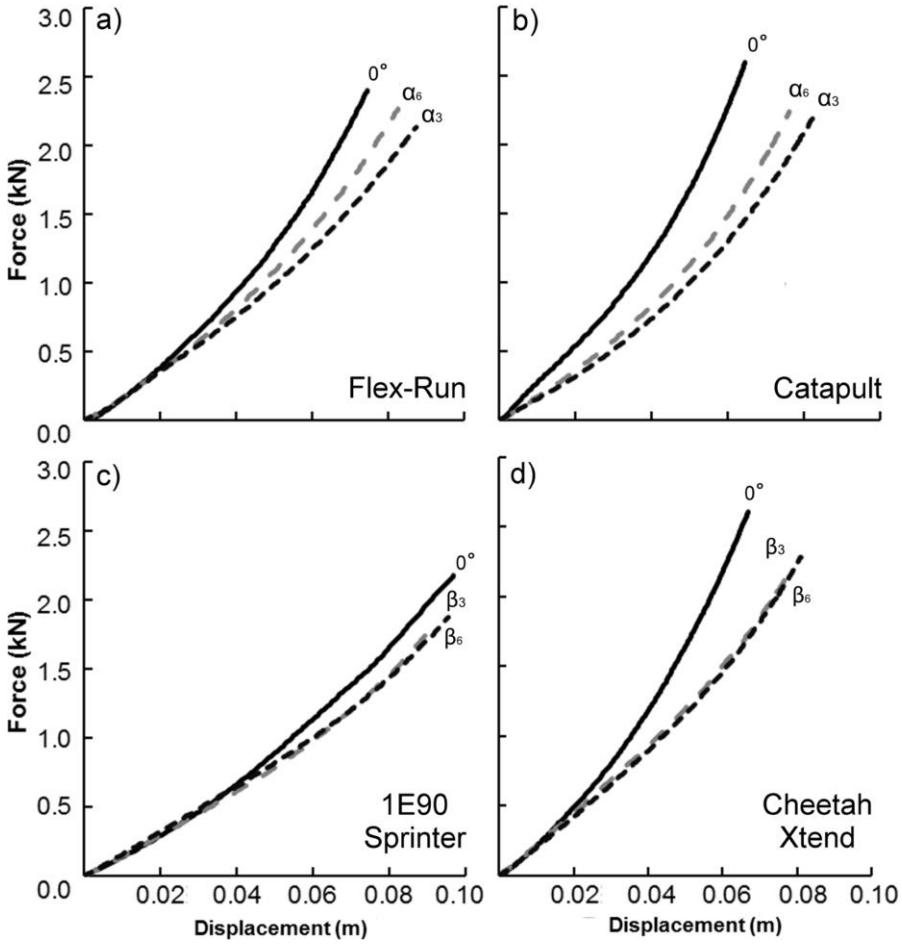

Figure 2.3. Representative force-displacement profiles for running-specific prosthetic models at each testing angle. Each running-specific prosthesis (RSP) is the manufacturer recommended stiffness category for a 70 kg distance runner. α_3 and β_3 indicate the measured angle between the RSP and peak resultant ground reaction force (GRF) vector while running 3 m/s using the C-shaped RSPs (Flex-Run and Catapult) and J-shaped RSPs (1E90 Sprinter and Cheetah Xtend), respectively. α_6 and β_6 indicate the measured angles between the RSP and peak resultant GRF vector while running 6 m/s using the C-shaped RSPs and J-shaped RSPs, respectively. a) The Flex-Run prosthesis at testing angles of 0°, α_3, and α_6, b) the Catapult prosthesis at testing angles of 0°, α_3, and α_6, c) the 1E90 Sprinter prosthesis at testing angles of 0°, β_3, and β_6, and d) the Cheetah Xtend prosthesis at testing angles of 0°, β_3, and β.

2.4.3 Prosthetic Prescription

Using the peak resultant GRFs and angles produced at 3 m/s, the actual stiffness of the manufacturer recommended Cheetah Xtend, which is prescribed based on user body mass, was 4% to 15% stiffer than the Flex-Run ($p<0.001$), 7% to 19% stiffer than the Catapult ($p<0.001$),

and 20% to 28% stiffer than the 1E90 Sprinter ($p<0.001$) prostheses across matched user body masses (Fig. 2.4). Using the peak resultant GRFs and angles produced at 6 m/s, the manufacturer recommended Cheetah Xtend prostheses were the same stiffness as the Flex-Run ($p=0.166$), 0% to 22% less stiff than the Catapult ($p=0.001$), and 3% to 21% stiffer than the 1E90 Sprinter ($p<0.001$) prostheses at matched user body masses (Fig. 2.4). The Flex-Run and Catapult prostheses are not specifically recommended for fast running/sprinting; therefore, we used manufacture recommended stiffness categories for distance running at 6 m/s.

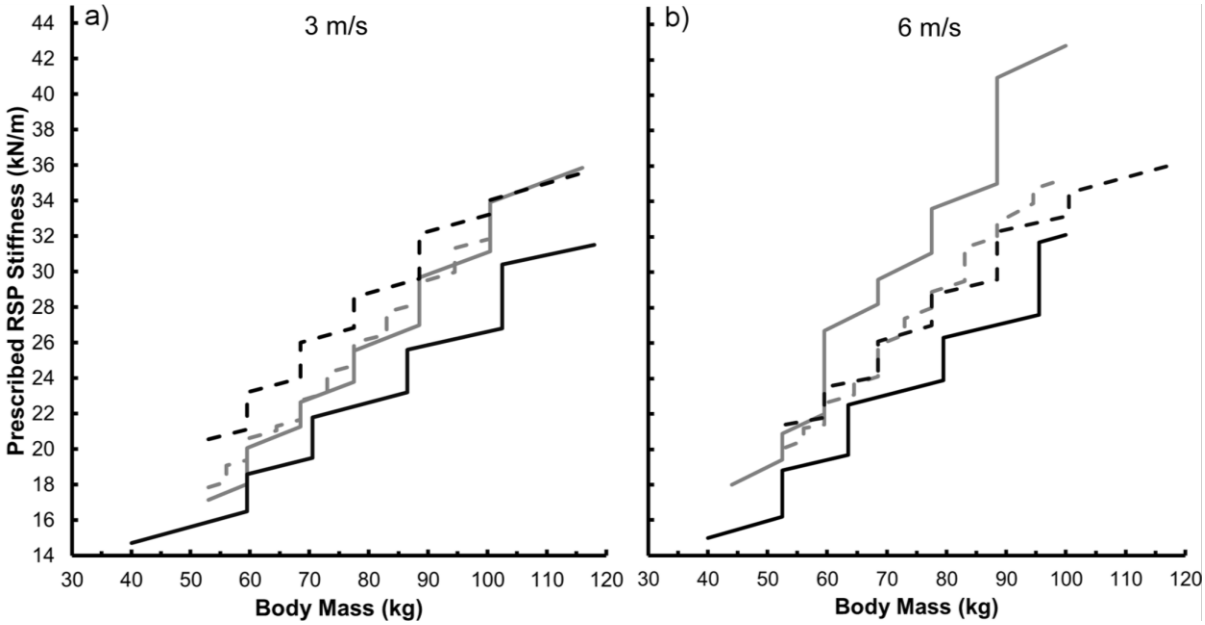

Figure 2.4. Prescribed prosthetic stiffness. The average stiffness (kN/m) of each running-specific prosthesis (RSP) as a function of the respective manufacturer's recommended user's body mass (kg) at running speeds of 3 m/s (a), and 6 m/s (b). The stiffness of each RSP was calculated using peak applied force magnitudes that simulated running 3 m/s (α_3 and β_3) and 6 m/s (α_6 and β_6). We then calculated displacement using the mean curvilinear force-displacement profiles with the appropriate applied force magnitudes. See supplementary tables 2.3-6 at end of chapter.

Prosthetic stiffness depends on peak GRF magnitude; hence we calculated the average 2nd order polynomial equations for each prosthetic model and stiffness category (supplementary tables 2.3-2.6) so that prosthetists can predict an athlete's prosthetic stiffness from the amount of

force they apply on the ground and/or prosthetic compression. For those unable to quantify force magnitudes or compression, and because of the relatively linear force-displacement relationships (average R^2=0.956), we also report average linear stiffness values (Table 2.2).

Users Mass (kg)	**3 m/s**				**6 m/s**			
	Flex-Run (kN/m)	**Catapult** (kN/m)	**1E90 Sprinter** (kN/m)	**Cheetah Xtend** (kN/m)	**Flex-Run** (kN/m)	**Catapult** (kN/m)	**1E90 Sprinter** (kN/m)	**Cheetah Xtend** (kN/m)
55	18.0	17.4	16.2	20.7	20.4	20.4	19.0	21.5
60	20.6	20.1	18.6	23.2	22.6	25.8	19.5	23.5
65	22.1	20.8	19.1	23.7	23.7	27.6	22.7	23.9
70	22.9	22.8	21.8	26.1	26.1	29.9	23.1	26.4
75	23.7	23.5	22.2	26.6	27.7	30.7	23.5	26.8
80	26.2	25.9	22.7	28.8	29.2	33.7	26.4	28.9
85	26.1	26.5	23.2	29.3	31.3	34.5	26.8	29.4
90	29.5	29.9	25.9	32.3	33.4	41.2	27.2	32.4
95	31.4	30.5	26.3	32.7	34.7	42.0	27.6	32.8
100	31.8	31.1	26.7	33.2	35.3	42.8	32.1	33.1

Table 2.2. The manufacturer recommended average prosthetic stiffness across models based on running 3 m/s and 6 m/s. All values include the rubber sole that comes with the prosthetic model, except for the Össur Cheetah Xtend, which was equipped with the Össur Flex-Run's rubber sole.

2.4.4 Hysteresis

The percentage of mechanical energy lost per cycle for C-shaped RSPs across conditions averaged 5.14% (SD: 0.70%). For every 1° increase in testing angle, the hysteresis magnitude decreased 0.04% ($p<0.001$). The average hysteresis for J-shaped RSPs across conditions was 4.28% (SD: 0.65%), which was lower than that of the C-shaped RSPs ($p<0.001$). Furthermore, testing angle affected the hysteresis of J-shaped RSPs ($p<0.001$), while height had no effect ($p=0.215$). For every 1° increase in testing angle, the hysteresis of the 1E90 Sprinter and Cheetah Xtend prostheses decreased 0.01% and 0.08%, respectively ($p<0.001$). Additionally, removing the rubber soles from C- and J-shaped RSPs reduced the hysteresis magnitudes by 42% ($p<0.001$).

2.4.5 Effect of angle and height on prosthetic stiffness

While controlling for prosthetic height, every 1° increase in testing angle decreased the stiffness of the Flex-Run and Catapult prostheses by 0.41 kN/m ($p<0.001$) and 0.79 kN/m ($p<0.001$), respectively (Fig. 2.3). Every 1° increase in testing angle decreased the stiffness of the 1E90 Sprinter and Cheetah Xtend prostheses by 0.45 kN/m ($p<0.001$) and 0.76 kN/m ($p<0.001$), respectively. Moreover, at a fixed testing angle, every 1 cm increase in height decreased the stiffness of both J-shaped RSPs by 0.27 kN/m ($p<0.001$). Despite a drastic pylon height difference (31.5 cm), preliminary testing revealed no effect of height on the stiffness of C-shaped RSPs; therefore, we did not further test the effect of height across C-shaped RSPs. Furthermore, removing the rubber soles did not affect RSP stiffness across prosthetic models ($p=0.151$).

2.5 Discussion

Despite well-characterizing the force-displacement relationships of the RSPs (average $R^2=0.956$), a linear function did not fit quite as well as a 2nd degree polynomial function ($p<0.001$), leading us to partially reject our initial hypothesis. Contrary to the notion that prosthetic stiffness is invariant during running [31, 32], our data suggest that as athletes exert greater forces on the ground and/or adjust the angle between the peak resultant GRF and their RSP during stance, prosthetic stiffness is altered. For example, a 70 kg athlete that produces peak resultant GRFs of 2.2, 2.6, 3.0, 3.4 times body weight with their affected leg using a manufacturer recommended Cheetah Xtend prosthesis (height: 38 cm; angle: 25.0°) would exhibit stiffness values of 25.1, 26.1, 27.1, and 28.1 kN/m, respectively. Yet, if the 70 kg athlete increased the angle of their RSP with respect to the resultant GRF from 15° to 30° in 5°

increments, the aforementioned prosthetic stiffness values would change to 32.7, 29.9, 27.1, 24.3 kN/m. It is possible that the inverse relationship between affected leg stiffness and running speed found in McGowan et al. [5] can be attributed to decreased prosthetic stiffness via increased angles between the resultant GRF vectors and RSPs at faster speeds.

Overall, mechanically testing RSPs at 0° overestimates prosthetic stiffness (linear) by 10% to 39% compared to using angles utilized by athletes with transtibial amputations while running at 3 m/s and 6 m/s. Previous studies have tested the stiffness of RSPs at 0° [31], and 30° [41]. We compared our methodology to that of Brüggeman et al. [31] by acquiring the same prosthetic model (Össur Cheetah) as the previous study, replicating their protocol (applied force: 1500 N, testing angle: 0°, loading velocity: 1 m/min), and then using our method (applied force: 2724 N, testing angle: 25°, loading velocity: 100 N/s) to determine stiffness. Brüggeman et al.'s protocol resulted in a prosthetic stiffness (linear) of 34.2 kN/m, whereas our protocol resulted in a linear stiffness of 29.2 kN/m. These discrepancies suggest that prosthetic stiffness testing procedures should be standardized.

We reject our second hypothesis; manufacturer recommended prosthetic stiffness varies across models for a given user body mass and activity. Additionally, we compared manufacturer recommended prosthetic stiffness during running at 3 m/s versus at 6 m/s. At a given body mass (prosthetic height of 38 cm), the manufacturer recommended 1E90 Sprinter prostheses were 11% stiffer at 6 m/s compared to 3 m/s across a 45 kg span in user body mass ($p=0.003$). Also, the recommended Catapult prosthetic stiffness increased 32% due to a greater recommended prosthetic stiffness category and reduced angle between the RSP and peak resultant GRF (Fig. 2.4). Conversely, the Cheetah Xtend prostheses are recommended at the same stiffness categories for 3 m/s and 6 m/s [46], and thus the stiffness values varied by <1% (Bonferroni

corrected p-value: p=0.080). Prosthetic stiffness requirements may be different for running at various speeds due to the different mechanical demands of the respective tasks. Future studies are needed to assess the effects of prosthetic stiffness on distance running and sprinting performance.

Since testing angle affected hysteresis, we also reject our third hypothesis stating that prosthetic hysteresis would be invariant across testing conditions. Intriguingly, RSPs dissipate less energy when their proximal end is rotated forward with respect to the applied force. Future studies are needed to examine prosthetic designs and decipher why RSPs display less hysteresis when rotated forward. Due to the importance of mechanical energy return on running and sprinting performance [6, 8], the designs of future RSPs should be developed to mitigate mechanical energy dissipation.

Moreover, prosthetic hysteresis was 42% lower when we removed the rubber soles, indicating that the rubber soles were responsible for almost half of the dissipated energy. Athletes with leg amputations should use soles with minimal damping to maximize the mechanical energy return of RSPs. In addition to the sole, energy dissipation probably occurs at the residual limb/socket interface. To our knowledge, no study has quantified the mechanical behavior of the residual limb and socket interface while running. Improving socket design by enhancing the connection between athletes and their RSPs may allow better utilization of the returned mechanical energy and potentially improve running performance.

Pylon height does not affect the stiffness of C-shaped RSPs; therefore, we reject our final hypothesis. The aluminum pylon of C-shaped RSPs has an annular section (i.e. an hollow cylinder) and appears less prone to bending due to the perpendicular components of the applied compression forces, and due to a higher area moment of inertia [51] compared to the rectangular

section of J-shaped RSPs. Increasing the overall length of the aluminum pylon technically reduces its overall stiffness, but the lengths used in our measurements were not enough to elicit a measurable difference. The height of RSPs needs to be within a relatively narrow range for athletes with unilateral amputations due to their unaffected leg length. Therefore, prosthetic stiffness adjustments would primarily be accomplished by changing stiffness category or sagittal plane angle. On the other hand, athletes with bilateral amputations can consider a wide range of heights and stiffness categories to achieve a specified prosthetic stiffness; however, height and stiffness may affect running performance in separate ways. In addition to stiffness, the effects of prosthetic height and alignment on performance warrant future research.

We assumed that the C-shaped RSPs were perpendicular to the respective pylons. Yet, the sagittal plane RSP-pylon alignment may have been slightly altered due to individual preference, thus our reported angles between the C-shaped RSPs and resultant GRF vectors may have been over/underestimated by a few degrees. We collected prosthetic angles and peak resultant GRFs from a cohort of exceptional athletes with unilateral transtibial amputations at 3 m/s and 6 m/s. Conceivably, less athletic individuals with amputations, or athletes with different amputation levels may not utilize the same prosthetic angles and/or generate the same resultant GRFs compared to those exhibited by our participants, and consequently prosthetic stiffness may differ. For example, athletes with transfemoral amputations with pylons connecting their RSPs to their sockets can use our reported values at 0°, as it is a fair approximation of their RSP-peak GRF angle to determine the prosthetic stiffness and hysteresis.

Our methodology does not account for the rotation of the RSP with respect to the resultant GRF throughout ground contact. It may be that RSPs are stiffer at initial and terminal ground contact than at mid-stance due to a smaller angle between the RSP and resultant GRF

vector. On the other hand, as applied force accrues RSPs become stiffer, implying that RSPs are stiffest at mid-stance. The influence of angle and force may counteract each other, exhibiting a constant prosthetic stiffness throughout stance; perhaps a deliberate design choice of prosthetic manufacturers. Future studies are warranted to include a rotational component to the mechanical stiffness testing of RSPs. Furthermore, we tested our RSPs with a loading rate (100 N/s) that is much lower than that recorded during running (over 4000 N/s [5, 33]). However, our low loading rate (100 N/s) enabled us to record force-displacement data from every 10 N of applied force, thus presenting ~150 to 400 data points per each loading cycle. When athletes with an amputation run 6 m/s, they have a ground contact time of ~0.2 seconds [33, 52]. If ground reaction forces were recorded at 2000 Hz, then 200 data points would have been collected from initial ground contact to mid-stance/peak GRF, which coincides with our material testing machines sampling versus loading rate data. Nevertheless, it is ideal for prosthetic testing to mimic the loading/unloading rates of those recorded during running; unfortunately, these rates are beyond the capability of our equipment.

2.6 Conclusions

We assessed prosthetic stiffness and hysteresis across a wide range of models, stiffness categories, and heights, at forces and angles that simulate those exhibited by athletes with transtibial amputations running at 3 m/s and 6 m/s. We found that the force-displacement profiles of RSPs are curvilinear, indicating that prosthetic stiffness varies with the magnitude of applied force. Yet, a linear force-displacement characterization is strongly predictive. We also found that manufacturer recommended prosthetic stiffness varies between models, and that the height of J-

shaped RSPs is inversely related to stiffness. Moreover, we provide evidence that prosthetic stiffness is much greater at 0° than at angles representative of those that occur during running.

When athletes with leg amputations change prosthetic models, height, and/or sagittal plane alignment, prosthetic stiffness also changes; therefore, variations in comfort, performance, etc. may be indirectly due to altered stiffness. We propose that prosthetic stiffness should be assessed under conditions that simulate the demands of the respective activity, and that manufacturers should provide the stiffness values of each RSP at specific heights. Until then, our study provides reference for the stiffness values of various prosthetic models across multiple stiffness categories and heights, and provides a foundation for future research to understand the potential effects of prosthetic stiffness on performance during distance running and sprinting.

Acknowledgements

We thank the Orthopedic Specialty Hospital in Murray, Utah. We also thank Freedom Innovations, Össur, and Ottobock for donating the running-specific prostheses used in this study. This project was supported by the BADER Consortium, a Department of Defense Congressionally Directed Medical Research Programs cooperative agreement (W81XWH-11-2-0222)**.** The authors have no conflicts of interest to disclose.

Supplementary Tables

Freedom Innovations Catapult FX6				
Condition (Angle)	**Stiffness Category**	**Force=ah^2+bh**	**Stiffness Variability (SD)**	**Percent Hysteresis Mean (SD)**
Neutral (0°)	2	297h^2+8h	(1.4)	6.5 (0.6)
	3	346h^2+11h	(2.2)	6.2 (0.2)
	4	359h^2+15h	(2.9)	5.8 (0.2)
	5	411h^2+17h	(1.6)	5.9 (0.1)
	6	381h^2+25h	(1.8)	6.1 (0.2)
	7	504h^2+25h	(2.0)	6.1 (0.2)
	7 No Sole	553h^2+43h	-	3.2
3 m/s (15°)	2	176h^2+4h	(0.2)	5.6 (0.1)
	3	195h^2+6h	(0.4)	5.8 (0.0)
	4	200h^2+8h	(2.2)	5.7 (0.7)
	5	237h^2+8h	(0.7)	5.4 (0.2)
	6	247h^2+12h	(0.2)	5.5 (0.0)
	7	293h^2+13h	(0.7)	5.5 (0.1)
6 m/s (10°)	2	195h^2+5h	(1.5)	5.7 (0.2)
	3	234h^2+5h	(1.7)	5.3 (0.2)
	4	307h^2+9h	(1.9)	5.4 (0.0)
	5	309h^2+11h	(1.1)	5.3 (0.1)
	6	318h^2+14h	(0.5)	5.3 (0.0)
	7	395h^2+18h	(4.3)	5.3 (0.0)

Table 2.3. The stiffness and hysteresis characteristics for Freedom Innovations Catapult FX6 prostheses at each testing condition. The equations indicate prosthetic displacement in meters (h) used to calculate the applied force in kN. Stiffness equals applied force divided by displacement. a and b are constants. All prostheses were tested with the manufacturer supplied sole, with the exception of stiffness category 7 No Sole.

Össur Flex-Run				
Condition (Angle)	**Stiffness Category**	**Force=ah^2+bh**	**Stiffness Variability (SD)**	**Percent Hysteresis Mean (SD)**
Neutral (0°)	3 Low	195h^2+10h	-	5.0
	3 High	199h^2+12h	-	5.4
	4 Low	187h^2+12h	-	5.5
	4 High	223h^2+12h	(1.3)	5.7 (0.2)
	5 Low	269h^2+12h	-	5.7
	5 High	271h^2+14h	(2.8)	6.2 (0.6)
	6 Low	270h^2+15h	-	5.4
	6 High	298h^2+17h	(0.7)	5.3 (0.2)
	7 Low	336h^2+18h	-	4.9
	7 High	354h^2+18h	(0.3)	5.7 (0.1)
	7 High No Sole	327h^2+21h	-	2.8
3 m/s (15°)	3 Low	102h^2+10h	-	4.7
	3 High	101h^2+12h	-	4.7
	4 Low	102h^2+13h	-	4.4
	4 High	109h^2+13h	(0.3)	4.7 (0.3)
	5 Low	121h^2+14h	-	6.8
	5 High	122h^2+15h	(0.6)	4.8 (0.0)
	6 Low	122h^2+17h	-	4.4
	6 High	137h^2+18h	(0.4)	4.6 (0.1)
	7 Low	161h^2+18h	-	4.5
	7 High	165h^2+19h	(0.7)	4.7 (0.1)
6 m/s (10°)	3 Low	134h^2+11h	-	5.8
	3 High	133h^2+12h	-	4.9
	4 Low	133h^2+13h	-	4.4
	4 High	147h^2+13h	(0.1)	4.8 (0.5)
	5 Low	175h^2+14h	-	4.9
	5 High	174h^2+15h	(0.4)	5.0 (0.3)
	6 Low	180h^2+16h	-	4.6
	6 High	206h^2+17h	(0.5)	4.7 (0.2)
	7 Low	232h^2+17h	-	4.6
	7 High	223h^2+19h	(0.0)	5.0 (0.1)

Table 2.4. The stiffness and hysteresis characteristics for Össur Flex-Run prostheses at each testing condition. The equations indicate prosthetic displacement in meters (h) used to calculate the applied force in kN. Stiffness equals applied force divided by displacement. a and b are constants. All prostheses were tested with the manufacturer supplied sole, with the exception of stiffness category 7 High No Sole.

Össur Cheetah Xtend										
Condition (Angle)	**Stiffness (Cat)**	**Force=ah²+bh**			**Stiffness Variability (SD)**			**Percent Hysteresis Mean (SD)**		
		31.5 cm	38.0 cm	44.5 cm	31.5 cm	38.0 cm	44.5 cm	31.5 cm	38.0 cm	44.5 cm
Neutral (0°)	2	$262h^2+16h$	$253h^2+14h$	$213h^2+15h$	(0.4)	(1.2)	-	5.1 (0.7)	5.1 (0.7)	5.0
	3	$306h^2+16h$	$322h^2+15h$	$291h^2+16h$	(0.4)	(0.2)	(0.0)	7.5 (0.1)	7.5 (0.1)	5.6 (0.0)
	4	$345h^2+16h$	$348h^2+16h$	$304h^2+15h$	(0.9)	(0.4)	(0.9)	7.1 (1.5)	7.1 (1.5)	6.2 (0.8)
	5	$387h^2+17h$	$359h^2+18h$	$321h^2+17h$	(1.3)	(0.6)	(0.3)	7.6 (0.3)	7.6 (0.3)	7.0 (0.3)
	6	$420h^2+18h$	$404h^2+19h$	$331h^2+18h$	(1.6)	(1.3)	(1.6)	8.1 (1.0)	8.1 (1.0)	6.5 (0.8)
	7	$440h^2+21h$	$429h^2+20h$	$344h^2+21h$	(0.7)	(0.4)	(0.7)	7.3 (0.5)	7.3 (0.5)	6.6 (1.2)
	7 No Sole	-	-	$484h^2+16h$	-	-	-	-	-	3.0
3 m/s (20°)	2	$99h^2+15h$	$95h^2+14h$	$94h^2+14h$	(0.3)	(0.3)	-	4.4 (0.1)	4.4 (0.1)	4.3
	3	$108h^2+17h$	$111h^2+16h$	$114h^2+15h$	(0.0)	(0.3)	(0.6)	4.9 (0.3)	4.9 (0.3)	4.8 (0.5)
	4	$130h^2+18h$	$131h^2+17h$	$130h^2+17h$	(0.5)	(0.4)	(0.1)	4.5 (0.4)	4.5 (0.4)	4.7 (0.3)
	5	$158h^2+18h$	$146h^2+19h$	$149h^2+18h$	(0.6)	(0.2)	(0.2)	5.4 (1.4)	5.4 (1.4)	4.5 (0.5)
	6	$177h^2+20h$	$167h^2+20h$	$167h^2+20h$	(0.1)	(0.1)	(0.1)	5.5 (0.2)	5.5 (0.2)	4.8 (0.3)
	7	$193h^2+20h$	$195h^2+19h$	$195h^2+19h$	(0.7)	(0.5)	(0.3)	5.4 (0.2)	5.4 (0.2)	4.6 (0.4)
6 m/s (25°)	2	$74h^2+16h$	$68h^2+17h$	$68h^2+17h$	(1.0)	(0.0)	-	4.3 (0.1)	4.3 (0.1)	3.8
	3	$90h^2+17h$	$82h^2+18h$	$82h^2+18h$	(1.0)	(0.3)	(0.6)	4.8 (0.9)	4.8 (0.9)	4.0 (0.0)
	4	$96h^2+20h$	$100h^2+19h$	$98h^2+19h$	(0.6)	(0.6)	(0.5)	4.2 (0.3)	4.2 (0.3)	3.8 (0.0)
	5	$121h^2+21h$	$116h^2+20h$	$115h^2+20h$	(0.1)	(0.2)	(0.4)	4.4 (0.0)	4.4 (0.0)	3.7 (0.0)
	6	$115h^2+24h$	$113h^2+24h$	$118h^2+23h$	(0.5)	(1.0)	(0.3)	4.1 (0.0)	4.1 (0.0)	4.9 (0.4)
	7	$154h^2+22h$	$159h^2+22h$	$149h^2+22h$	(0.1)	(0.0)	(0.8)	5.3 (0.8)	5.3 (0.8)	4.3 (0.5)

Table 2.5. The stiffness and hysteresis characteristics for the Össur Cheetah Xtend prostheses at each testing condition. The equations indicate prosthetic displacement in meters (h) used to calculate the applied force in kN. Stiffness equals applied force divided by displacement. a and b are constants. All RSPs were tested with the supplied sole from the Össur Flex-Run prostheses, with the exception of stiffness category 7 No Sole.

Ottobock 1E90 Sprinter											
Condition (Angle)	**Stiffness (Cat)**	**Force=ah²+bh**			**Stiffness Variability (SD)**			**Percent Hysteresis Mean (SD)**			
		25.0 cm	31.5 cm	38.0 cm	25.0 cm	31.5 cm	38.0 cm	25.0 cm	31.5 cm	38.0 cm	
Neutral (0°)	1	$147h^2+11h$	$132h^2+11h$	$102h^2+11h$	(0.7)	(0.0)	(0.8)	3.6 (0.4)	3.6 (0.4)	3.7 (0.4)	
	2	$152h^2+14h$	$143h^2+13h$	$109h^2+13h$	(2.2)	(0.1)	(0.3)	5.3 (1.1)	5.3 (1.1)	3.8 (0.0)	
	3	$189h^2+16h$	$169h^2+15h$	$119h^2+14h$	(0.7)	(0.8)	(1.5)	4.1 (0.2)	4.1 (0.2)	4.4 (0.8)	
	4	$214h^2+20h$	$168h^2+17h$	$140h^2+18h$	(2.3)	(1.4)	(2.6)	3.6 (0.1)	3.6 (0.1)	4.0 (0.5)	
	5	$234h^2+22h$	$196h^2+22h$	$126h^2+21h$	(0.0)	(1.9)	(0.9)	4.4 (1.1)	4.4 (1.1)	4.4 (0.4)	
	5 No Sole	-	-	$231h^2+20h$	-	-	-	-	-	1.2	
3 m/s (20°)	1	$90h^2+9h$	$90h^2+9h$	$85h^2+9h$	(0.3)	(0.0)	(0.1)	3.8 (0.1)	3.8 (0.1)	3.8 (0.0)	
	2	$102h^2+12h$	$97h^2+12h$	$94h^2+11h$	(0.2)	(0.3)	(0.3)	3.6 (0.1)	3.6 (0.1)	3.7 (0.0)	
	3	$123h^2+14h$	$117h^2+14h$	$115h^2+13h$	(0.6)	(0.4)	(0.5)	3.8 (0.1)	3.8 (0.1)	4.0 (0.1)	
	4	$139h^2+17h$	$149h^2+16h$	$122h^2+16h$	(0.9)	(2.6)	(0.5)	4.0 (0.2)	4.0 (0.2)	4.1 (0.2)	
	5	$146h^2+22h$	$142h^2+21h$	$127h^2+20h$	(0.4)	(0.2)	(0.3)	5.1 (1.4)	5.1 (1.4)	4.5 (0.2)	
6 m/s (25°)	1	$78h^2+10h$	$79h^2+10h$	$77h^2+9h$	(0.4)	(0.5)	(0.7)	3.7 (0.1)	3.7 (0.1)	3.7 (0.2)	
	2	$86h^2+13h$	$84h^2+13h$	$82h^2+13h$	(0.4)	(0.1)	(0.2)	4.0 (0.4)	4.0 (0.4)	3.8 (0.1)	
	3	$103h^2+15h$	$97h^2+15h$	$98h^2+15h$	(0.9)	(0.7)	(0.7)	3.9 (0.5)	3.9 (0.5)	3.6 (0.1)	
	4	$117h^2+18h$	$112h^2+18h$	$107h^2+17h$	(0.8)	(0.8)	(0.7)	4.0 (0.5)	4.0 (0.5)	4.4 (1.0)	
	5	$122h^2+24h$	$133h^2+23h$	$117h^2+22h$	(0.8)	(1.6)	(0.5)	4.0 (0.1)	4.0 (0.1)	4.1 (0.5)	

Table 2.6. The stiffness and hysteresis characteristics of Ottobock 1E90 Sprinter prostheses at each testing condition. The equations indicate prosthetic displacement in meters (h) used to calculate the applied force in kN. Stiffness equals applied force divided by displacement. a and b are constants. All prostheses were tested with the manufacturer supplied sole, with the exception of stiffness category 5 No Sole.

3 Chapter 2: Reduced prosthetic stiffness lowers the metabolic cost of running for athletes with bilateral transtibial amputations

3.1 Abstract

Inspired by the spring-like action of biological legs, running-specific prostheses are designed to enable athletes with lower-limb amputations to run. Yet, manufacturer recommendations for prosthetic stiffness and height may not optimize running performance. Therefore, we investigated the effects of using different prosthetic configurations on the metabolic cost and biomechanics of running. Five athletes with bilateral transtibial amputations each performed fifteen trials on a force-measuring treadmill at 2.5 or 3.0 m/s. Athletes ran using each of three different prosthetic models (Freedom Catapult FX6, Össur Flex-Run, and Ottobock 1E90 Sprinter) with five combinations of stiffness categories (manufacturer recommended and ± 1) and heights (International Paralympic Committee's maximum competition height and ± 2 cm) while we measured metabolic rates and ground reaction forces. Overall, prosthetic stiffness (fixed effect (β)=0.036; p=0.008) but not height ($p \geq 0.089$) affected the net metabolic cost of transport; less stiff prostheses reduced metabolic cost. While controlling for prosthetic stiffness (kN/m), using the Flex-Run (β=-0.139; p=0.044) and 1E90 Sprinter prostheses (β=-0.176; p=0.009) reduced net metabolic costs by 4.3% to 4.9% compared to using the Catapult prostheses, respectively. The metabolic cost of running improved when athletes used prosthetic configurations that decreased peak horizontal braking ground reaction forces (β=2.786; p=0.001), stride frequencies (β=0.911; $p<0.001$), and leg stiffness values (β=0.053; p=0.009). Remarkably, athletes did not maintain overall leg stiffness across prosthetic stiffness conditions. Rather, the in-series prosthetic stiffness governed overall leg stiffness. The metabolic cost of

running in athletes with bilateral transtibial amputations is influenced by prosthetic model and stiffness, but not height.

3.2 Introduction

Running is a bouncing gait that is mechanically well-characterized by a spring-mass model, which depicts the stance leg as a massless linear spring and the body as a point mass (Fig. 3.1) [1-3]. In the model, the leg spring compresses and stores elastic energy during the first half of the stance phase. Subsequently, the leg spring releases energy as it lengthens from mid-stance through the end of ground contact [6]. During running, elastic elements such as tendons and ligaments act as springs that stretch and recoil [6, 53-55]. Inspired by the spring-like action of biological legs, passive-elastic carbon-fiber running-specific prostheses (RSPs) are designed to enable athletes with lower-limb amputations to run. RSPs are shaped like the uppercase letters "C" or "J", attach in-series to the residual limb (Fig. 3.2), and emulate the spring-like function of biological legs during level-ground running [6, 53-55] by storing and returning elastic energy during ground contact [30, 31]. Since conserving mechanical energy via elastic mechanisms theoretically reduces the metabolic cost of running [6, 53-55], the elastic function of RSPs likely contributes to the 14% lower metabolic cost of running for athletes with transtibial amputations using RSPs compared to using relatively rigid, conventional walking prostheses [56].

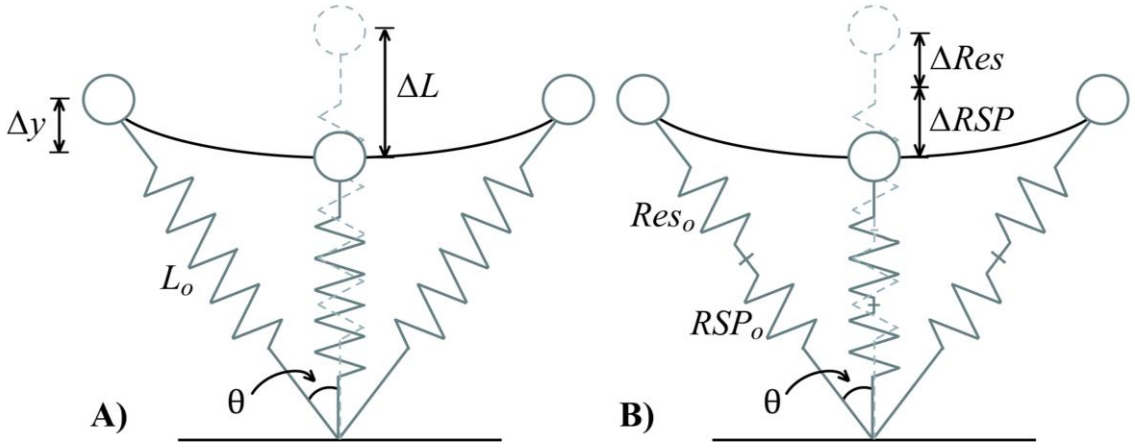

Figure 3.1. Illustration of a spring-mass model of running (A), and a spring-mass model of running with an in-series leg spring (B). Body mass is represented as a point mass (circle) and the touch-down angle is indicated by theta (θ). The stance leg is represented by a massless linear spring for non-amputees (A), or two in-series massless linear springs for athletes with bilateral amputations (B). The initial leg length (L_0) shortens (ΔL), as does its vertical height (Δy) during the stance phase of running. Modeled residual limb length (Res_0) and prosthetic height (RSP_0) compress and extend (ΔRes and ΔRSP) during the stance phase of running.

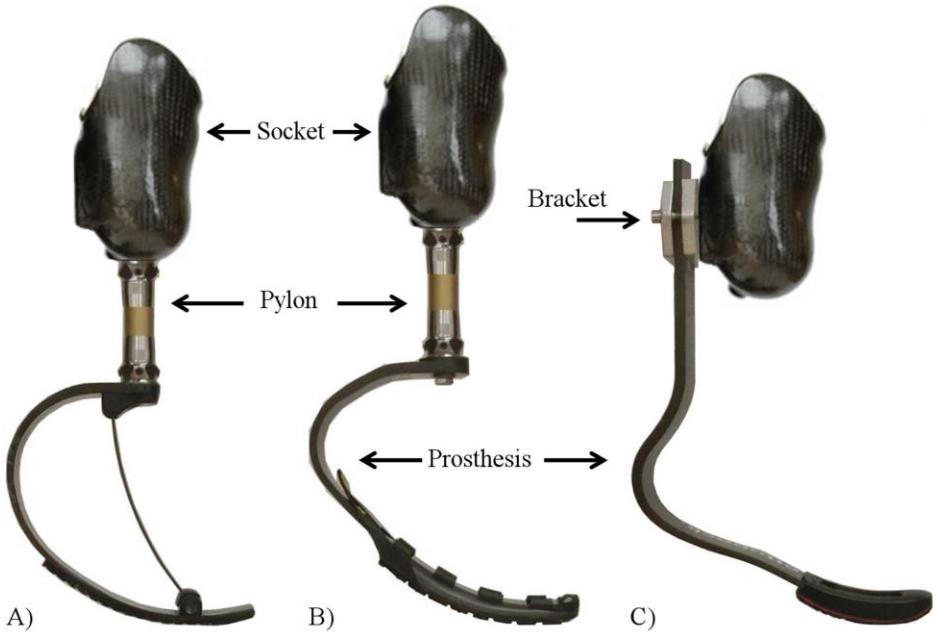

Figure 3.2. Running-specific prostheses. From left to right, A) the Freedom Innovations Catapult FX6 prosthesis (C-shaped) at a representative recommended height, B) the Össur Flex-Run prosthesis (C-shaped) at a representative height of +2 cm, and C) the Ottobock 1E90 Sprinter prosthesis (J-shaped) at a representative height of -2 cm. The C-shaped prostheses are connected

to sockets via aluminum pylons, and the J-shaped prostheses are connected to sockets via custom aluminum brackets.

Despite reducing the metabolic cost of running [56] and improving athletic performances compared to the use of previous prosthetic designs [57], current manufacturer recommendations for prosthetic stiffness may not optimize the running performance of athletes with bilateral transtibial amputations. For athletes with *unilateral* amputations, the aim of the current manufacturer recommended prosthetic configurations are to mitigate stride kinematic asymmetries between the affected and unaffected legs (e.g. asymmetric ground contact times) [45]. For athletes with *bilateral* amputations, prosthetists simply match the left and right legs' RSPs at the manufacturer recommended stiffness category, which is based on the same prosthetic stiffness to body mass ratio as athletes with unilateral amputations [43, 45, 58].

Surface stiffness, which is in-series with the stance leg, affects the running performance of non-amputees [3, 59]. For example, Kerdok et al. [59] reported that changing surface stiffness from 945 kN/m to 75 kN/m decreased the metabolic cost of running in non-amputees by 12%. This decreased metabolic cost was primarily attributed to the greater mechanical energy return from the compliant surface to the runner. Furthermore, when surface compliance changes, non-amputees maintain a constant overall surface plus leg stiffness by altering leg joint stiffness and/or segment geometries during running [59-61]. Straighter limb posture generally results in lower joint moments, and in turn reduces the muscular force needed to support body weight [27, 62], which is the primary determinant of the metabolic cost of running [24-26, 63]. These previous studies suggest that decreasing prosthetic stiffness will reduce the metabolic cost of running. However, the effects of prosthetic stiffness on overall leg stiffness and metabolic cost during running have yet to be determined.

Analogous to prosthetic stiffness recommendations, current prosthetic height recommendations may not optimize distance running performance. Prosthetic height is set at the discretion of the athlete, their prosthetist, and/or in accordance to the International Paralympic Committee (IPC) guidelines [64]. Anecdotally, the potential effects of increased prosthetic height were brought to light at the 2012 Paralympic games, when it appeared that athletes with bilateral transtibial amputations improved their sprinting performance by using taller RSPs. Hypothetically, longer legs could improve running speed by increasing the forward distance traveled during ground contact, while accounting for step frequency and the stance average vertical ground reaction force (GRF) [65]. Previous research indicates that the metabolic cost of running is not associated with the leg lengths of non-amputees [23], however simple correlations fail to account for potential covariates such as increased lower limb mass with longer legs. No study has systemically altered prosthetic height for athletes with bilateral leg amputations and assessed its influence on distance running performance.

We sought to determine how the use of RSPs with different stiffness values and heights affect the metabolic cost of running for athletes with bilateral transtibial amputations. Since reduced prosthetic stiffness may enhance mechanical energy conservation and improve the stance leg's effective mechanical advantage, we hypothesized that using RSPs with a lower stiffness than manufacturer recommended would decrease the metabolic cost of running. Given the lack of previous data, we tested the null hypothesis that altering prosthetic height would not affect the metabolic cost of running. Based on several studies [59-61], we hypothesized that residual limb stiffness (comprising knee and hip joints) would be inversely associated with prosthetic stiffness, such that athletes would maintain overall leg stiffness across different prosthetic stiffness configurations.

Finally, the metabolic cost of running is often associated with biomechanical variables such as vertical [25, 66] and horizontal GRF magnitude [24, 67], ground contact time [25, 68], stride frequency [38, 69], and leg stiffness [4, 38, 69]. For those reasons, we sought to quantify how the metabolic cost of running relates to these biomechanical variables in athletes with bilateral transtibial amputations.

3.3 Methods

3.3.1 Participants

Five male athletes with bilateral transtibial amputations participated (Table 3.1). Each athlete had over one year of experience using RSPs, which included track and field races, and gave informed written consent according to the Colorado Multiple Institutional Review Board and the USAMRMC Office of Research Protection, Human Research Protection Office.

Partic-ipants	**Age** (yrs)	**Mass** (kg)	**Standing Met Power** (W/kg)	**Event(s)**	**Max IPC Height** (m)	**Max IPC Leg length** (m)	**Catapult Leg length** (m)	**Flex-Run Leg length** (m)	**1E90 Sprinter Leg length** (m)
1	25	69.8	1.6	100m/ 200m	1.80	0.97	1.12	1.12	0.97
2	23	76.1	1.5	Long Jump	1.88	1.07	1.07	1.07	1.04
3	18	73.2	1.7	100m/ 200m	1.87	1.05	1.05	1.05	1.05
4	31	69.6	1.3	400m	1.90	1.10	1.10	1.10	1.10
5	27	68.9	1.5	5000m	1.87	1.06	1.06	1.06	1.06
Avg	24.8	71.5	1.5		1.86	1.05	1.08	1.08	1.04
SD	4.8	3.0	0.2		0.04	0.05	0.03	0.03	0.04

Table 3.1. Participant characteristics: age, mass, average standing metabolic (Met) power, cause of amputations, and primary event. The maximum standing height and corresponding leg lengths allowed in track and field races sanctioned by the International Paralympic Committee (IPC) [64]. The resulting Catapult, Flex-Run, and 1E90 Sprinter prosthesis leg lengths represent the closest attainable maximum IPC-regulated leg lengths from each participant and prosthetic

model combination [64]. Leg lengths were measured from the greater trochanters to the most distal locations of the unloaded prostheses.

3.3.2 Protocol

Initially, each participant completed a fitting and accommodation session. During this session, we collected anthropometric measurements to determine the tallest height that each participant could use to compete in track and field races according to the IPC [64]. Next, a certified prosthetist fit each participant with three different prosthetic models (Freedom Innovations Catapult FX6, Irvine, CA, USA; Össur Flex-Run, Reykjavik, Iceland; Ottobock 1E90 Sprinter, Duderstadt, Germany) at the manufacturer's recommended stiffness category and ±1 stiffness categories and at leg lengths that produced the IPC maximum competition height and ±2 cm. Prosthetic stiffness categories are recommended to athletes based on user body mass with larger athletes recommended numerically greater stiffness categories [43, 45, 58]. The Catapult and Flex-Run prostheses are shaped like a "C" and attach distally to the sockets that encompass the residual limbs, via connective aluminum pylons (Fig. 3.2). The 1E90 Sprinter prostheses are shaped like a "J" and mount to the posterior wall of each socket (Fig. 3.2). After establishing the heights for J-shaped RSPs, they are typically bolted directly to the sockets. Instead, we constructed custom aluminum brackets that were bolted to the sockets, thus allowing us to preserve the RSPs, secure them to the sockets, and alter height between trials (Fig. 3.2). Sockets are carbon-fiber or fiber-glass (check sockets) negative composites of a residual limb and are secured to the limb via suction or locking mechanisms.

Due to the combined lengths of the participant's residual legs and the heights of prosthetic components, we were unable to match the maximum IPC competition height for some participants with certain prosthetic models. The build height of C-shaped RSPs limit the minimum participant height (Fig. 3.2). For example, the minimum height of the Flex-Run

prosthesis is 277 mm prior to adding the components necessary for socket attachment (4). Thus, if the maximum IPC competition height for a participant is less than the length from the top of their head to the end of their residual limb plus 277 mm, they will exceed the maximum IPC height with the respective prosthetic model under all conditions. Also, the maximum achievable height was limited while using J-shaped RSPs. The 1E90 Sprinter prostheses could not exceed their build height; consequently, a participant with short residual limbs was unable reach the maximum IPC height using the 1E90 Sprinter prostheses (Table 3.1); whereas, the C-shaped RSPs could be made as tall as necessary through the use of connective pylons. For these cases, we set prosthetic height as close as feasible to the maximum IPC competition height. If the closest achievable height was taller than the maximum IPC competition height, ensuing prosthetic height alterations were +2 cm and +4 cm. If the closest achievable height was shorter than the maximum IPC competition height, ensuing prosthetic height alterations were −2 cm and −4 cm (Table 3.1).

After being fit with different prosthetic configurations, participants ran on a treadmill at self-selected speeds until both the prosthetist and participant were satisfied. Generally, athletes were accommodated to each prosthetic model at the recommended stiffness category and height. When using C-shaped RSPs, athletes also ran at additional heights (i.e. ±2 cm) to determine proper alignment with taller/shorter pylons. When using J-shaped RSPs, the components and alignment were the same for each height, thus athletes were not typically accommodated to additional heights. The accommodation sessions lasted approximately 6-7 hours per participant. All participants used their personal competition sockets for the trials with the respective prosthetic shape (4 used J-shaped and 1 used C-shaped RSPs). The four athletes who compete with J-shaped RSPs used their everyday walking sockets for the C-shaped RSP trials. For the

athlete who competes with C-shaped RSPs, a prosthetist fabricated custom check sockets that replicated the participant's competition sockets (suspension, internal dimensions, etc.) for the J-shaped RSP trials.

On subsequent days, participants performed a 5-minute standing trial (using their personal walking prostheses) and up to six, 5-minute running trials per session with at least 5 minutes of rest between trials. The combination of the rest periods and the moderate intensity running trials adequately prevented any potential effects of fatigue. Previous studies reported that subjects who run at a moderate intensity for trial lengths up to 7 minutes display no signs of fatigue [47, 70].

Participants ran on a 3D force-measuring treadmill (Treadmetrix, Park City, UT, USA) at 3 m/s. If a participant was unable to maintain primarily oxidative metabolism at 3 m/s, as indicated by a respiratory exchange ratio >1.0, running speed was set to 2.5 m/s for all of their respective trials. Each participant ran using 15 different prosthetic model, stiffness category, and height combinations. Initially, participants ran using each prosthetic model at three stiffness categories (recommended and ± 1) and the maximum competition height. The stiffness category for each prosthetic model that elicited the lowest net metabolic cost of transport (CoT in J/kg/m) was deemed optimal. Subsequently, participants ran using the optimal stiffness category of each prosthetic model at two additional heights (e.g. ±2 cm). We randomized the trial order beginning with the nine prosthetic model and stiffness category combinations at the maximum IPC height. Once a participant completed trials at all three stiffness categories with a prosthetic model, the altered height trials for the respective model at the optimal stiffness category were randomly inserted into the trial order. Data were collected over three to five sessions, and all participants completed the protocol within nine days following the accommodation session.

3.3.3 Metabolic Cost of Transport

We instructed participants to fast for at least three hours prior to testing. We measured their rates of oxygen consumption ($\dot{V}O_2$) and carbon dioxide production ($\dot{V}CO_2$) using open-circuit expired gas analysis (TrueOne 2400, ParvoMedic, Sandy, UT, USA) throughout each trial and averaged these rates during the last two minutes of each trial to calculate steady-state metabolic rates. We used the Brockway equation [71] to convert the average $\dot{V}O_2$ and $\dot{V}CO_2$ into metabolic power (W). Then, we subtracted the average metabolic power consumed during standing of the corresponding day from each running trial to yield net metabolic power. We normalized net metabolic power by the mass of the participant (W/kg) for each prosthetic condition. Participant mass included running gear. Finally, to compare 3.0 and 2.5 m/s trials, we divided net metabolic power by running velocity to calculate the net metabolic cost of transport (CoT) in J/kg/m. We tested each participant at the same time of day for all of their respective sessions.

3.3.4 Prosthetic stiffness

Recommended prosthetic stiffness (kN/m) differs between models [30]. Therefore, we assessed the influence of the manufacturer's recommended prosthetic stiffness category, as well as actual prosthetic stiffness (kN/m) on the net CoT during running [30], using established data. We calculated prosthetic stiffness from the mean peak GRF measured from both legs during each trial (present study) and the force-displacement equations from [30] to estimate prosthetic displacement. Subsequently, we divided the measured peak GRF magnitude by the estimated prosthetic displacement to yield stiffness.

3.3.5 Biomechanics

We measured vertical and anterior-posterior components of the ground reaction forces (GRFs) between minutes 2.0 and 3.0, and between minutes 3.5 and 5.0 of each trial. We collected GRFs at 1000 Hz, filtered them using a 4th order low-pass Butterworth filter with a 30 Hz cutoff frequency, and then used filtered data to calculate GRF parameters, stride kinematics, and leg stiffness values from 10 consecutive strides (20 steps) with a custom MATLAB script (Math Inc., Natick, MA, USA). We set our GRF threshold at 1% of user body weight to detect periods of ground contact.

We calculated overall leg stiffness (k_{leg}) as the quotient of peak vertical GRF (F_{peak}) and maximum leg spring compression (ΔL) during ground contact [2].

$$k_{leg} = \frac{F_{peak}}{\Delta L} \tag{3.1}$$

To calculate the maximum compression of the leg spring (ΔL), we measured initial leg length (L_0) as the distance from the greater trochanter to the distal end of the unloaded RSP [5, 33]. Next, we used initial leg lengths to calculate theta (θ), which is the angle of the leg spring at initial ground contact relative to vertical, using equation 3.2.

$$\theta = sin^{-1}(\frac{v\ t_c}{2\ L_0}) \tag{3.2}$$

Because the spring-mass model assumes step symmetry about the vertical axis [1-3], theta (θ) equals half the angle swept by the stance leg, as determined from running velocity (v), ground contact time (t_c), and initial leg length (L_0). The maximum stance leg spring compression (ΔL) was calculated using equation 3.3:

$$\Delta L = \Delta y + L_0(1 - \cos\theta) \tag{3.3}$$

which incorporates peak vertical displacement of the center of mass during ground contact (Δy), calculated by twice integrating the vertical acceleration of the center of mass with respect to time

[72]. The instantaneous vertical acceleration of the center of mass was calculated by subtracting the participant's body weight from the vertical GRF magnitude (net force), and dividing by body mass [72].

Since biological legs and RSPs have relatively linear force-displacement profiles [2, 30], we modeled overall leg stiffness (k_{leg}) as two in-series springs (Fig. 3.1). We used previously established measurements of prosthetic stiffness (k_{RSP}) [30], to estimate residual limb stiffness (k_{res}) using equation 3.4.

$$\frac{1}{k_{leg}} = \frac{1}{k_{res}} + \frac{1}{k_{RSP}} \tag{3.4}$$

Due to the potential association between the mechanical energy delivered by the RSPs and the metabolic cost of running, we calculated mechanical power return from the RSPs for each step ($\dot{P}_{RSP}$):

$$\dot{P}_{RSP} = \frac{k_{RSP}(\Delta d)^2(1-Hst_{RSP}/100)}{2\,t_{step}} \tag{3.5}$$

determined by prosthetic stiffness (k_{RSP}), peak prosthetic displacement (Δd), percent prosthetic hysteresis (Hst_{RSP}) [30], and step time (t_{step}). In order to relate prosthetic mechanical energy return to metabolic cost of transport (J/kg/m), we divided the energy return averaged per step by user body mass (m) and running velocity (v) to calculate mechanical energy return ($\dot{E}_{RSP}$) per kilogram per meter (J/kg/m):

$$\dot{E}_{RSP} = \frac{P_{RSP}}{m\,v} \tag{3.6}$$

3.3.6 Statistical Analyses

We used a linear mixed model to evaluate the effects of using different prosthetic models, stiffness categories, and heights on net CoT. We used a second statistical linear mixed model

with actual prosthetic stiffness (kN/m) instead of stiffness category to evaluate the effects of using different prosthetic models, stiffness, and heights on net CoT.

Three of our participants ran at 3.0 m/s and two ran at 2.5 m/s. Accordingly, we used linear mixed models to control for speed while independently testing the associations of the predetermined GRF parameters (stance average vertical GRF, peak vertical GRF, and peak horizontal braking and propulsive GRFs), stride kinematics (ground contact time, and stride frequency), and leg stiffness on the net CoT. To evaluate the influence of prosthetic mechanical energy return on net CoT, in addition to the relationships between leg stiffness, prosthetic stiffness, and residual limb stiffness, we performed simple linear regressions. We performed paired two-tailed t-tests to compare each biomechanical variable from minutes 2.0 to 3.0 to the respective variable from minutes 3.5 to 5.0 to ensure participants achieved a biomechanical steady-state. We reported the fixed effect (β) from each statistically significant association (dependent variable = β independent variable + intercept). When appropriate, we implemented a Bonferroni correction, and tested for potential interaction effects across all statistical comparisons. We set the level of significance at $\alpha=0.05$, and performed statistical analyses using R-studio software (Boston, MA, USA).

3.4 Results

While controlling for covariates, use of different prosthetic stiffness (category and kN/m) ($p\leq0.008$) (Fig. 3.3), but not height ($p\geq0.089$) (Fig. 3.4), affected the net CoT of athletes with bilateral transtibial amputations. Each integer reduction in stiffness category decreased the average net CoT by 3.7% ($\beta=0.135$; $p<0.001$). Actual prosthetic stiffness values ranged from 19.3 to 29.6 kN/m and averaged 22.9 ± 2.3 kN/m (±SD). Overall, every 1 kN/m reduction in prosthetic stiffness decreased net CoT by 1.3% ($\beta=0.036$; $p=0.008$) (Fig. 3.3).

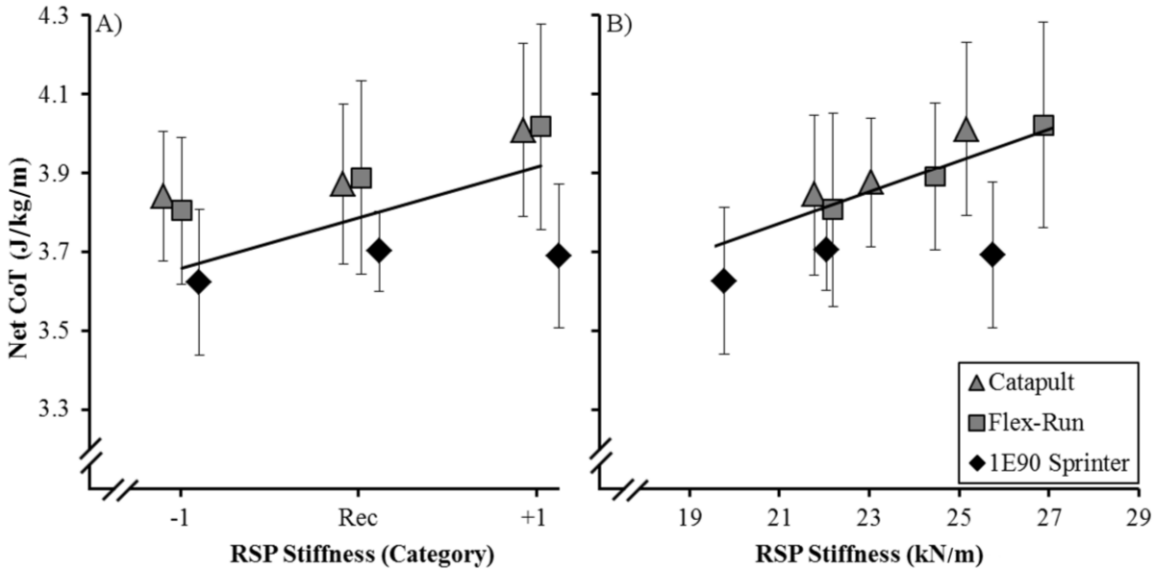

Figure 3.3. A) Mean (±SEM) net metabolic cost of transport (CoT) as a function of using different models of running-specific prostheses (RSPs) with different stiffness categories (Cat). Symbols are offset for clarity. Regression equation: Net CoT = 0.129 ΔCat + 3.786. B) Mean (±SEM) net metabolic cost of transport (CoT) as a function of actual prosthetic stiffness (kN/m) across prosthetic models. Regression equation: Net CoT = 0.036 ΔkN/m + 2.931. Triangles represent use of the C-shaped Catapult, squares represent use of the C-shaped Flex-Run, and diamonds represent use of the J-shaped 1E90 Sprinter prostheses.

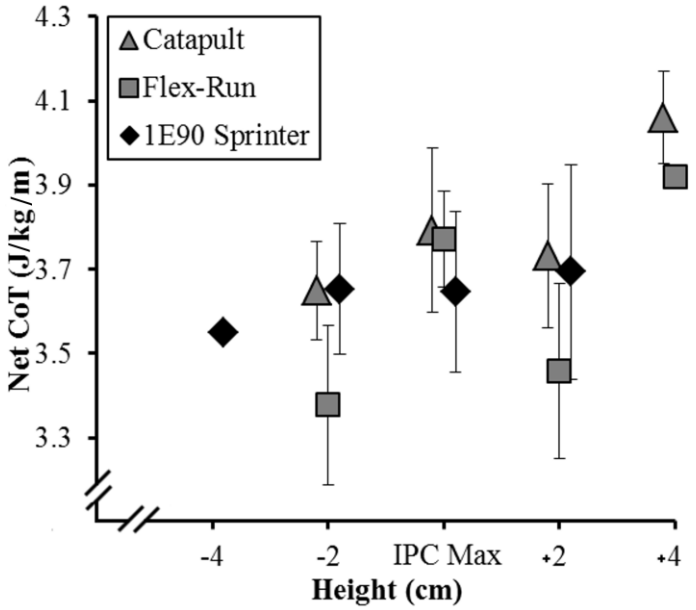

Figure 3.4. Mean (±SEM) net metabolic cost of transport (CoT) as a function of using different models of running-specific prostheses (RSPs) at different heights (cm) using the stiffness category that produced the lowest net CoT. Symbols are offset for clarity. IPC Max indicates the prosthetic height for each participant that elicits the maximum competition height based on the International Paralympic Committee guidelines (1) and deviations indicate heights of ±2 cm and ±4 cm. Triangles represent use of the C-shaped Catapult, squares represent use of the C-shaped Flex-Run, and diamonds represent use of the J-shaped 1E90 Sprinter prostheses.

The metabolic cost of running was associated with the equipped prosthetic model. The influence of prosthetic model on net CoT was largely the same when controlling for either prosthetic stiffness category or actual stiffness (kN/m), thus unless otherwise specified, we will interpret prosthetic model effects while controlling for actual prosthetic stiffness (kN/m). Within our prosthetic stiffness range, when athletes with bilateral transtibial amputations used the 1E90 Sprinter prostheses, their net CoT was 4.3 to 4.7% lower compared to using Catapult prostheses (β=-0.176; p=0.009). The net CoT was similar when athletes used the Flex-Run versus 1E90 Sprinter prostheses (p=0.597). When controlling for stiffness category, the use of Flex-Run prostheses elicited similar net CoT values compared to the use of Catapult prostheses (p=0.138), whereas while controlling for actual prosthetic stiffness (kN/m), the use of Flex-Run prostheses reduced net CoT 4.4% to 4.9% compared to the use of Catapult prostheses (β=-0.139; p=0.044), highlighting the dissimilarity in manufacturer recommended stiffness values (Fig. 3.3). There were no significant interaction effects between prosthetic model, stiffness, and/or height on net CoT ($p \geq 0.230$). Additionally, there was an extremely weak, but significant correlation between the RSP mechanical energy return and the elicited net CoT (p=0.042; R^2=0.055; net CoT = –0.660 RSP mechanical energy return + 4.360) (Fig. 3.5).

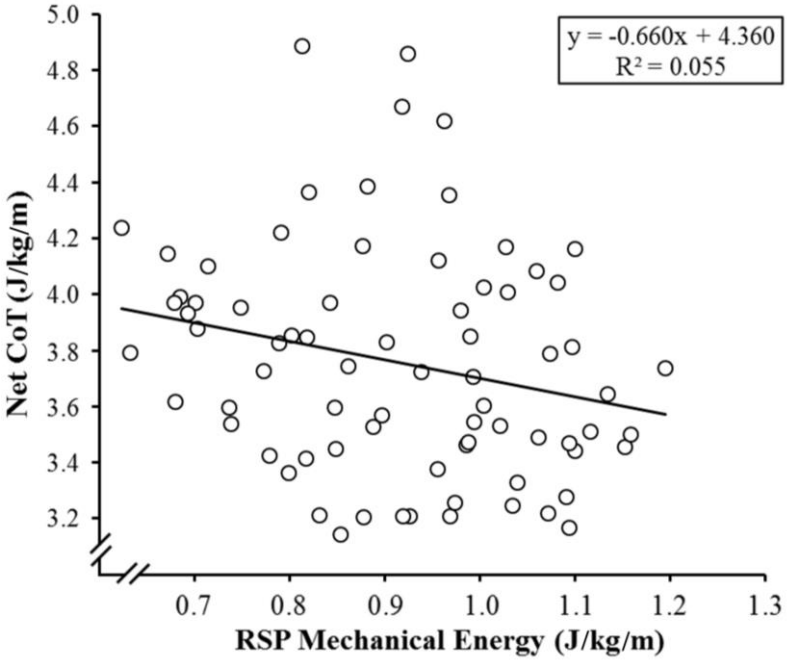

Figure 3.5. The net metabolic cost of transport (CoT) as a function of running-specific prosthesis (RSP) mechanical energy return for each running trial. Increased prosthetic mechanical energy return lowered net CoT (p=0.042).

There were no differences between any tested biomechanical parameters from minutes 2.0 to 3.0 compared to minutes 3.5 to 5.0 ($p \geq 0.430$). Consequently, we only report biomechanical data collected between minutes 3.5 to 5.0 of each trial. Residual limb stiffness values ranged from 18.7 to 82.8 kN/m and averaged 42.5 ± 15.1 kN/m (±SD) (Fig. 3.6). There was a moderate positive association between prosthetic stiffness (kN/m) and leg stiffness ($p<0.001$; $R^2=0.437$; leg stiffness = 0.703 prosthetic stiffness – 1.623) (Fig. 3.6), and a strong positive association between residual limb stiffness and leg stiffness ($p<0.001$; $R^2=0.825$; leg stiffness = 0.149 residual limb stiffness + 8.159). There was a weak, yet statistically significant, positive association between prosthetic stiffness (kN/m) and residual limb stiffness ($p=0.003$; $R^2=0.115$; residual limb stiffness = 2.186 prosthetic stiffness – 7.704) (Fig. 3.6).

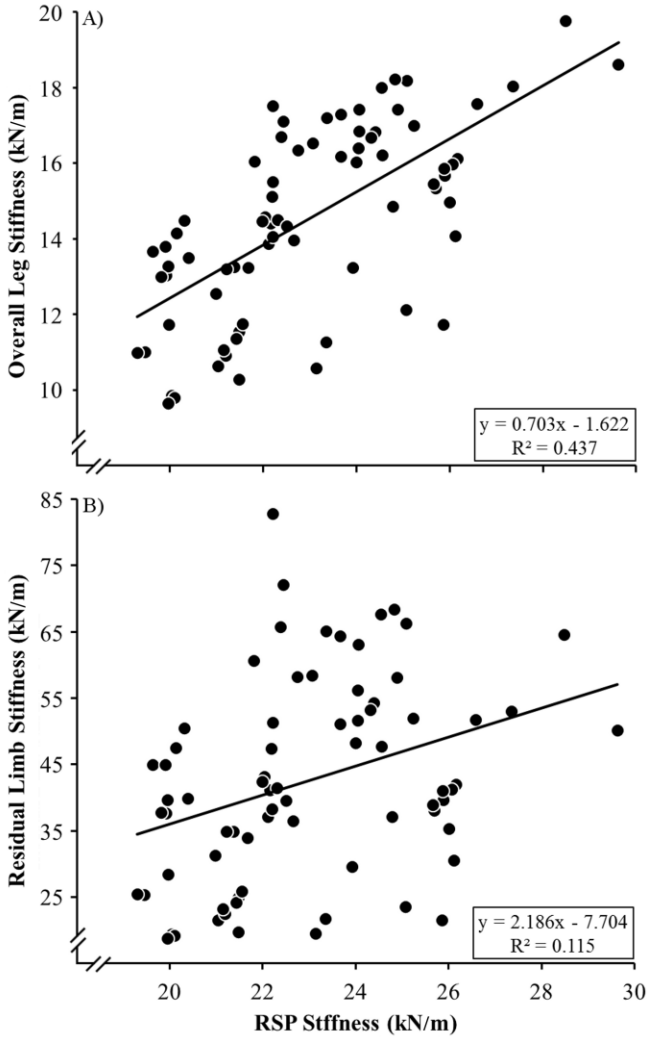

Figure 3.6. A) Overall leg stiffness compared to running-specific prosthesis (RSP) stiffness ($p<0.001$), and B) Residual limb stiffness compared to prosthetic stiffness ($p=0.003$). There was a positive association between both overall leg stiffness and residual limb stiffness compared to prosthetic stiffness.

Net CoT was associated with peak braking horizontal GRF, stride frequency, and leg stiffness. Independently, every 0.1 times body weight decrease in peak braking horizontal GRF was related to a 6.4% reduced net CoT (net CoT = 2.789 peak braking GRF + 4.354; $p=0.001$), every 0.1 Hz decrease in stride frequency was related to an 8.3% reduced net CoT (net CoT = 0.911 stride frequency + 1.099; $p<0.001$), and each 1 kN/m decrease in leg stiffness was

associated with a 1.8% reduced net CoT (net CoT = 0.053 leg stiffness + 2.991; p=0.009). Neither stance average vertical GRF (p=0.592), peak vertical GRF (p=0.723), peak propulsive horizontal GRF (p=0.063), nor ground contact time (p=0.116) were associated with net CoT.

3.5 Discussion

We accept our initial hypothesis based on our findings that athletes with bilateral transtibial amputations consume less metabolic energy while running with RSPs that are less stiff than manufacturer recommended. Since prosthetic stiffness category recommendations are based on user body mass, we ran a linear mixed model with prosthetic stiffness (kN/m) normalized to each corresponding participant's body mass. Every 0.1 kN/m/kg decrease in prosthetic stiffness (while controlling for prosthetic model) reduced net CoT by 9.2% (β=2.499; p=0.012), further supporting the notion that the use of less stiff RSPs reduces the metabolic cost of running for athletes with bilateral transtibial amputations. The decreased metabolic cost while using less stiff RSPs is likely related to improved biomechanics. Overall, the use of less stiff RSPs lowered peak braking GRF, stride frequency, and leg stiffness ($p \leq 0.022$). Moreover, while considering prosthetic models, further linear mixed model analyses revealed that for every 1 kN/m prosthetic stiffness reduction, net CoT decreased while using the Catapult (β=0.085; $p<0.001$) and Flex-Run (β=0.084; $p<0.001$), but not the 1E90 Sprinter (p=0.258) prostheses (Fig. 3.3). Therefore, the effects of prosthetic stiffness on net CoT depend on the prosthetic model. Future studies should investigate whether use of C-shaped RSPs that are more than one stiffness category lower than the manufacturer recommended optimize net CoT, and whether net CoT remains independent of the 1E90 Sprinter or J-shaped prosthetic stiffness across a wider range of stiffness values.

In addition to improved biomechanics, the metabolic cost of running when using the J-shaped 1E90 Sprinter prostheses compared to the C-shaped RSPs may be due to better sagittal plane alignment, reduced mechanical energy dissipation (less hysteresis), and/or enhanced stability. The sagittal plane alignment of the 1E90 Sprinter prostheses may have elicited GRF vectors that were more aligned with the stance limb, thus mitigating muscular force requirements [27, 62]. Also, J-shaped RSPs return ~1% more of the stored elastic energy (~1% less hysteresis) than C-shaped RSPs [30], thus potentially minimizing mechanical work performed by the muscles when using the 1E90 Sprinter prostheses compared to the C-shaped RSPs. Another possible explanation for the reduced metabolic cost of running with the 1E90 Sprinter prostheses compared to the C-shaped RSPs may have been owed to improved lateral stability [24, 49, 73, 74]. Arellano et al. [32] found that an athlete with bilateral transtibial amputations had greater mediolateral ”foot” placement variability than non-amputees while running at fast speeds [32], indicating that lateral balance may be compromised compared to non-amputees. Accordingly, it is possible that there is a considerable metabolic cost of maintaining lateral balance during running for athletes with bilateral transtibial amputations [24, 49, 73, 74]. Overall, 1E90 Sprinter prostheses are wider (0 to 2.5 cm) and thicker (0.1 to 0.9 cm) than the C-shaped RSPs at each segment (i.e. proximal, medial, distal) [43, 45, 58]. Thus, the design of the 1E90 Sprinter prostheses may have improved mediolateral stability, and consequently reduced the metabolic cost of running compared to the use of C-shaped RSPs.

The improved metabolic cost of running with the J-shaped 1E90 Sprinter versus C-shaped RSPs was in spite of the relatively heavy attachments used for the 1E90 Sprinter prostheses. The mass of two brackets plus 1E90 Sprinter prostheses (2008 g) were 384 g and 630 g greater than the mass of the Catapult and Flex-Run prostheses, respectively. Adding mass to

the lower legs or feet of non-amputees increases the metabolic cost of running, such that 100 g added to the feet increases metabolic cost by ~1% [75, 76]. It is likely that the use of standard, lighter attachments for the J-shaped 1E90 Sprinter prostheses would further decrease the metabolic cost of running.

Numerical reductions in three biomechanical variables, peak braking GRF, stride frequency, and leg stiffness, were associated with improved net CoT. Decreased peak braking GRFs may reduce metabolic cost by mitigating the muscular force generated by the legs during running [24, 67]. The potential influence of stride frequency and leg stiffness on metabolic cost is not straightforward. The metabolic cost of running for non-amputees increases when they adopt unnatural stride frequencies [38, 69]. Yet, in the present study participants used a self-selected stride frequency for each prosthetic configuration. Similarly, when non-amputees adopt higher or lower leg stiffness values than preferred, their metabolic cost of running increases [4, 38, 77]. Hypothetically, compliant leg springs decrease the metabolic cost of running compared to stiffer leg springs by prolonging ground contact time and by storing and returning more elastic energy per unit of applied force. Longer ground contact time enables athletes to produce the required vertical force on the ground with slower, more economical muscle fibers [25, 78]. Also, storing and returning more elastic energy during running mitigates the muscular mechanical work needed to sustain running, which also elicits more economical muscular force production [6-8, 55]. However, the notion that force generated by isometric muscle contractions is more economical than continuous stretching-shortening contractions has been challenged. Holt et al. [79] reported that while generating force, frog muscles *in vitro* consume metabolic energy at the same rate when continuously stretching and shortening versus operating isometrically. Moreover, stiffer leg springs generally have an improved effective mechanical advantage compared to

compliant leg springs [27, 62] due to reduced ankle, knee, and hip joint flexion [80, 81]. Because the greatest GRF magnitudes are approximately vertical and occur when the runner's center of mass is directly above the body's center of pressure (Fig. 3.1) [1-3], reduced joint flexion theoretically decreases peak GRF-joint moments due to shorter moment arm lengths, mitigating muscular force requirements. Collectively, moderate leg stiffness seems to minimize the metabolic cost of running by optimizing the interplay of multiple biomechanical factors.

We accept our second (null) hypothesis; the metabolic cost of running was independent of prosthetic height. Since the influence of prosthetic height did not achieve statistical significance, our results support those of Williams and Cavanagh [23] who also reported no relationship between the metabolic cost of running and the leg lengths of non-amputees. Athletes with long residual limbs that compete in sprint events within the T43 classification (athletes with bilateral below knee amputations) may not able to use C-shaped RSPs because their overall height would exceed the IPC's regulated competition height [64]. However, based on the disassociation between prosthetic height and net CoT from our study, these athletes could increase their height beyond the IPC's regulated competition height without affecting their distance running performance. Further linear mixed model analyses reveal that prosthetic height was unrelated to stride frequency ($p=0.162$) or leg stiffness ($p=0.914$), but was associated with peak braking GRF ($\beta=0.005$; $p=0.049$). For every 2 cm increase in prosthetic height, peak braking GRF magnitude increased 4.8%. Additional paired two-tailed t-tests revealed that prosthetic mass was similar across height alterations ($p\geq0.352$); indicating that prosthetic mass did not statistically affect our prosthetic height results.

To our knowledge, only one study has investigated the influence of prosthetic configuration on a facet of running performance. Tominaga et al. [82] altered the RSPs' sagittal

plane alignment ±4° for athletes with unilateral transtibial amputations, and found no association between alignment and running speed during the acceleration phase of an all-out sprint [82]. Yet, sagittal plane alignment may affect net CoT based on our previous finding that a 1° alignment change alters prosthetic stiffness 0.46 to 0.79 kN/m, depending on the prosthetic model [30].

Similar to Kerdok et al. [59], we found that reduced in-series stiffness with respect to the stance leg, as well as increased mechanical energy return from the in-series spring were associated with a reduced metabolic cost of running. In contrast to Kerdok et al. [59], who found a strong correlation between the metabolic cost of running and the mechanical energy return of the in-series compliant surface, we found an extremely weak correlation between the metabolic cost of running and the mechanical energy returned by the in-series RSPs (R^2=0.055). Furthermore, we found that prosthetic mechanical energy return was independent of prosthetic stiffness (linear regression: p=0.718) and that overall leg stiffness decreased with reduced in-series stiffness. Collectively, it appears that athletes *with* and *without* amputations both run with lower metabolic costs when in-series stiffness is reduced, yet the underlying mechanisms responsible for these changes are different.

We found that the overall leg stiffness (residual limb plus RSP in-series stiffness) of athletes with bilateral transtibial amputations is affected by changes in prosthetic stiffness. Our results coincide with those of McGowan et al. [5], suggesting that prosthetic stiffness governs overall leg stiffness. We found a positive association between residual limb stiffness (biological limb stiffness) and prosthetic stiffness (in-series stiffness) (Fig. 3.5). Therefore, we reject our third hypothesis. Our results contrast with those of non-amputee runners whom adjust their biological leg stiffness with altered in-series (surface) stiffness to maintain overall leg plus in-series stiffness [59-61]. Our results indicate that in-series prosthetic stiffness affects the running

mechanics of athletes with bilateral transtibial amputations; consequently, traversing terrain of varying compliance likely alters their running mechanics. Biomechanically, leg stiffness is a composite of sagittal plane joint torsional stiffness and leg segment geometries [80, 81, 83]. Since RSP stiffness cannot yet be modulated neurally [30], and the hip joint has a negligible influence on leg stiffness [80, 81, 83], it is possible that athletes with bilateral transitibial amputations primarily rely on knee joint mechanics to alter leg stiffness. Future studies are needed to understand the mechanisms underlying the unique leg stiffness results of athletes with bilateral transtibial amputations.

Previously, the metabolic cost of running had only been reported for two athletes with bilateral transtibial amputations [52, 84]; this dataset now totals seven athletes with bilateral transtibial amputations (Table 3.2). Selecting the most economical trial for each of our participants and the reported values in the literature, average gross CoT (ml O_2/kg/km) from these seven athletes with bilateral transtibial amputations is 188.9 ± 16.3 ml O_2/kg/km (mean ± SD). For context, Olympic qualifying, sub-elite, and recreational non-amputee runners tested by Morgan et al. [22] elicited mean gross CoT values of 181.9 ± 9.1, 187.5 ± 9.7, and 190.5 ± 13.6 ml O_2/kg/km (mean ± SD), respectively. Furthermore, our study demonstrates the importance of optimizing prosthetic model and stiffness recommendations since the least economical prosthetic configuration for each of our participants yielded average gross CoT values that were 21.9% higher than their most economical trials (227.0 ± 22.7 vs. 186.2 ± 12.3 ml O_2/kg/km) (paired two-tailed t-test; p=0.001) (Table 3.2).

Athletes with bilateral transtibial amputations	**Lowest gross CoT** (ml O_2/kg/km)	**Highest gross CoT** (ml O_2/kg/km)
1	207.0	264.0
2	185.6	216.0
3	182.0	230.2
4	174.2	204.2
5	182.4	220.7
Avg ± SD	186.2 ± 12.3	227.0 ± 22.7
6	174.9	N/A
7	216.5	N/A
Avg ± SD	188.9 ± 16.3	

Table 3.2. The lowest and highest elicited gross metabolic cost of transport (CoT) (ml O_2/kg/km) values for the participants in the present study (Athletes 1 through 5), as well as those reported in the literature (Athletes 6 and 7). Athlete 6 is from Weyand et al. [52], athlete 7 was tested in Brown et al. [56], and their individual CoT data were reported by Kram et al. [84].

We were unable to match the maximum IPC competition height for all participants and prosthetic models due to residual limb lengths and/or prosthetic component dimensions. In turn, we adopted a statistical approach that accounted for the discrepancies in participant height across trials. Also, our participants used two sets of sockets to complete our protocol (one set for C-shaped RSPs, and one set for J-shaped RSPs), thus there could have been unequal residual limb movement within the different sockets. This may have led to varying levels of muscular co-contraction and/or mechanical energy dissipation. Unfortunately, little is known regarding how prosthetic sockets affect athletic performance. Future studies aimed to understand the influence of socket design on the performance of athletes with lower limb amputations are warranted. Furthermore, two of the five participants were unable to complete all trials at 3.0 m/s while maintaining primarily aerobic metabolism. As a consequence, those two participants completed their trials at 2.5 m/s, therefore we used net CoT because of its general independence with running speed [22, 24, 85], which we confirmed with our dataset using a linear mixed model

analysis (p=0.572). Even though we present the largest dataset of running metabolic costs and biomechanics from athletes with bilateral transtibial amputations to date, our relatively small sample size may have lead us to falsely accept null hypotheses (type II error) that would be detected with a larger participant cohort.

3.6 Conclusion

Prosthetic model and stiffness, but not height, influence the metabolic cost of running for athletes with bilateral transtibial amputations. While controlling for prosthetic stiffness (kN/m), using the Flex-Run and the 1E90 Sprinter prostheses yielded lower net metabolic cost of transports compared to using the Catapult prostheses. Across prosthetic models, use of RSPs that are less stiff than manufacturer recommended (e.g. numerically lower stiffness category) reduced the metabolic cost of running. The use of RSPs of different heights spanning a 4 cm range had no effect on the metabolic cost of running. Mechanically, the leg stiffness of athletes with bilateral transtibial amputations is governed by in-series prosthetic stiffness. In all, athletes with bilateral leg amputations can minimize their metabolic cost of running through the use of RSPs that are optimally designed, and have lower prosthetic stiffness compared to the manufacturer recommended.

Acknowledgements

We thank Mike Litavish CPO and Angela Montgomery CPO for their invaluable assistance throughout our study. We extend our gratitude to Dr. Rodger Kram for his support throughout this project. We also thank Freedom Innovations, Össur, and Ottobock for donating the running-specific prostheses used in this study.

4 Chapter 3: Prosthetic model, but not stiffness or height, affects the metabolic cost of running for athletes with unilateral transtibial amputations

4.1 Abstract

Running-specific prostheses enable athletes with lower limb amputations to run by emulating the spring-like function of biological legs. Current prosthetic stiffness and height recommendations aim to mitigate kinematic asymmetries for athletes with unilateral transtibial amputations. However, it's unclear how different prosthetic configurations influence the biomechanics and metabolic costs of running. Consequently, we investigated how prosthetic model, stiffness, and height affect the biomechanics and metabolic costs of running. Ten athletes with unilateral transtibial amputations each performed fifteen running trials at 2.5 or 3.0 m/s while we measured ground reaction forces and metabolic rates. Athletes ran using three different prosthetic models with five different stiffness category and height combinations per model. Use of an Ottobock 1E90 Sprinter prosthesis reduced metabolic cost by 4.3% and 3.4% compared to use of Freedom Innovations Catapult (fixed effect (β)=-0.177; $p<0.001$) and Össur Flex-Run (β=-0.139; p=0.002) prostheses, respectively. Neither prosthetic stiffness ($p\geq0.180$) nor height (p=0.062) affected the metabolic cost of running. The metabolic cost of running was related to lower peak (β=0.649; p=0.001) and stance average (β=0.772; p=0.018) vertical ground reaction forces, prolonged ground contact times (β=-4.349; p=0.012), and decreased leg stiffness (β=0.071; $p<0.001$) averaged from both legs. Metabolic cost was reduced with more symmetric peak vertical ground reaction forces (β=0.007; p=0.003), but was unrelated to symmetric stride kinematics ($p\geq0.636$). Therefore, prosthetic recommendations based on stride kinematics do not necessarily minimize the metabolic cost of running. Instead, an optimal prosthetic model, which

improves overall biomechanics, minimizes the metabolic cost of running for athletes with unilateral transtibial amputations.

4.2 Introduction

Biological legs behave like linear springs during level-ground running [2, 3]. From initial ground contact through mid-stance, tensile forces elongate and store considerable mechanical energy in the elastic structures of the runner's stance leg (i.e. tendons and ligaments) [6, 53, 86-88]. Subsequently, the stored energy is released as the elastic structures recoil and help extend the leg throughout the second half of stance [6]. These stance phase running mechanics are well-characterized by a spring-mass model, which depicts the stance leg as a massless linear spring supporting a point mass that represents the runner's center of mass [2, 3, 35] (Fig. 4.1).

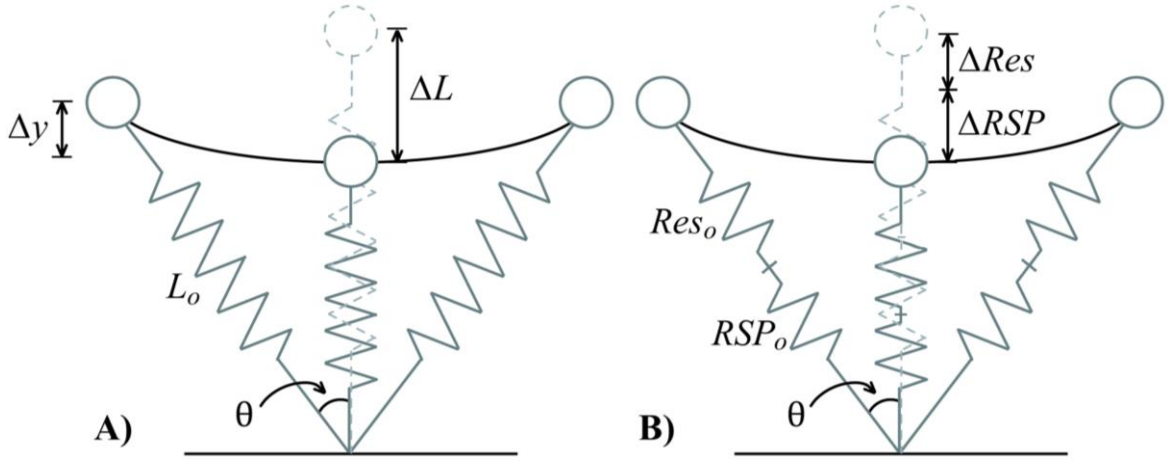

Figure 4.1. A) Illustration of the spring-mass model of running for non-amputees and the unaffected leg of athletes with a transtibial amputation. B) Illustration of a spring-mass model of running with an in-series leg spring for the affected leg of athletes with a transtibial amputation. Body mass is represented as a point mass (circle) and the touch-down angle is indicated by theta (θ). The stance leg is represented by a massless linear spring (A), or two in-series massless linear springs (B). The initial leg length (L_0) shortens (ΔL), as its vertical height (Δy) lowers during the stance phase of running. Modeled residual limb length (Res0) and prosthetic height (RSP_0) compress (ΔRes and ΔRSP) during the stance phase of running.

The spring-mass model well-characterizes running mechanics [2, 3, 35], but fails to explain the metabolic cost of running. Unlike the model's depiction, muscles produce force to

allow elastic energy storage, thus consuming metabolic energy [25, 68, 88]. Furthermore, biological legs do not recycle all of the mechanical energy needed to sustain running [53, 86], therefore leg muscles change length while producing force, which may constitute a portion of the metabolic cost of running [89]. Moreover, athletes modulate their muscular demands by changing running mechanics, accordingly affecting their metabolic cost. For instance, prolonging ground contact time and reducing stance average ground reaction force (GRF) magnitude during running yields more economical muscular force production [24-26, 67, 68]. Muscular force magnitude also depends on the leg's effective mechanical advantage [27, 62], which along with the rate of producing force (ground contact time), is associated with leg stiffness and step frequency [4] at a given running speed. Thus, by changing stride kinematics and kinetics, athletes may be able to minimize their metabolic cost of running, and improve their distance running performance [90].

The use of passive-elastic running-specific prostheses (RSPs), which emulate the spring-like function of biological legs, allow athletes with unilateral transtibial amputations to run. An RSP connects in-series to the residual limb via a prosthetic socket. RSPs emulate the mechanics of biological legs by storing and returning elastic energy during running [31]. Since the commercialization of RSPs in the 1980s, the athletic achievements of athletes with transtibial amputations have improved remarkably [57]. Ensuing prosthetic design iterations, such as the removal of the prosthetic "heel" component, have further enhanced running performance [57, 91]. Yet, despite the improved performance of athletes with transtibial amputations, the prescription of prosthetic model, stiffness, and height are subjective, and may not optimize running performance.

After prosthetists and athletes arbitrarily select a prosthetic model, which vary in design (1-3, 13), prosthetists recommend stiffness and height based on the manufacturer's recommendations and their own experience. Prosthetic stiffness recommendations are based on the mass of the athlete, with larger/heavier athletes prescribed stiffer RSPs [30, 43, 45, 58]. The recommended prosthetic stiffness (kN/m) for a given user body mass has yet to be standardized across prosthetic models [30], thus considerable variability exists among recommended prosthetic stiffness. Prosthetic height is recommended so that the affected leg length, which includes the RSP, is 2 to 5 cm longer than the unaffected leg length. In reality, affected leg length is set at the discretion of the prosthetist and athlete, and has been reported to range 0.3 to 8.0 cm taller than the unaffected leg [10]. Rather than using subjective prosthetic model, stiffness, and height recommendations that may not optimize the metabolic cost of running [30], we aim to determine whether prosthetic model, stiffness, and/or height affect the metabolic cost of running, and if so, we seek to determine the prosthetic configuration that minimizes metabolic cost, thus optimizing distance running performance [90].

Previous research of non-amputees indicates that reducing surface stiffness lowers the metabolic cost of running [92], therefore reducing prosthetic stiffness may lower the metabolic cost of running for athletes with unilateral transtibial amputations. While running, non-amputees adjust their leg stiffness to accommodate different surface stiffness so that the combination of their leg and the surface maintains a constant total stiffness [60, 61]. They adapt to complaint surfaces in part by better aligning their leg joints with the resultant GRF vector [83], thereby improving the effective mechanical advantage of their leg joints [27, 62]. Additionally, compliant elastic surfaces recycle mechanical energy [59], theoretically mitigating the required muscular work needed to sustain running velocity. Together, these biomechanical adaptations to

running on compliant surfaces have been related to a reduced metabolic cost of running [59, 92]. For example, Kerdok et al. [59] reported that a 12.5 fold decrease in surface stiffness reduced the metabolic cost of running 3.7 m/s by 12% [59]. Hence, reduced prosthetic stiffness compared to the manufacturer recommended stiffness may lower the metabolic cost of running for athletes with unilateral transtibial amputations due to decreased muscular work and improved residual limb stiffness (better effective mechanical advantage).

Prosthetic height may also influence the metabolic cost of running. Increased prosthetic height may prolong the affected leg's ground contact time [12, 13], enabling more economical force production [25, 78]. Alternatively, the effective mechanical advantage of the leg joints would worsen with invariant joint angles and taller prostheses. Nonetheless, it is unknown whether prosthetic height affects the metabolic cost of running for athletes with unilateral transtibial amputations.

Athletes with unilateral transtibial amputations exhibit asymmetric stride kinematics and kinetics [5, 11, 32, 34, 36, 44, 93-96], which are likely a consequence of the RSPs' inability to replicate biological lower leg function. Accordingly, prosthetic manufacturers and prosthetists recommend stiffness and height configurations that mitigate stride kinematic asymmetries between the legs of athletes with unilateral transtibial amputations [43, 45, 58]. In line with these recommendations, a preliminary study by Wilson et al. [34] reported that changing prosthetic stiffness and height altered the stride kinematic and kinetic asymmetry for two athletes with unilateral transtibial amputations during running. Perhaps the metabolic cost of running is correlated with the severity of stride kinematic and/or kinetic asymmetry. Previous studies have reported positive associations between stride kinematic and kinetics asymmetries and the metabolic cost of walking for young healthy subjects [98, 99], and for individuals with unilateral

transtibial amputations [100]. On the other hand, Mattes et al. [101] reported that the metabolic cost of using passive prostheses during walking for individuals with unilateral transtibial amputations is greater when lower limb mass and moments of inertia are symmetric between legs. Yet, it is uncertain if these walking studies translate to running. Seminati et al. [102] reported that non-amputees with slightly asymmetric lower limbs run with more pronounced stride kinematic asymmetries while consuming metabolic energy at the same rate as non-amputees with symmetric lower limbs and biomechanics. Additionally, Brown et al. [56] reported that athletes with unilateral transtibial amputations (with presumably asymmetric biomechanics) consume oxygen at similar rates as age and fitness matched non-amputees (with presumably symmetric biomechanics) across running speeds; indicating that asymmetric running biomechanics may not exacerbate the metabolic cost of running for athletes with unilateral transtibial amputations. Due to the current prescription of RSPs, which aim to minimize kinematic asymmetries for athletes with unilateral transtibial amputations, we seek to investigate how different prosthetic configurations affect the stride kinematic and kinetic asymmetries of athletes with unilateral transtibial amputations, and whether these asymmetries are associated with the metabolic cost of running.

The purpose of our study was to determine the prosthetic model, stiffness, and height configuration that minimizes the metabolic cost of running for athletes with unilateral transtibial amputations, thus optimizing distance running performance [90]. To explain the potential effects of prosthetic configuration on metabolic cost, we also determined the associations between prosthetic model, stiffness, and height on the elicited biomechanics (overall and asymmetric). We also investigated the relationships between running biomechanics (overall and asymmetric) and metabolic cost. We hypothesized that the metabolic cost of running for athletes with

unilateral transtibial amputations would be minimized when they used an RSP less stiff than the respective manufacturer's recommended stiffness category and when they used an RSP set at the manufacturer/prosthetist recommended height. We hypothesized that leg stiffness would be invariant across different prosthetic stiffness, thus residual limb stiffness would be inversely correlated with prosthetic stiffness. We also hypothesized that the metabolic cost of running for athletes with unilateral transtibial amputations would be correlated with overall and asymmetric biomechanics. Lastly, we hypothesized that the prosthetic model, stiffness, and height that minimize metabolic cost would be associated with the biomechanical variables that optimize the metabolic cost of running. Due to their influence on the metabolic cost of running, we investigated the following biomechanical variables: peak and stance average vertical GRFs [25, 66, 68], peak horizontal GRFs [24, 67], ground contact time [25, 68], stride frequency [37, 38, 69], and leg stiffness [4, 37, 38, 69].

4.3 Methods

4.3.1 Participants

Ten athletes with a unilateral transtibial amputation (seven males and three females) participated (Table 4.1). Each participant had at least one year of experience running using a passive-elastic RSP and gave informed consent according to our protocol, which was approved by the Colorado Multiple Institutional Review Board and the USAMRMC Office of Research Protection, Human Research Protection Office.

Age	33.4 ± 6.1 yrs
Height	1.77 ± 0.08 m
Body mass	76.1 ± 14.1 kg
UL leg length	0.95 ± 0.05 m
Rec Catapult AL length	1.01 ± 0.07 m*
Rec Flex-Run AL length	1.00 ± 0.07 m*
Rec 1E90 Sprinter AL length	0.98 ± 0.07 m
Standing metabolic rate	1.3 ± 0.1 W/kg

Table 4.1. Average (±SD) anthropometric measurements and standing metabolic rates of athletes with unilateral transtibial amputations (7M, 3F). *indicates a significant difference between recommended (Rec) affected leg (AL) and unaffected leg (UL) lengths ($p<0.05$), following a Bonferroni corrected paired two-tailed t-test.

4.3.2 Protocol

Initially, each participant completed an alignment and accommodation session, which entailed a certified prosthetist aligning each participant with three different prosthetic models (Freedom Innovations Catapult FX6, Irvine, CA, USA; Össur Flex-Run, Reykjavik, Iceland; Ottobock 1E90 Sprinter, Duderstadt, Germany) at each manufacturer's recommended stiffness category and ±1 stiffness category, and at each manufacturer's recommended prosthetic height and ±2 cm. The Catapult and Flex-Run prostheses are "C" shaped and attach distally to the socket via a connective aluminum pylon (Fig. 4.2). The 1E90 Sprinter prosthesis is "J" shaped and mounts to the posterior wall of the socket. After establishing the height for a J-shaped prosthesis, the device is typically bolted directly to the socket. For this study, we constructed a custom aluminum height adjustment bracket that was bolted to an athlete's socket, allowing us to secure the 1E90 Sprinter prosthesis to the socket, alter prosthetic height between trials, while preserving the RSP (Fig. 4.2).

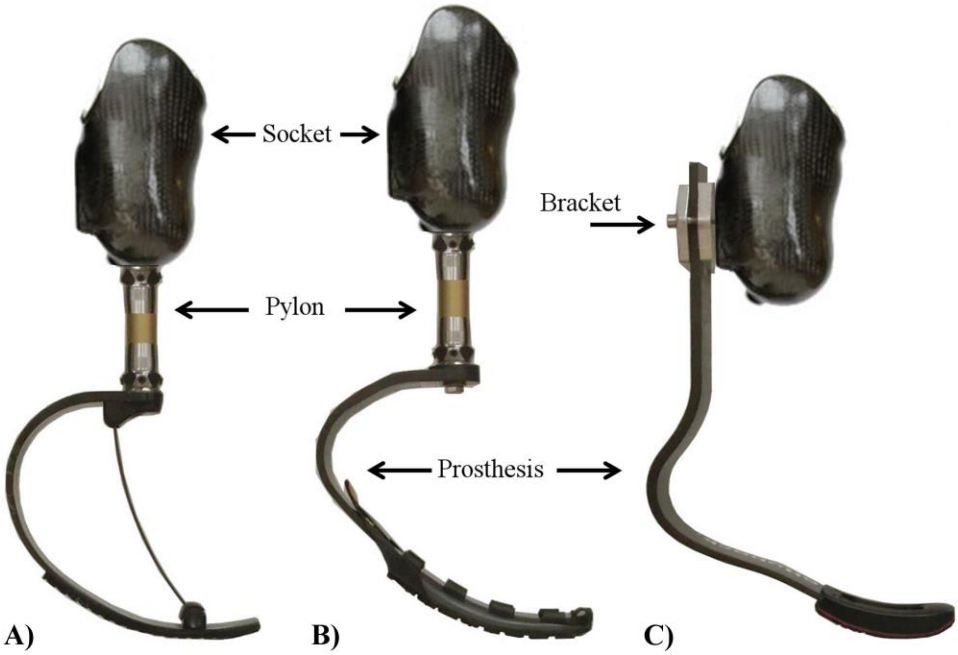

Figure 4.2. A) Freedom Innovations Catapult FX6 prosthesis (C-shaped) at a representative recommended height, B) Össur Flex-Run prosthesis (C-shaped) at a representative height of +2 cm, and C) Ottobock 1E90 Sprinter prosthesis (J-shaped) at a representative height of -2 cm. The C-shaped prostheses are connected beneath the socket via an aluminum pylon, and the J-shaped prosthesis is connected behind the socket via a custom aluminum bracket.

During the accommodation session, participants ran using each prosthetic model on a treadmill at self-selected speeds until both the participant and prosthetist were satisfied with the recommended height and the alignment at each height. Generally, athletes accommodated to each prosthetic model at the recommended stiffness category and height. For the C-shaped RSPs, the athletes ran at all three heights (recommended and ±2 cm) to determine proper alignment for each connective pylon. For the J-shaped RSP, the alignment of the custom bracket that connected the RSP to the socket remained unaltered across height conditions, thus athletes did not typically accommodate to the non-recommended heights prior to the experimental sessions.

On subsequent days, participants performed a five minute standing trial (using their personal walking prosthesis) and up to six, five minute running trials per session with at least

five minutes of rest between trials. Participants ran on a 3D force-measuring treadmill (Treadmetrix, Park City, UT, USA) at 3 m/s. If a participant was unable to maintain primarily oxidative metabolism at 3 m/s, indicated by a respiratory exchange ratio >1.0, running speed was reduced to 2.5 m/s. All running trials for a participant were performed at the same speed; therefore, if running speed was reduced to 2.5 m/s, all of the trials for the respective participant were (re)tested at 2.5 m/s.

Each participant ran using 15 different combinations of prosthetic model, stiffness category, and height. Initially, participants ran using each prosthetic model at three different stiffness categories (recommended and ±1) and the recommended affected leg length (nine trials, three per prosthetic model). The stiffness category for each prosthetic model that elicited the lowest net metabolic cost of transport (CoT in J/kg/m) was deemed optimal. Subsequently, participants ran using the optimal stiffness category of each prosthetic model at two additional affected leg lengths (±2 cm) (six additional trials). We randomized the trial order beginning with the nine prosthetic model and stiffness category combinations at the recommended affected leg length. Once a participant completed trials at all three stiffness categories for a prosthetic model at the recommended affected leg length, the height alteration trials for the respective prosthetic model at the optimal stiffness category were randomly inserted into the trial order. We tested each participant at the same time of day for all of their sessions to minimize any potential day-to-day variability.

4.3.3 Protocol

The recommended prosthetic stiffness (kN/m) for each prosthetic model varies [30]. Accordingly, we evaluated the influence of each manufacturer's recommended prosthetic stiffness category, as well as the influence of actual prosthetic stiffness (kN/m) on the net CoT

during running using recently published data from our lab [30]. Concisely, we calculated prosthetic stiffness using the mean peak vertical GRF magnitude measured from the affected leg during each trial (present study) and estimated prosthetic displacement using the force-displacement equations from Beck et al. [30]. Subsequently, we divided the measured peak GRF magnitude by the respective RSP displacements to yield prosthetic stiffness.

4.3.4 Biomechanics

Participants ran on a 3D force-measuring treadmill. We collected and analyzed the vertical and anterior-posterior components of the ground reaction forces (GRFs) during the last two minutes of each trial. We collected GRFs at 1000 Hz and filtered them using a 4th order low pass Butterworth filter with a 30 Hz cutoff. We used the filtered data to calculate peak and stance average vertical GRFs, peak horizontal (braking and propulsive) GRFs, in addition to ground contact time, step frequency, and leg stiffness values from 10 consecutive strides (10 affected leg steps and 10 unaffected leg steps) with a custom MATLAB script (Mathworks Inc., Natick, MA, USA). To detect periods of ground contact, we set the vertical GRF threshold to 1% of participant body weight.

Leg stiffness (k_{leg}) was computed as the quotient of peak vertical GRF (F_{peak}) and the maximum compression of the leg spring (ΔL) during ground contact (Fig. 4.1), as per Farley et al. [2].

$$k_{leg} = \frac{F_{peak}}{\Delta L} \tag{4.1}$$

To calculate the maximum compression of the leg spring (ΔL), we measured initial unaffected leg length (L_0) from the greater trochanter to the floor during standing, and affected leg length (L_0) as the distance from the greater trochanter to the distal end of the unloaded RSP [9]. Next,

we used initial leg lengths to calculate theta (θ), which is the angle of the leg spring at initial ground contact relative to vertical.

$$\theta = sin^{-1}(\frac{v\ t_c}{2\ L_0}) \tag{4.2}$$

Mathematically, theta (θ) equals half the angle swept by the stance leg, as determined from running velocity (v), ground contact time (t_c), and initial leg length (L_0). The maximum stance leg spring compression (ΔL) was calculated using equation 4.3,

$$\Delta L = \Delta y + L_0(1 - \cos\theta) \tag{4.3}$$

which incorporates the peak vertical displacement of the center of mass during ground contact (Δy), calculated by twice integrating the vertical acceleration of the center of mass with respect to time [72]. The instantaneous vertical acceleration of the center of mass was calculated by subtracting the participant's body weight from the vertical GRF magnitude (net force), and dividing by body mass [72].

Since biological legs and RSPs act as relatively linear springs [2, 30, 103, 104], we modeled the affected leg stiffness as two in-series linear springs comprised of the RSP and residual limb (Fig. 4.1; Equation 4.4).

$$\frac{1}{k_{leg}} = \frac{1}{k_{RSP}} + \frac{1}{k_{res}} \tag{4.4}$$

Thus, we used the measured leg stiffness (k_{leg}) and the calculated prosthetic stiffness (k_{RSP}) to solve for the residual limb stiffness (k_{res}) during running.

To assess inter-limb symmetry, we used the absolute value of the symmetry index [34, 105, 106] expressed as a percentage (Equation 4.5). Taking the absolute value of the symmetry index is necessary to discern symmetry from asymmetry using linear statistical models. Perfect inter-limb symmetry is equal to zero percent.

$$\left|\frac{UL - AL}{0.5\ (UL + AL)}\right| \times 100 \tag{4.5}$$

Due to the potential association between RSP mechanical energy return and the metabolic cost of running, we calculated absolute mechanical energy return per affected leg step ($\dot{E}_{step}$),

$$\dot{E}_{step} = \frac{1}{2} k_{RSP} (\Delta d)^2 (1 - Hyst_{RSP}/100) \tag{4.6}$$

determined from prosthetic stiffness (k_{RSP}), peak prosthetic displacement (Δd), and percent prosthetic hysteresis ($Hyst_{RSP}$) [30]. Next, we divided absolute mechanical energy return ($\dot{E}_{RSP}$) by user body mass (m) and stride length (L_{stride}) to calculate normalized mechanical energy return ($\dot{E}_{RSP}$) per stride (J/kg/m).

$$\dot{E}_{RSP} = \frac{\dot{E}_{step}}{m\ (L_{stride})} \tag{4.7}$$

4.3.5 Metabolic Cost of Transport

We instructed participants to fast for at least three hours prior to testing. We measured each participant's rate of oxygen consumption ($\dot{V}O_2$) and carbon dioxide production ($\dot{V}CO_2$) using open-circuit expired gas analysis (TrueOne 2400, ParvoMedic, Sandy, UT, USA) throughout each trial and averaged these rates during the last two minutes of each trial to calculate steady-state metabolic power (W) using a standard equation [71]. Then, we subtracted the average metabolic power consumed during standing of the corresponding day from each running trial to yield net metabolic power. We normalized net metabolic power by the mass of each participant, which included running gear (e.g. RSP, socket, shoe, and clothes) for each respective trial. Finally, to combine data from 3.0 and 2.5 m/s, we divided net metabolic power by running velocity to calculate the net metabolic cost of transport (CoT) in J/kg/m.

4.3.6 Statistical Analyses

We used a linear mixed model to evaluate the effects of using different prosthetic models, stiffness categories, and heights on net CoT. We used a second linear mixed model to evaluate the effects of using different prosthetic models, actual prosthetic stiffness (kN/m), and heights on net CoT. We used linear regressions to assess the independent relationships between affected leg stiffness, prosthetic stiffness, and residual limb stiffness. We also tested whether affected and unaffected leg stiffness are correlated, and if net CoT is influenced by the absolute RSP mechanical energy return per step and/or per unit distance traveled with linear regressions.

Four participants ran at 3.0 m/s and six ran at 2.5 m/s. For this reason, we used additional linear mixed models to control for speed while independently testing the associations between overall (affected leg and unaffected leg averaged) and asymmetric GRFs (stance average vertical GRF, peak vertical GRF, and peak horizontal braking and propulsive GRFs), stride kinematics (ground contact time and step frequency), and leg stiffness on net CoT. We also performed a linear mixed model to evaluate the relationship between prosthetic model, stiffness, and height on the overall and asymmetric biomechanical variables that influence net CoT.

We used paired two-tailed t-tests to assess leg length discrepancies between affected and unaffected legs and implemented Bonferroni corrections when appropriate. For the linear mixed models and linear regressions, we report the fixed effect (β) from each statistically significant association (dependent variable = β independent variable + intercept). We tested all potential independent variable interactions with linear mixed models. If independent variables or interactions were non-significant, they were dropped from the model for the interpretation of the significant variables and interactions. We set the level of significance at α=0.05, and performed all statistical analyses using R-studio software (Boston, MA, USA).

4.4 Results

All prosthetic models were set at statistically similar recommended heights ($p \geq 0.053$) (Table 4.1). The recommended affected leg lengths were statistically longer than the corresponding unaffected leg lengths when using the Catapult (1.01 ± 0.07 m; $p<0.001$) and Flex-Run prostheses (1.00 ± 0.07 m; $p=0.001$), but not when using the 1E90 Sprinter prosthesis (0.98 ± 0.07 m; Bonferroni corrected $p=0.080$). Furthermore, our highest stiffness category Flex-Run prosthesis was the manufacturer recommended stiffness category for two participants. Hence, these participants were tested at the stiffness categories of recommended, -1, and -2 with the Flex-Run prosthesis. Due to residual leg lengths and component heights, we were unable to perfectly match prosthetic heights at -2 cm for five participants. Therefore, the actual prosthetic heights for the shortest condition for five participants were -1.2, -1.3, -2.6, -0.5, and -1.2 cm with the C-shaped RSPs. We accounted for these disparities with our statistical analyses. Additionally, due to RSP component and logistical limitations, we were unable to complete four trials for three different participants; hence our results include 146 trials (Table 4.2) rather than 150 (15 trials per 10 participants).

		Catapult			**Flex-Run**			**1E90 Sprinter**		
		-1 Cat	**Rec Cat**	**+1 Cat**	**-1 Cat**	**Rec Cat**	**+1 Cat**	**-1 Cat**	**Rec Cat**	**+1 Cat**
Number of Participants	**+2 cm**	5	2	2	4	5	1	5	2	2
	Rec Ht	10	10	10	10	10	8	10	10	10
	-2 cm	5	2	2	4	4	1	6	2	2

Table 4.2. The number of participants for each prosthetic model, at recommended (Rec) and ±1 stiffness categories, and Rec and ±2 cm height (Ht) configurations.

While controlling for covariates (i.e. controlling for two of the following while assessing the third: prosthetic model, stiffness, and height), the net CoT for athletes with unilateral transtibial amputations was independent of prosthetic stiffness category ($p=0.180$), actual prosthetic stiffness ($p=0.327$) (Fig. 4.3), and height ($p=0.062$). In contrast, prosthetic model had a significant effect on net CoT. Use of a 1E90 Sprinter prosthesis resulted in 4.3% and 3.4% lower net CoT compared to use of the Catapult ($\beta=-0.177$; $p<0.001$) and Flex-Run ($\beta=-0.139$; $p=0.002$) prostheses, respectively. Net CoT was similar with use of the Catapult versus Flex-Run prosthesis ($p=0.393$) (Fig. 4.3). There were no prosthetic model, stiffness, or height interactions affecting net CoT ($p\geq0.151$).

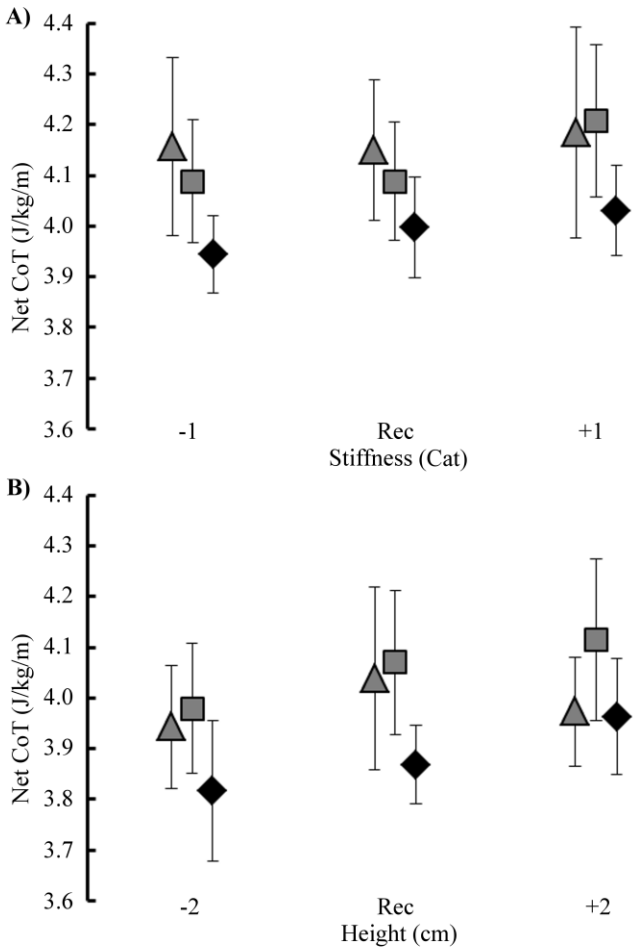

Figure 4.3. The average (±SE) net cost of transport (CoT) across prosthetic stiffness categories (Cat) for each prosthetic model. B) The average (±SE) net CoT across recommended (Rec) and ±2 cm prosthetic height alterations. Triangles represent Catapult prostheses, squares indicate Flex-Run prostheses, and diamonds signify 1E90 Sprinter prostheses. Symbols are offset for visual representation. See table 2 for sample size in visual depiction. We performed linear mixed models from all of our collected data to determine that there was no effect of stiffness category ($p=0.180$) or height ($p=0.062$) on net CoT, and that net CoT was reduced when participants used the 1E90 Sprinter prosthesis compared to using the Catapult ($p<0.001$) or Flex-Run ($p=0.002$) prosthesis.

The affected leg stiffness of athletes with unilateral transtibial amputations was positively correlated with prosthetic stiffness ($p<0.001$; $R^2=0.708$; affected leg stiffness = 0.558 prosthetic stiffness + 0.814) (Fig. 4.4) and residual limb stiffness ($p<0.001$; $R^2=0.728$; affected leg stiffness = 0.196 residual limb stiffness + 6.777). Increased prosthetic stiffness was associated with

increased residual limb stiffness ($p<0.001$; $R^2=0.212$; Residual limb stiffness = 0.159 prosthetic stiffness + 17.336) (Fig. 4). Unaffected leg stiffness was positively correlated with affected leg stiffness ($p<0.001$; $R^2=0.509$; unaffected leg stiffness = 0.693 affected leg stiffness + 5.270), and prosthetic stiffness ($p<0.001$; $R^2=0.398$; unaffected leg stiffness = 0.398 prosthetic stiffness + 5.583).

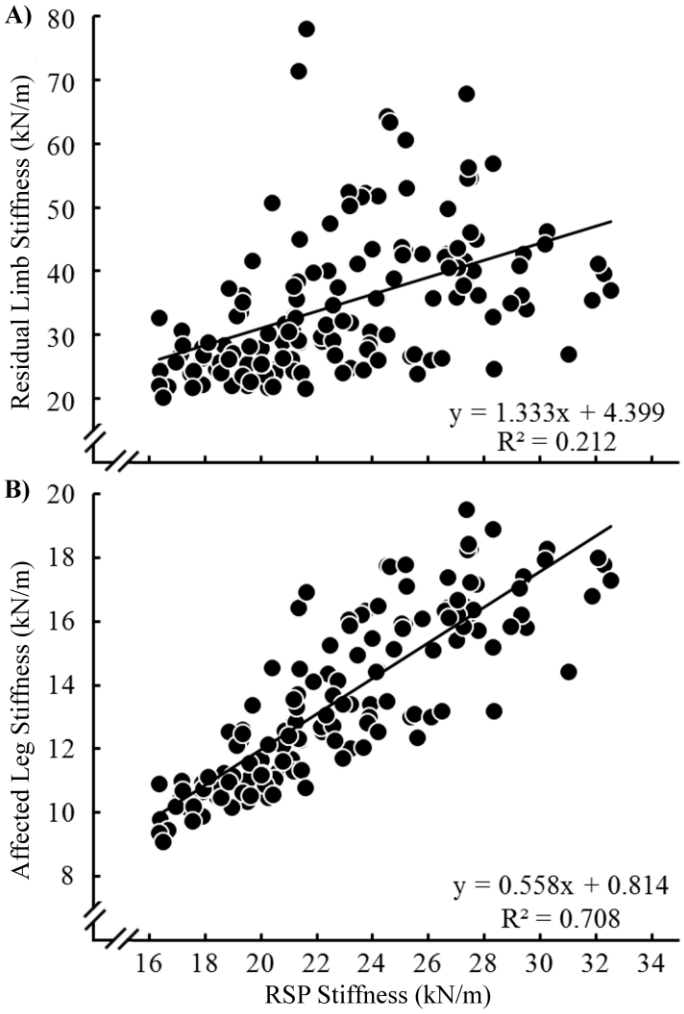

Figure 4.4. A) Residual limb stiffness compared to running-specific prosthetic (RSP) stiffness ($p<0.001$), and B) Affected leg stiffness compared to prosthetic stiffness. We performed linear regressions across all collected data to determine significant correlations between A) residual limb stiffness and RSP stiffness ($p<0.001$), as well as between B) affected leg stiffness and RSP stiffness ($p<0.001$).

The majority of overall (affected leg and unaffected leg average) biomechanical parameters affected net CoT. Namely, for every 0.1 times body weight reduction in peak (β=0.649; p=0.001) and stance average vertical GRF (β=0.772; p=0.018), net CoT decreased 2.6%. For every 0.1 second increase in ground contact time, net CoT decreased 8.4% (β=-0.435; p=0.012). For every 1 kN/m reduction in leg stiffness, net CoT decreased 2.3% (β=0.071; p<0.001). Net CoT was not affected by peak horizontal braking (p=0.502) or propulsive (p=0.899) GRFs, nor step frequency (p=0.773). Additionally, neither the amount of RSP mechanical energy returned per step nor per unit distance traveled influenced net CoT ($p \geq 0.060$).

Of the investigated stride kinematic and kinetic asymmetries, net CoT was only related to peak vertical GRF asymmetry (β=0.007; p=0.003) (Fig. 4.5). Across all prosthetic configurations, for every 10.0% reduction in peak vertical GRF asymmetry, net CoT decreased 1.9%. For perspective, if the mean elicited peak vertical GRF asymmetry (15.7%) between the affected and unaffected legs became perfectly symmetric (0.0%), net CoT would decrease 3.0%. The elicited net CoT was independent of the following asymmetries: stance average vertical GRF (p=0.410), peak braking (p=0.119) and peak propulsive (p=0.917) horizontal GRF, ground contact time (p=0.867), step frequency (p=0.754), and leg stiffness (p=0.636) (Table 4.3 and Table 4.4). Within our protocol, running speed did not alter the influence of biomechanics on metabolic cost ($p \geq 0.170$).

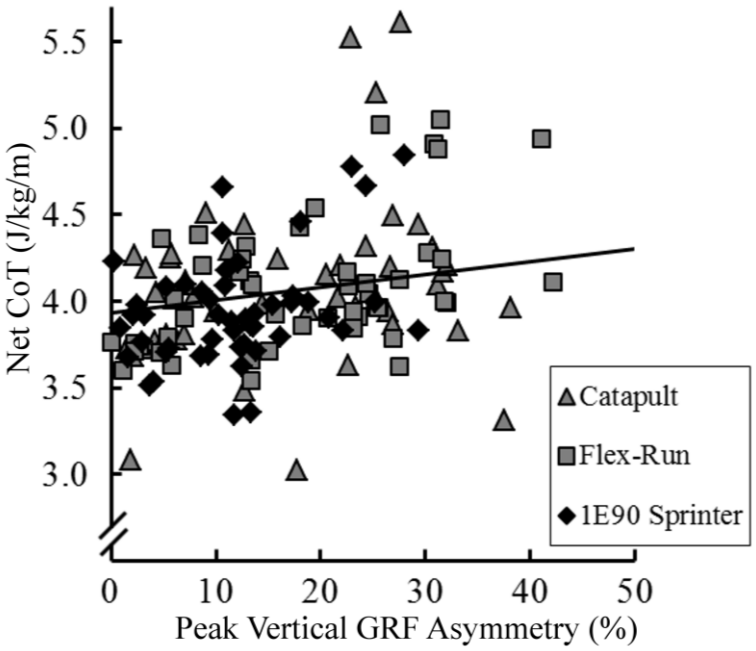

Figure 4.5. Individual net cost of transport (CoT) values plotted as a function of absolute peak vertical ground reaction force (GRF) asymmetry. Triangles represent Catapult prostheses, squares indicate Flex-Run prostheses, and diamonds signify 1E90 Sprinter prostheses. Using all of our collected data, we performed a linear mixed model to determine that reducing peak vertical GRF asymmetry lowered net CoT (net CoT = 0.007 peak vertical GRF asymmetry + 3.933).

	Catapult			**Flex-Run**			**1E90 Sprinter**		
Biomechanics	**-1 Cat**	**Rec Cat**	**+1 Cat**	**-1 Cat**	**Rec Cat**	**+1 Cat**	**-1 Cat**	**Rec Cat**	**+1 Cat**
Peak vGRF (BW)	2.40	2.39	2.40	2.38	2.40	2.43	2.37	2.37	2.40
Avg vGRF (BW)*	1.32	1.34	1.35	1.38	1.39	1.41	1.34	1.35	1.39
$\mathbf{t_c}$ (sec)*	0.27	0.26	0.25	0.25	0.25	0.24	0.27	0.26	0.25
$\mathbf{k_{leg}}$ (kN/m)*	14.0	14.4	15.0	14.3	14.5	14.3	13.2	13.6	14.5
Peak vGRF (SI)	15.0	18.4	18.8	14.6	16.9	17.6	9.2	10.3	13.1

Table 4.3. The biomechanical variables that influenced net CoT: overall peak vertical ground reaction force (vGRF), stance average vGRF (Avg vGRF), ground contact time (tc), leg stiffness (kleg), and peak vGRF asymmetry at each stiffness category (Recommended (Rec) and ±1 category) for each prosthetic model at the recommended height. "BW" indicates body weight, and "SI" indicates symmetry index as a percent. * indicates significant effect of prosthetic stiffness (kN/m) on the biomechanical variable across all of our data using linear mixed model analyses.

Biomechanics	Catapult			Flex-Run			1E90 Sprinter		
	-2 cm	Rec Ht	+2 cm	-2 cm	Rec Ht	+2 cm	-2 cm	Rec Ht	+2 cm
Peak vGRF (BW)	2.40	2.40	2.36	2.51	2.38	2.37	2.35	2.38	2.38
Avg vGRF (BW)	1.33	1.33	1.30	1.45	1.38	1.36	1.33	1.36	1.34
$\mathbf{t_c}$ (sec)	0.26	0.26	0.27	0.25	0.25	0.26	0.27	0.26	0.27
$\mathbf{k_{leg}}$ (kN/m)	14.6	14.4	14.3	15.3	14.5	14.4	13.2	13.8	13.4
Peak vGRF (SI)*	8.8	17.4	23.8	13.8	16.6	27.1	8.9	10.8	19.0

Table 4.4. The biomechanical variables that influenced net CoT: overall peak vertical ground reaction force (vGRF), stance average vGRF (Avg vGRF), ground contact time (tc), leg stiffness (kleg), and peak vGRF asymmetry at each prosthetic height (Ht) (Recommended (Rec) and ±2 cm) for every prosthetic model across stiffness categories. "BW" indicates body weight, and "SI" indicates symmetry index. * indicates significant effect of prosthetic height on biomechanical variable across all our data using linear mixed model analyses.

Increased prosthetic stiffness (kN/m) resulted in greater stance average vertical GRFs (β=0.007; $p<0.001$), shorter ground contact times (β=-0.002; $p<0.001$) (Table 4.3 and Fig. 4.6), and greater leg stiffness (β=0.194; $p<0.001$) (Table 4.3). Increased prosthetic height resulted in more asymmetric peak vertical GRFs (β=4.062; $p<0.001$) (Table 4.4 and Fig. 4.7). The 1E90 Sprinter prosthesis resulted in greater stance average vertical GRF compared to the Catapult (β=0.033; p=0.001) but not Flex-Run prosthesis (p=0.137), longer ground contact time (β=0.008; $p<0.001$) compared to the Flex-Run but not the Catapult (p=0.395) prosthesis, and lower leg stiffness compared to both C-shaped RSPs ($\beta \geq -0.556$; $p<0.001$). The 1E90 Sprinter prosthesis resulted in 8.3 to 8.7% (symmetry index percentage) more symmetric peak vertical GRFs compared to the use of the C-shaped RSPs ($p<0.001$) (Fig. 4.6 and Fig. 4.7). Neither prosthetic model, stiffness, nor height affected overall peak vertical GRF magnitude ($p \geq 0.050$). Prosthetic stiffness was independent of peak vertical GRF asymmetry (p=0.108) (Table 4.3 and Fig. 4.6), and

prosthetic height was independent of stance average vertical GRF (p=0.959), ground contact time (p=0.353), and leg stiffness (p=0.348).

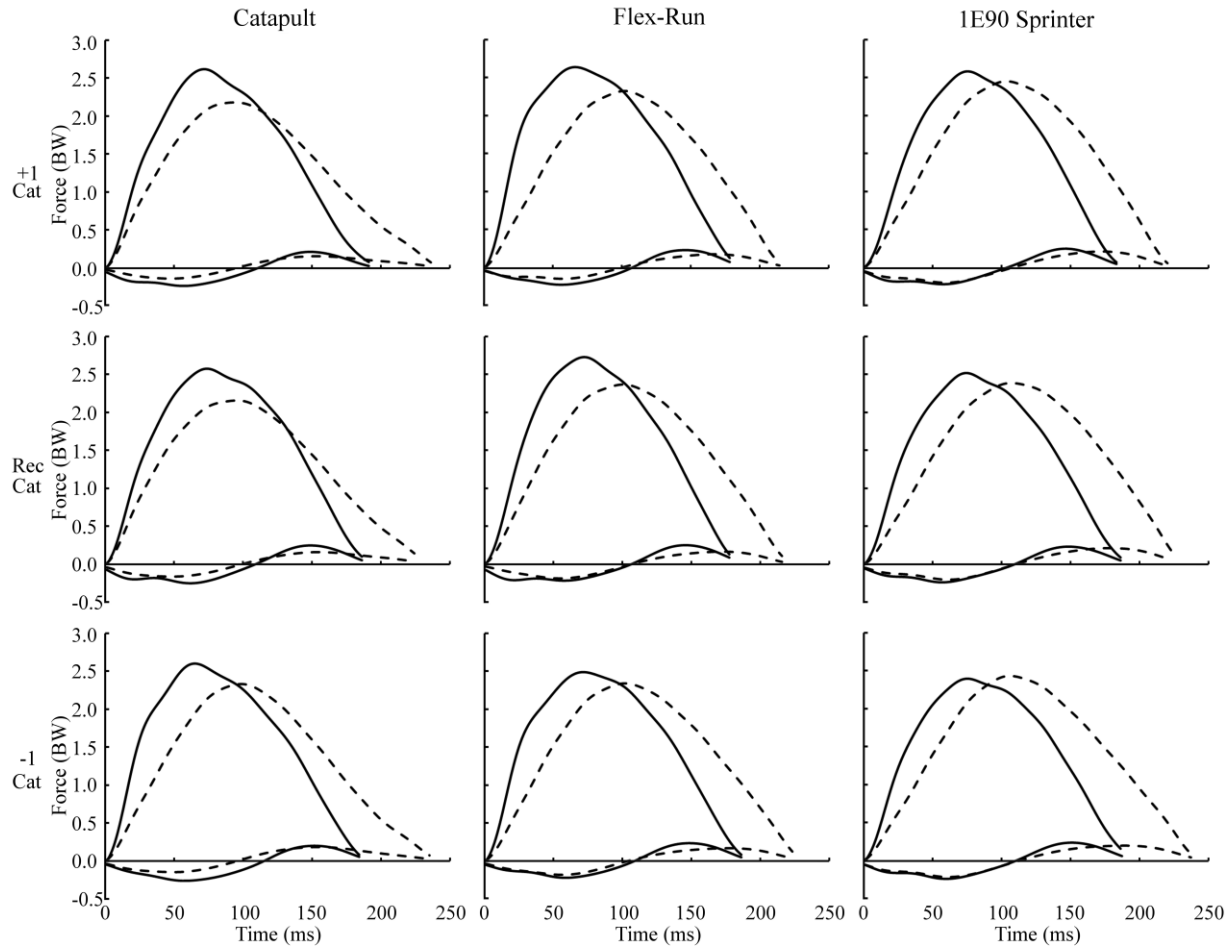

Figure 4.6. Mean vertical and horizontal ground reaction forces (GRFs) from ten consecutive affected (dashed line) and unaffected (solid line) leg steps from a representative participant running at 3 m/s. Columns left to right indicate the Freedom Innovations Catapult FX6, Össur Flex-Run, and Ottobock 1E90 Sprinter prostheses. Rows top to bottom indicate prosthetic stiffness category: -1, recommended (Rec), and +1.

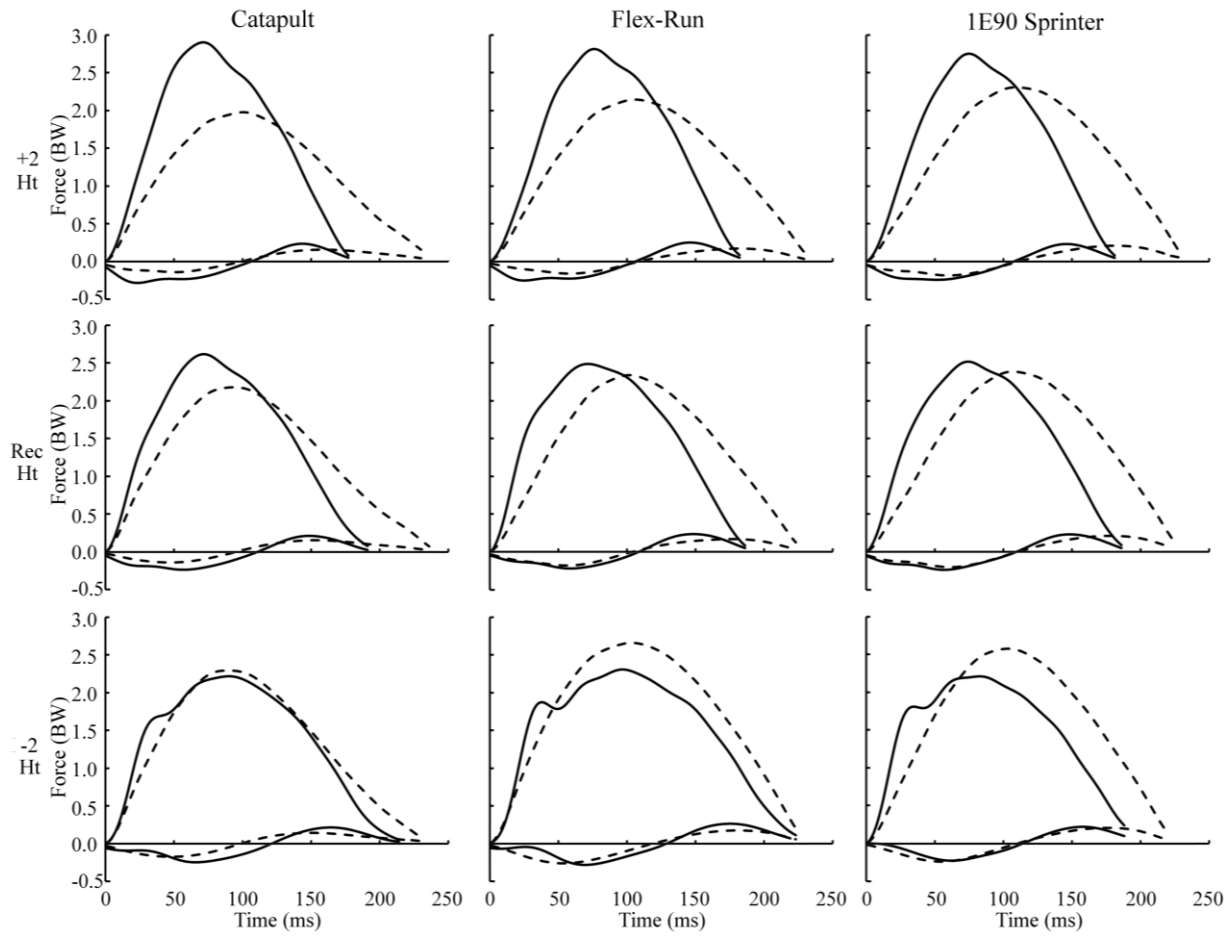

Figure 4.7 Mean vertical and horizontal ground reaction forces (GRFs) from ten consecutive affected (dashed line) and unaffected (solid line) leg steps from a representative participant running at 3 m/s. Columns left to right indicate the Freedom Innovations Catapult FX6, Össur Flex-Run, and Ottobock 1E90 Sprinter prostheses. Rows top to bottom indicate prosthetic height: +2 cm, recommended (Rec), and -2 cm.

4.5 Discussion

Within the study's parameters, neither prosthetic stiffness nor height affected the net CoT during running for athletes with unilateral transtibial amputations; therefore, we reject our initial hypothesis. Unlike prosthetic stiffness and height, net CoT was affected by prosthetic model. The use of the J-shaped 1E90 Sprinter prosthesis lowered the metabolic cost of running compared to the use of the C-shaped Catapult and Flex-Run prostheses; the 1E90 Sprinter prosthesis was metabolically optimal for 9 out of 10 athletes. These results occurred despite the heavier custom

bracket used for the 1E90 Sprinter prosthesis compared to the typical J-shaped RSP configuration. Rather than bolting the prosthesis directly to the socket, we used a relatively large bracket (~400 g) to connect the RSP to the socket (Fig. 4.2). As a result, the combined mass of the 1E90 Sprinter prosthesis and attachment was ~425 g greater than that of the Catapult and Flex-Run prostheses. Previous non-amputee running studies demonstrate that adding 100 g to each foot increases the metabolic cost of running by ~1% [75, 76], indicating that our testing configuration for the 1E90 Sprinter prosthesis may have artificially increased the metabolic cost of running. Thus, the lower metabolic cost while using the J-shaped 1E90 Sprinter prosthesis versus the use of C-shaped prostheses would have likely been further reduced through the use of a typical, light weight, configuration.

The best prosthetic configuration (model, stiffness, and height combination) for each participant resulted in an 18.9% lower net CoT compared to the worst configuration (paired t-test; $p<0.001$; 3.65 ± 0.37 vs. 4.50 ± 0.45 J/kg/m). Our results coincide with previous research demonstrating the sensitivity of the metabolic cost of running to prosthetic model for athletes with unilateral transtibial amputations [91]. In 1999, Hsu et al. [91] reported that athletes with unilateral transtibial amputations consumed oxygen at 8 – 11% greater rates while running at 2.01 – 2.45 m/s using a solid-ankle cushioned heel (SACH) prosthesis compared to using a passive-elastic Re-Flex Vertical Shock Pylon prosthesis. The SACH prosthesis uses a static, rigid design whereas the Re-Flex Vertical Shock Pylon prosthesis uses a vertical leaf spring and piston-cylinder pylon design [91]. In 2009, Brown et al. [56] reported that athletes with transtibial amputations consumed 14% less oxygen while running at 2.23 m/s using RSPs (the athlete's personal RSP), similar to those used in the present study, compared to using relatively rigid passive-elastic walking prostheses that have an incorporated "heel" component.

Remarkably, the most and least economical RSPs for each participant in the present study elicited a wider range of metabolic costs compared to the previous research that compared the use of RSPs to walking prostheses [56, 91]. This may be due to inconsistent sagittal plane alignment, the use of different sockets, and/or the faster running speeds used in the present study compared to previous investigations [56, 91]. Altogether, prosthetic model strongly influences the metabolic cost of running for athletes with unilateral transtibial amputations.

We reject our second hypothesis because residual limb stiffness was positively correlated with prosthetic stiffness (Fig. 4.4). This positive correlation accentuated the leg stiffness changes of our participants with altered in-series (prosthetic) stiffness, contrasting that of non-amputee runners [60, 61]. Consequently, running mechanics and center of mass dynamics of athletes with unilateral transtibial amputations may be affected by the in-series (RSP or surface) stiffness (Table 4.3 and Fig. 4.6). The residual limb stiffness of athletes with bilateral transtibial amputations are also positively correlated with prosthetic stiffness [9], indicating that the absence of biological lower legs may yield novel biomechanical adaptations to in-series stiffness changes.

Due to the effects of different biomechanical parameters on the metabolic cost of running, we accept our third hypothesis. Regarding overall biomechanics, the metabolic cost of running was reduced with lower peak and stance average vertical GRFs, longer ground contact times, and decreased leg stiffness (Table 4.3 and Table 4.4). Thus, it is likely that the optimal combination of these biomechanical variables minimize the metabolic cost of running for athletes with unilateral transtibial amputations. For instance, in our study, running with compliant leg springs resulted in prolonged ground contact time and decreased stance average vertical GRFs. Longer ground contact time extends the duration that athletes are able to generate

force on the ground, enabling the recruitment of slower, more economical muscle fibers [25, 78]. Lower stance average vertical GRFs reduce the number of active, ATP consuming actin-myosin cross-bridges needed to sustain running [25, 78]. However, reduced leg stiffness also decreases the effective mechanical advantage of the leg joints. Thus, there is likely an optimal leg stiffness that elicits the ideal combination of the rate and magnitude of muscular force production. Furthermore, reduced peak vertical GRF asymmetries resulted in an improved metabolic cost of running for athletes with unilateral transtibial amputations. Within the range of observed asymmetries, peak vertical GRF asymmetry was the only such parameter that changed net CoT. Six of the seven observed asymmetries had no effect on the metabolic cost of running, including all of the measured stride kinematics. Therefore, current prosthetic prescriptions, which aim to mitigate stride kinematic asymmetries (1-3), may not necessarily minimize the metabolic cost of running. Rather, prosthetic prescriptions focused on both legs' biomechanics may optimize the distance running performance of athletes with unilateral transtibial amputations.

Our last hypothesis was supported because the J-shaped prosthetic model that minimized the metabolic cost of running for athletes with unilateral transtibial amputations was associated with reduced leg stiffness, and more symmetric peak vertical GRFs compared to the use of the C-shaped RSPs ($p<0.001$). In addition, the use of the 1E90 Sprinter prosthesis may have led to enhanced sagittal plane alignment, and/or improved lateral balance during running compared to the C-shaped RSPs. The sagittal plane alignment of the 1E90 Sprinter prosthesis may have yielded shorter GRF-leg joint moment arms, mitigating joint moments and the muscular force requirements during running [27, 62]. Moreover, through a series of studies Arellano and Kram [24, 49, 73, 74] demonstrated that there is a measurable metabolic cost associated with maintaining lateral balance during running. Hence, the wider (0 to 2.5 cm) and thicker (0.1 to 0.9

cm) design of the 1E90 Sprinter prosthesis versus the C-shaped RSPs at each segment (i.e. proximal, medial, distal) [43, 45, 58] may have improved lateral balance, consequently reducing the metabolic cost of running.

It has been widely accepted that athletes with unilateral transtibial amputations generate lower peak and stance average vertical GRFs with their affected leg compared to their unaffected leg [11, 93, 107]. Our study supports this notion; the unaffected leg of our participants averaged 15.4% greater peak vertical GRFs than those of the affected leg. Lower affected leg peak vertical GRFs have been attributed to residual limb discomfort [93], weakness , as well as to the lack of net positive RSP mechanical power . However, our data indicate that peak vertical GRF asymmetry occurred because of unequal leg lengths. The affected leg's peak vertical GRF production is inversely correlated with its relative length (linear regression; $p<0.001$; $R^2=0.417$; peak vertical GRFs = -0.052 relative affected leg length (cm) + 2.449) (Fig. 4.7). Unaffected leg peak vertical GRFs were independent of affected leg length (linear regression; $p=0.052$). Of our study's 18 trials (spanning 5 participants) where affected leg length was shorter or equal to unaffected leg length, the peak ($p=0.421$) and stance average ($p=0.686$) vertical GRFs were statistically similar between legs. Simply stated, reducing affected leg length, by decreasing prosthetic height, yields more symmetric peak and stance average vertical GRFs between the legs of athletes with unilateral transtibial amputations (Fig. 4.7).

Future studies are needed to optimize RSP configuration across multiple amputation levels (e.g. transfemoral, transtibial, etc.) and over a broad range of athletic endeavors (e.g. sprinting, cycling, and jumping). Socket design may also influence the metabolic cost of running. In the current study, our participants used two different sockets to complete the protocol (one for C-shaped RSPs and one for the J-shaped RSP). As a result, there may have been unequal residual

limb movement within the different sockets, potentially leading to varying levels of muscular contraction, which may have affected the metabolic cost of running [108]. Additionally, the use of two separate testing speeds may have limited our study, however we verified that running speed did not affect net CoT ($p=0.454$) or any of the investigated biomechanical parameters ($p \geq 0.170$) using linear mixed models. We risk reporting type I errors due to our procedure of assessing each dependent variable with a separate statistical test. In addition, the effect of prosthetic height may have been confounded by our pseudo-randomized trial order. Ideally, height alteration trials would have been inserted into the initial randomized trial order rather than after all the prosthetic stiffness category trials at the recommended height for each of the respective prosthetic models.

4.6 Conclusions

Prosthetic model, but not stiffness or height, affected the metabolic cost of running for athletes with unilateral transtibial amputations. The use of a J-shaped, 1E90 Sprinter prosthesis elicited lower metabolic costs during running compared to the use of C-shaped prostheses. Furthermore, athletes with transtibial amputations appear to modulate biological leg stiffness with altered in-series stiffness differently than non-amputees. As such, changes to in-series prosthetic stiffness and surface stiffness likely alter the running mechanics of athletes with unilateral transtibial amputations. Despite the current prescriptions of running-specific prostheses, which aim to mitigate kinematic asymmetries between the affected and unaffected legs of athletes with unilateral transtibial amputations, the metabolic cost of running was independent of stride kinematic asymmetries, and only related to one kinetic asymmetry (peak vertical GRFs). Instead, the metabolic cost of running was reduced with decreased overall

(affected and unaffected leg average) peak and stance average vertical GRFs, prolonged ground contact times, and reduced leg stiffness. Therefore, current prosthetic manufacturer recommendations do not necessarily reduce the metabolic cost of running (or optimize distance-running performance). Instead, recommendations based on prosthetic design and the affected and unaffected leg's average biomechanics, rather than asymmetries, likely optimize distance-running performance for athletes with unilateral transtibial amputations.

Acknowledgements

We thank Mike Litavish CPO and Angela Montgomery CPO for their invaluable assistance throughout our study. We extend our gratitude to Dr. Rodger Kram for his support throughout this project. We also thank Freedom Innovations, Össur, and Ottobock for donating the running-specific prostheses used in this study.

5 CHAPTER 4: Running economy is similar between athletes with and without transtibial amputations

5.1 Abstract

The best distance running performances of athletes with transtibial amputations are considerably worse than those of non-amputees. Accordingly, running economy may be impaired for athletes with versus without transtibial amputations. However, current data support the hypothesis that despite different lower leg architecture and biomechanics, running economy is not inherently different between athletes with unilateral, bilateral, and without transtibial amputations.

5.2 Introduction

Athletes who reach the Olympic podium in distance running events (≥1500 m) typically possess a high aerobic capacity [16-18] and exceptional running economy [16, 18]. Across a heterogeneous group of athletes, aerobic capacity is a moderate-to-strong predictor of distance running performance (R^2 = 0.83-0.92) [17]. Alternatively, among a homogeneous group of athletes, like Olympic distance runners, running economy can vary by ~21% [22, 23] and better correlates with distance running performance than aerobic capacity (running economy vs. performance: R^2 = 0.42-0.69; aerobic capacity vs. performance: R^2 = 0.01-0.20) [18, 109, 110]. While considering aerobic capacity and lactate metabolism, superior running economy enables athletes to outperform their competitors through the ability to run faster at a given relative aerobic intensity [16, 21-23].

Athletes with transtibial amputations use passive-elastic carbon-fiber running-specific prostheses (RSPs) to compete in running events. RSPs connect in-series to the athletes' residual

limbs via carbon fiber sockets and emulate the spring-like behavior of biological legs by recycling mechanical energy during ground contact [28, 30]. RSPs do not fully replicate biological leg function [30], thus athletes with transtibial amputations using RSPs adopt stride kinematics and kinetics that are dissimilar to those of non-amputees [5, 31, 52]. Regardless, distance-running performance is constrained by the aforementioned physiological parameters. Since running economy relates to biomechanics [23, 24], the dissimilar biomechanics of athletes with versus without transtibial amputations may elicit running economy values that differ between cohorts.

Currently, the best distance running performances of athletes with transtibial amputations are inferior to those of non-amputees [111, 112]. For example, the International Paralympic Committee's (IPC's) 1500 m world records for male and female athletes with transtibial amputations are 33% and 30% slower than the corresponding non-amputee world records [111, 112]. The distance running performance discrepancies between athletes with and without transtibial amputations may be due to running economy differences. Yet, the results from peer-reviewed research support the hypothesis that despite differences in lower leg architecture and biomechanics, running economy is not inherently different between athletes with transtibial amputations using RSPs and non-amputees. Therefore, it is unlikely that running economy relates to the inferior distance running performances of athletes with transtibial amputations (unilateral and bilateral) compared to non-amputees.

To support this hypothesis, we will compare the published running economy data for athletes with unilateral and bilateral transtibial amputations to those of non-amputees. Subsequently, we will report the main biomechanical differences between athletes with versus without transtibial amputations that may affect running economy.

5.2.1 Running Economy

To compare running economy across athletes tested at different running speeds, we define running economy as the gross rate of oxygen consumed per unit of mass (physiological body mass plus running gear mass) and per unit of horizontal distance traveled (cost of transport, CoT). Most studies report that CoT is independent of running speed [24, 85, 113], though some studies show that CoT is greater (worse) at running speeds <2.5 m/s or >3.5-4.0 m/s [114-116]. Nonetheless, due to the general independence of CoT and running speed [24, 85, 113], we used CoT to enable running economy comparisons across athletes and running speeds.

5.2.2. Running-Specific Prostheses

Prosthetic configuration affects the running economy of athletes with transtibial amputations [9, 29, 56, 91]. For instance, Brown et al. [56] reported that athletes with unilateral transtibial amputations elicit ~14% better CoTs while running with RSPs compared to with passive-elastic prostheses with incorporated heel components that are designed for walking (Fig. 5.1). Furthermore, Beck et al. [9] reported that prosthetic model and stiffness both relate to the CoT of athletes with bilateral transtibial amputations. Hence, we limited our analyses to the running economy data of athletes with transtibial amputations using passive-elastic carbon fiber RSPs that exclude incorporated heel components (Fig. 5.1). If a study reported an athlete's running economy with more than one RSP configuration, we used the lowest elicited running economy value for the respective athlete.

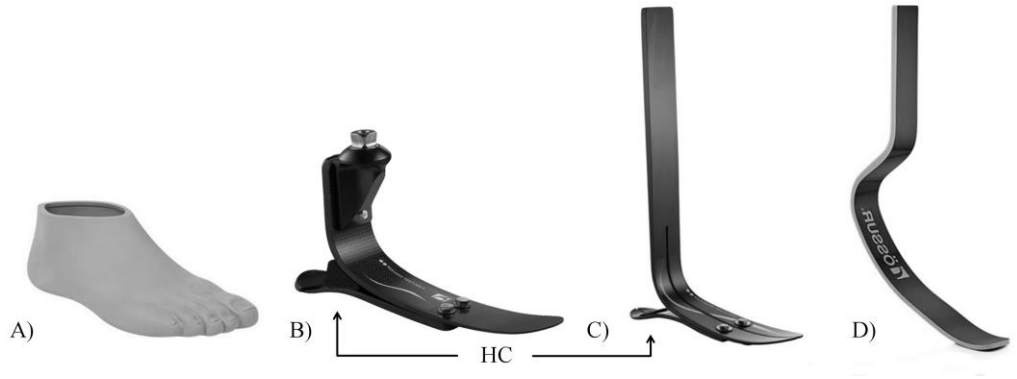

Figure 5.1. A) A representative polyurethane prosthetic cover (primarily used with walking prostheses), B) a prosthesis designed for walking that includes an incorporated heel component (HC), C) a prosthesis designed for higher level ambulation, including walking and running, with an incorporated HC, and D) a J-shaped running-specific prosthesis.

5.3 Running economy for athletes with transtibial amputations

Even though there have been minimal prosthetic design changes since the early 1990s, to date, merely fifteen athletes with unilateral transtibial amputations have had their steady-state running economy data reported [29, 56, 84]. Collectively, the average CoT for athletes with unilateral transtibial amputations is 208.9 ml O_2/kg/km (SD N/A) (Table 5.1) [29, 56, 84]. Furthermore, the running economies of seven athletes with bilateral transtibial amputations have been published [9, 52, 56, 84]. Collectively, the average (± SD) CoT for athletes with bilateral transtibial amputations is 188.9 ± 16.3 ml O_2/kg/km [9, 52, 56, 84]. Due to delayed oxygen uptake kinetics [117, 118], we excluded running economy data from athletes with transitibial amputations measured within the first two minutes of their running trials [119].

Amputation Level	Reference	CoT (ml O_2/kg/km)	Running Speed (m/s)	Sample Size (n)
Unilateral	Brown et al. [56]	227.8	2.23	5
Unilateral	Beck et al. [29]	199.4 ± 12.9	2.5 & 3.0	10
Bilateral	Weyand et al. [52]	174.2	2.5 - 4.5	1
Bilateral	Brown et al. [56]	216.5	2.23	1
Bilateral	Beck et al. (6)	186.2 ± 12.3	2.5 & 3.0	5

Table 5.1. Gross cost of transport (CoT) from athletes with transtibial amputations using running-specific prostheses. Average ± SD when available.

5.4 Running Economy Comparisons

We compared the highest, average, and lowest CoT between athletes with unilateral, bilateral, and without transtibial amputations to determine if there are differences in running economy due to amputation status. The highest and lowest CoT enables us to compute the range of running economy data within and across groups. The lowest CoT also establishes the best running economy that each athlete cohort has attained. Athletes with unilateral transtibial amputations exhibit CoTs that vary by 25%, athletes with bilateral transtibial amputations have CoTs that vary by 20%, and homogenous non-amputee runners have CoTs can that vary by ~21% [22, 23]. The numerically greater CoT range for athletes with unilateral transtibial amputations versus non-amputees may be due to the grouping of athletes by amputation status rather than by performance or training experience, which usually determines homogeneity for non-amputee runners [22, 23].

5.4.1. Athletes with Unilateral versus Bilateral Transtibial Amputations

The highest elicited CoT from athletes with unilateral transtibial amputations was 5% greater than that from athletes with bilateral transtibial amputations (227.8 versus 216.5 ml O_2/kg/km, respectively) (Fig. 5.2) [56, 84]. We used the average CoT from Brown et al. [56] as the highest CoT for athletes with unilateral transtibial amputations because Brown et al.'s cohort

average running economy value was greater than the least economical athlete reported by Beck et al. [29]. The superior running economy values from Beck et al. [29] versus Brown et al. [56] may be due to a number of factors, including the number of RSP configurations tested per athlete in each study (15 versus 1, respectively). Moreover, the average CoT reported from fifteen athletes with unilateral transtibial amputations [9, 52, 56] was 11% worse than the average CoT from seven athletes with bilateral transtibial amputations (208.9 versus 188.9 ml O_2/kg/km, respectively) (Fig. 5.2) [29, 56]. In contrast, the lowest reported CoT from athletes with unilateral transtibial amputations was 1% less than that of athletes with bilateral transtibial amputations (171.8 versus 174.2 ml O_2/kg/km, respectively) (Fig. 5.2) [9, 29].

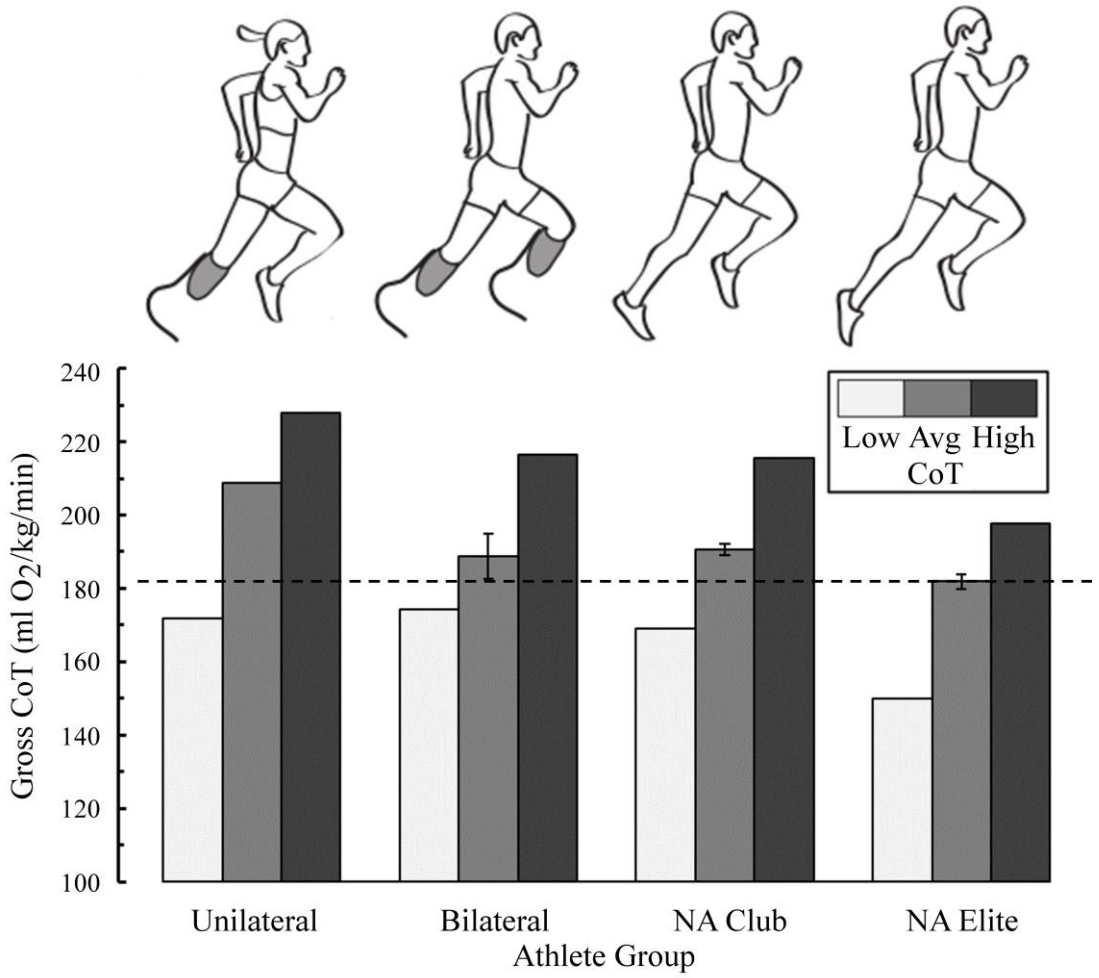

Figure 5.2. The lowest (light grey), average (medium grey), and highest (dark grey) gross cost of transport (CoT) reported from athletes with unilateral and bilateral transtibial amputations using running-specific prostheses, and from non-amputee (NA) club and elite runners. Error bars indicate standard error (SE), and the dashed line indicates the mean CoT from NA elite runners [22]. There was insufficient detail from the data of athletes with unilateral amputations to determine SE. For athletes with unilateral transtibial amputations, the lowest CoT value is from Beck et al. [29], the average CoT value is from Beck et al. [29] and Brown et al. [56], and the highest CoT value is from Brown et al. [56]. For athletes with bilateral transtibial amputations, the lowest CoT value is from Beck et al. [9], the average CoT value is from Beck et al. [9], Brown et al. [56] (reported by Weyand et al. [52]), and the highest CoT value is from Brown et al. [56]. For NA club runners (36 to 46 minute 10 km runners), all CoT are from Morgan et al. [22]. For NA elite male runners, the lowest CoT value is from Lucia et al. [120], and the mean and highest CoT are from Morgan et al. [22].

Overall, the highest and average CoTs from the fifteen athletes with unilateral transtibial amputations versus seven athletes with bilateral transtibial amputations suggest that the athletes

with bilateral transtibial amputations possess inherently better running economy compared to athletes with unilateral transtibial amputations. Notably, athletes who had their running economies reported across 15 different prosthetic configurations comprised 66 and 71% of the total athletes with unilateral and bilateral transtibial amputations, respectively; the remaining athletes were only tested with one RSP configuration. Since RSP configuration affects running economy [9, 29], the difference in average CoT may relate to the larger percentage of athletes with bilateral versus unilateral transtibial amputations that were tested across multiple RSP configurations. Furthermore, the most economical value from each athlete group was nearly identical, with a numerically lower CoT from an athlete with a unilateral transtibial amputation, indicating that having unilateral versus bilateral transtibial amputations does not affect running economy.

5.4.2. Athletes with versus without Transtibial Amputations

The highest CoT measured from athletes with unilateral transtibial amputations (227.8 ml O_2/kg/km) was within one standard deviation from the mean CoT from non-amputee college aged runners (215.4 ± 24.3 ml O_2/kg/km) [121] and similar to the maximum CoT from ten physically active non-amputee non-runners (~224 ml O_2/kg/km) [22]. The highest CoT from athletes with bilateral transitibial amputations (216.4 ml O_2/kg/km) is similar to the worst CoT elicited by 36 to 46 min 10 km non-amputee runners (~217 ml O_2/kg/km) [22].

The average CoT of fifteen athletes with unilateral transtibial amputations was 208.9 ml O_2/kg/km, which is similar to the reported average CoT of ten physically active non-amputee non-runners (201.0 ± 11.9 ml O_2/kg/km). The average CoT of athletes with bilateral transtibial amputations (188.9 ± 16.3 ml O_2/kg/km) is numerically similar to the average of 36 to 46 min 10 km non-amputee runners (190.5 ± 13.6 ml O_2/kg/km) [22], 10.4 ± 0.95 min 3 km non-amputee

runners (189.5 ml O_2/kg/km) [122], as well as collegiate and <35 min 10 km non-amputee runners (187.5 ± 9.7 ml O_2/kg/km) (Fig. 5.2) [22].

The lowest CoTs from athletes with unilateral (171.8 ml O_2/kg/km) and bilateral (174.2 ml O_2/kg/km) transtibial amputations are considerably higher (worse) than the lowest, and seemingly fictional, CoT from an elite male non-amputee distance runner (150 ml O_2/kg/km) [120]. Other exceptional non-amputee CoTs include those of the current female marathon world record holder (165 ml O_2/kg/km) [123], as well as those from an elite male (~164 ml O_2/kg/km) and a collegiate or club level male non-amputee distance runner (161.7 ml O_2/kg/km) [22]. We define elite male distance runners as those who run 5 km <13:50, 10 km <28:46 km, and/or marathon <2:20:00 in accordance with [22].

In all, the highest CoTs exhibited by athletes with unilateral and bilateral transtibial amputations coincide with those of some non-amputees. The average running economy values of athletes with unilateral and bilateral transtibial amputations are approximately three and one standard deviations above the average of elite male non-amputee distance runners [22]. However, the lowest elicited CoTs from athletes with unilateral and bilateral transtibial amputations are roughly one standard deviation below that of the average elite male non-amputee distance runner CoT [22], and well within the range of elite non-amputee distance runner CoTs in the literature (Fig. 5.2) [22, 120, 123].

5.4.3. Normalizing running economy

Normalizing CoT to only physiological body mass, rather than including running gear mass, yields relatively worse CoTs for athletes with transtibial amputations compared to non-amputees, particularly for athletes with bilateral transtibial amputations. For instance, the mass of a competition socket plus RSP is typically ~1.5 kg [9, 31, 52], while the mass of a marathon

running shoe is only ~0.23 kg [122]. By normalizing rates of oxygen consumption to physiological body mass (minus 1.5 kg per amputated leg), average CoT increases 2.1 (208.9 to 213.3 ml O_2/kg/km) and 4.3% (188.9 to 197.1 ml O_2/kg/km) for athletes with unilateral and bilateral transtibial amputations, respectively (assuming the mass of the athlete with bilateral transtibial amputations tested by Brown et al. [56] matches their average participant mass). When using CoT and body mass values indicative of competitive male non-amputee runners (CoT: 190 ml O_2/kg/km, physiological body mass plus running gear mass: 70 kg), removing running shoe mass increases CoT by a mere 0.03% [122]. By increasing CoT the respective 2.1, 4.3, and 0.03%, the most economical athletes with unilateral and bilateral transtibial amputations still exhibit CoTs that are within the range of elite male non-amputee distance runners [22].

5.5 Lower leg Architecture and Elicited Biomechanics of Athletes with versus without Transtibial Amputations: Implications for Running Economy

The dissimilar lower leg architecture and biomechanics observed between athletes with transtibial amputations using RSPs and non-amputees may affect running economy. For example, RSP mass is considerably less than the corresponding biological leg segment [31]. As such, athletes with transtibial amputations may have a reduced metabolic cost of swinging their legs versus non-amputees [24, 124]; leg swing comprises ~7% of the net metabolic cost of running [24]. Moreover, RSPs recycle more of the stored elastic energy during ground contact than passive viscoelastic structures of biological lower legs. RSP hysteresis (1-7%) [30] is less than that of the Achilles tendon (7-11%) [54] and the foot arch (22%) [53]. Additionally, unlike biological lower legs, RSPs are unable to generate net positive mechanical work [36]. Further, the residual limb's movement within the socket may be an additional source of mechanical

energy loss. Thus, athletes with transtibial amputations likely compensate for the RSP's and user-socket interface's mechanical energy loss by producing relatively more positive mechanical work with their hip and/or knee joints [125]. Because extensor muscles of the knee and hip are less efficient than those of the ankle [126], using more proximal muscles potentially elicits less economical running. Athletes with unilateral transtibial amputations may elicit slightly worse running economies than non-amputees due to their relatively asymmetric biomechanics [29]. Lastly, from 3 to 5 m/s, the medio-lateral 'foot' placement variability of athletes with and without transtibial amputations is similar [32], but athletes with transtibial amputations exhibit less stable affected leg dynamics compared to biological legs [127]. Yet, their center of mass dynamics during running are more stable than those of non-amputees [127]. Thus, the metabolic cost of maintaining lateral balance during running, which comprises ~3% of the net metabolic cost of running [24], may not differ between athletes with and without transtibial amputations.

Advances in prosthetic design that optimize stiffness, mass, mechanical power, user-socket interface, and lateral balance could potentially improve the running economy of athletes with transtibial amputations. Additionally, optimizing RSP sagittal plane alignment to improve the leg's effective mechanical advantage would likely enhance running economy [27]. In addition to 'optimized' passive-elastic RSPs, the future development of lightweight powered RSPs may further improve running economy beyond what is possible for non-amputees without the use of assistive devices.

Analogous to the conversation regarding the sprinting ability of athletes with bilateral transtibial amputations versus non-amputees [65, 84], it is difficult to determine whether athletes with transtibial amputations using RSPs are predicted to be more or less economical runners than non-amputees based on their biomechanics that *theoretically* increase/decrease running

economy. Nevertheless, for this review we present the current running economy values in the literature, which support the notion that running economy is similar between athletes with transtibial amputations using RSPs and non-amputees (Fig. 5.2).

5.6. Limitations

The supporting evidence of our novel hypothesis has a few potential limitations. First, one or more athletes with transtibial amputations may have participated in multiple studies. Accordingly, we might have included the same athlete's running economy data more than once when determining cohort averages. In addition, comparing CoTs across athletes tested in different labs may be influenced by the study's running speed [114, 115], altitude [128], and treadmill deck compliance [59]. Lastly, numerous articles report non-amputee running economy data, making it possible to find non-amputee running economy data that are better or worse than those of athletes with transtibial amputations. But, regardless of the non-amputee comparison, running economy data of athletes with unilateral and bilateral transtibial amputations are within the range of non-amputee runners, with some values comparable to those of elite non-amputee distance runners.

5.7 Future Directions

Many studies attribute aerobic capacity, lactate threshold, and running economy as the main factors that govern distance running performance [14, 129]. Hence, if running economy is similar between athletes with and without transtibial amputations, future studies should investigate whether aerobic capacity and lactate threshold are inherently different between athletes with and without transtibial amputations. Alternatively, if no physiological parameters

are different between athlete cohorts, social restrictions may limit the distance running performance of athletes with transtibial amputations. This could occur because neither of the pinnacle track and field competitions for these athletes (Paralympic Games or the IPC World Championships) offer distance-running events. Accordingly, the best athletes with transtibial amputations may opt to train and compete in sprinting events or in other sports to reach the prestigious Paralympics and/or IPC World Championships, rather than embarking on the lonely pursuit of competitive distance running.

5.8 Conclusions

Based on current data in the literature, running economy is similar between athletes with unilateral and bilateral transtibial amputations using RSPs and non-amputee athletes despite differences in lower leg architecture and biomechanics. Therefore, running economy is not likely responsible for the inferior distance running performances of athletes with transtibial amputations compared to those of non-amputees.

6 CHAPTER 4: How do prosthetic stiffness, height, and running speed affect the biomechanics of athletes with bilateral transtibial amputations?

6.1 Abstract

Limited available information describes how running-specific prostheses and running speed affect the biomechanics of athletes with bilateral transtibial amputations. Accordingly, we quantified the effects of prosthetic stiffness, height, and speed on the biomechanics of five athletes with bilateral transtibial amputations during treadmill running. Each athlete performed a set of running trials with fifteen different prosthetic model, stiffness, and height combinations. Each set of trials began with the athlete running on a force-measuring treadmill at 3 m/s, subsequent trials incremented by 1 m/s until they achieved their fastest attainable speed. We collected ground reaction forces during each trial. Prosthetic stiffness, height, and running speed each affected biomechanics. Specifically, with stiffer prostheses athletes exhibited greater peak and stance average vertical ground reaction forces (β=0.03; $p<0.001$), increased overall leg stiffness (β=0.21; $p<0.001$), decreased ground contact time (β=-0.07; $p<0.001$), and increased step frequency (β=0.042; $p<0.001$). Prosthetic height inversely associated with step frequency (β=-0.021; $p<0.001$). Running speed inversely associated with leg stiffness (β=-0.58; $p<0.001$). Moreover, at faster running speeds the effect of prosthetic stiffness and height on biomechanics was mitigated and unchanged, respectively. Thus, prosthetic stiffness, but not height, likely influences distance running performance more than sprinting performance for athletes with bilateral transtibial amputations.

6.2 Introduction

During running, the vertical position of an athlete's centre of mass (CoM) reaches its lowest position at mid-stance and its highest position at the middle of the aerial phase. This fundamental cyclic movement is due to the spring-like behaviour of the stance leg and is well-described by a spring-mass model [1-5]. The model simplifies the leg's musculoskeletal system during running to a massless linear leg spring supporting a point mass that represents the athlete's CoM [1-5] (Fig. 6.1). During the first half of ground contact, elastic potential energy is stored in the compressed leg spring. Subsequently, the stored mechanical energy is released during the second half of ground contact as the leg spring recoils, thereby accelerating the CoM forward and upward into the aerial phase [6]. The magnitude of the stored and returned mechanical energy is inversely related to leg stiffness, and is thought to influence running performance by altering the generation of muscular mechanical work [6-8], and contraction velocities [88].

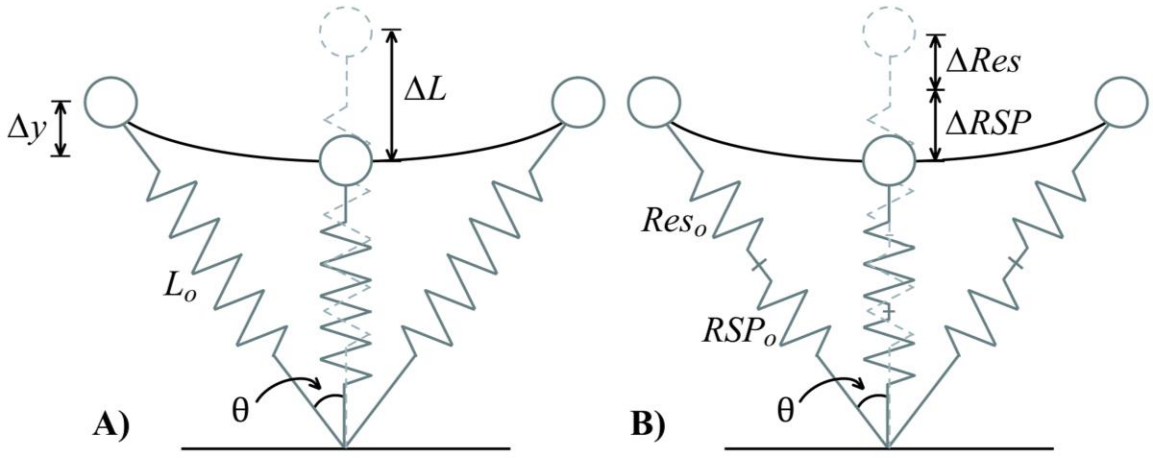

Figure 6.1. Illustration of a (*a*) spring–mass model and (*b*) spring–mass model with two in-series leg springs. Body mass is represented as a point mass (circle) and the touch-down angle is indicated by θ. (*a*) The stance leg is represented by a massless linear spring for non-amputees, and (*b*) two in-series massless linear springs for athletes with bilateral amputations. The initial leg length (L_0) shortens (ΔL), and vertical height (Δy) decreases during the stance phase of running. Modelled residual limb length (Res_0) and prosthetic height (RSP_0) compress and extend (ΔRes and ΔRSP) during the stance phase of running.

Fundamentally, the spring-mass model characterizes running biomechanics for athletes with [5, 9-11] and without lower limb amputations [1-5]; however, the product of step length and step frequency ultimately dictates running speed. Step length can be determined from the product of the horizontal distance traveled by the CoM during ground contact (contact length) and the stance average vertical ground reaction force (GRF) magnitude normalized to body weight [12, 13]. Step frequency can be calculated from the reciprocal of the sum of ground contact time and aerial time [12, 13]. Thus, the spring-mass model describes running biomechanics while kinematic and kinetic parameters dictate running speed.

There is limited available information regarding how athletes with bilateral transtibial amputations, who run with passive-elastic running-specific prostheses (RSPs), adapt their biomechanics to achieve different running speeds. That is because to date merely three studies have reported biomechanics from a total of two athletes with bilateral transtibial amputations across running speeds [5, 49, 52], and since the running biomechanics of athletes with unilateral transtibial amputations (affected and unaffected leg) and non-amputees differ from those of athletes with bilateral transtibial amputations [5, 49, 52]. Collectively, as constant running speed is increased from 2.5 to 8.0 m/s, athletes with bilateral transtibial amputations decrease leg stiffness, increase contact length [5], increase stance average vertical GRF [52], decrease contact time, and maintain a nearly constant aerial time [52]. Beyond 8 m/s, the same biomechanical

trends persist except that stance average vertical GRFs plateau and aerial times decrease [52]. Therefore, athletes with bilateral transtibial amputations increase both step length and step frequency to achieve running speeds from 2.5 to 8.0 m/s, while they primarily increase step frequency to achieve speeds faster than 8.0 m/s. However, these trends are based on data from two athletes, thus a greater sample size is needed to confirm or refute these results.

Further, it is uncertain if the biomechanical changes with altered running speeds are inherent to athletes with bilateral transtibial amputations or if they are due to the characteristics of their RSPs. For example, many researchers and governing institutions speculate that prosthetic stiffness and height have a strong influence on the biomechanics and running performance of athletes with bilateral transtibial amputations [5, 9, 64, 65]. In our previous study [9], we found that the use of stiffer RSPs by athletes with bilateral transtibial amputations was correlated with increased overall leg stiffness, increased residual limb stiffness, faster step frequencies, and increased metabolic cost at relatively slow running speeds (2.5 and 3.0 m/s). Thus, it remains uncertain whether running speed alters the influence of prosthetic stiffness on biomechanics. Since prosthetic stiffness slightly increases with greater applied force [30], and residual limb stiffness is positively associated with prosthetic stiffness [9], the leg stiffness and step frequency of athletes with bilateral transtibial amputations should theoretically increase with running speed. Yet, the leg stiffness of such athletes has been reported to decrease at faster running speeds [5], indicating that the influence of prosthetic stiffness may be mitigated at faster running speeds.

Athletes with bilateral transtibial amputations participate in events that span a broad range of running speeds, therefore it is important to understand how prosthetic stiffness, height, and speed affect biomechanics. Accordingly, the purpose of this study was to quantify how changes in prosthetic stiffness, height, and running speed affect the biomechanics of athletes

with bilateral transtibial amputations. Based on our previous study [9], we hypothesized that across running speeds 1) the use of stiffer RSPs would increase leg stiffness and step frequency, and 2) the use of taller RSPs would be independent of the biomechanical variables that govern leg stiffness and running speed. We also hypothesized that 3) faster running speeds would lessen the influence of prosthetic stiffness on biomechanical parameters.

6.3 Methods

6.3.1 Subject Recruitment

Five male athletes with bilateral transtibial amputations participated (Table 6.1). Four athletes primarily compete in sprinting (≤400m) and/or jumping track and field events and one athlete primarily competes in distance running events (≥5000m) (Table 6.1). Each athlete had over one year of experience running with passive-elastic RSPs, and gave informed written consent according to the protocol that was approved by the Colorado Multiple Institutional Review Board and the USAMRMC Office of Research Protection, Human Research Protection Office.

Partici-pants	**Age** (yrs)	**Mass** (kg)	**Primary Event(s)**	**Max IPC Height** (m)	**Max IPC Leg length** (m)	**Catapult Leg length** (m)	**Cheetah Xtend Leg length** (m)	**1E90 Sprinter Leg length** (m)
1	25	69.3	100m/200m	1.80	0.97	1.12	0.97	0.97
2	23	76.3	Long Jump	1.88	1.07	1.07	1.07	1.04
3	18	75.0	100m/200m	1.87	1.05	1.05	1.05	1.05
4	31	70.4	400m	1.90	1.10	1.10	1.10	1.10
5	27	70.5	5000m	1.87	1.06	1.06	1.06	1.06
Average	24.8	72.3		1.86	1.05	1.08	1.05	1.04
SD	4.8	3.1		0.04	0.05	0.03	0.05	0.04

Table 6.1. Participant characteristics: age, mass, and primary event(s). The maximum standing height and corresponding leg lengths allowed in track and field races sanctioned by the International Paralympic Committee (IPC). The resulting Catapult, Cheetah Xtend and 1E90 Sprinter prosthesis leg lengths represent the closest attainable maximum IPC-regulated leg lengths from each participant and prosthetic model combination. Leg lengths were measured from the greater trochanters to the most distal locations of the unloaded prostheses.

6.3.2 Experimental Protocol

Initially, each participant completed a fitting and accommodation session. During this session, we collected anthropometric measurements to determine the tallest prosthetic height that each participant could use to compete in track and field races according to the International Paralympic Committee (IPC) guidelines [64]. Next, a certified prosthetist aligned each participant with three commonly used prosthetic models (Freedom Innovations Catapult FX6, Irvine, CA, USA; Össur Cheetah Xtend, Reykjavik, Iceland; Ottobock 1E90 Sprinter, Duderstadt, Germany) at the manufacturer's recommended and ±1 stiffness categories at the prosthetic height that produced the IPC maximum competition height and ±2 cm. We chose these stiffness and height configurations because they have been reported to elicit biomechanical changes during running in athletes with transtibial amputations [9, 29, 34] and they enabled us to recruit athletes spanning a wide range of body masses and heights.

Each RSP functions as a spring through the storage and return of mechanical energy during stance. The Catapult prostheses are "C" shaped and attach distally to sockets via connecting aluminum pylons. Each carbon-fibre or fibreglass socket (check socket) surrounds a residual limb and is secured with suction or a locking mechanism (Fig. 6.2). The Cheetah Xtend and 1E90 Sprinter prostheses are "J" shaped and mount to the posterior wall of the socket. After establishing the heights of the J-shaped RSPs, the prostheses are typically bolted directly to the sockets. To preserve the J-shaped RSPs, secure them to the sockets, and alter prosthetic height

between trials, we constructed custom aluminum brackets that were bolted to the sockets (Fig. 6.2).

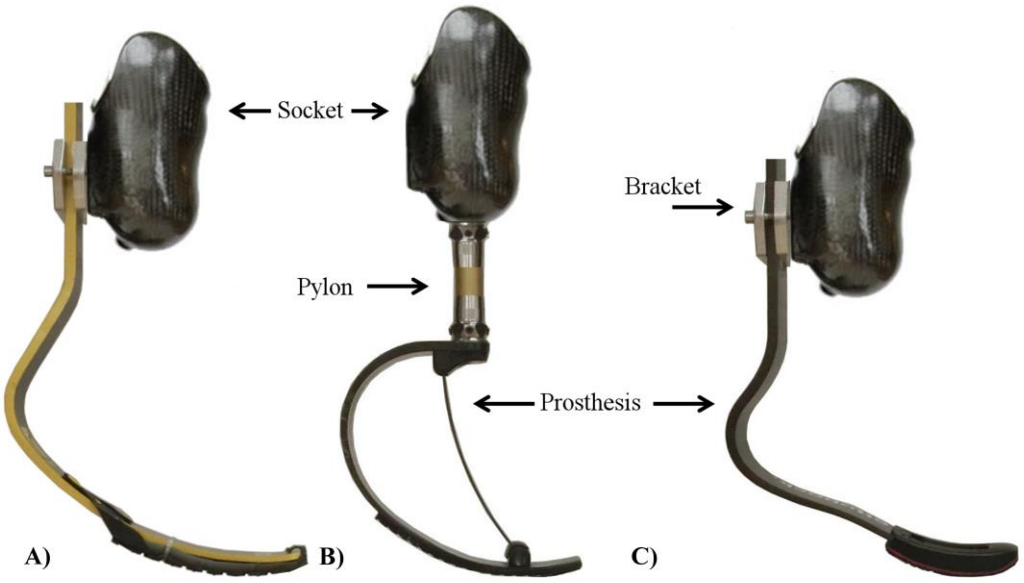

Figure 6.2. From left to right, (*a*) the Össur Cheetah Xtend prosthesis (J-shaped) at a representative recommended height, (*b*) the Freedom Catapult FX6 prosthesis (C-shaped) at a representative height of +2 cm and (*c*) the Ottobock 1E90 Sprinter prosthesis (J-shaped) at a representative height of −2 cm. The C-shaped prostheses are connected to sockets via aluminium pylons, and the J-shaped prostheses are connected to sockets via custom aluminium brackets.

Due to participant residual limb lengths and available prosthetic components, we were unable to match the maximum IPC competition height for some participants with certain prosthetic models. For these cases, we set prosthetic height as close as possible to the maximum IPC competition height. If the closest attainable height was taller than the maximum IPC competition height, we set that height as the baseline height for the respective participant and RSP combination and ensuing prosthetic height alterations were +2 cm and +4 cm. If the closest achievable height was shorter than the maximum IPC competition height, we set that height as the baseline height for the respective participant and RSP combination and subsequent prosthetic height alterations were -2 cm and -4 cm (Table 6.1).

After participants were aligned to a prosthetic configuration, they ran on a motorized force-measuring treadmill (Treadmetrix, Park City, UT, USA) at self-selected speeds until both the prosthetist and participant were satisfied with the comfort and function of the respective RSPs. Generally, athletes accommodated to each prosthetic model at the recommended stiffness category and height. When using C-shaped RSPs, athletes also ran at additional heights (i.e. ±2 cm) to determine proper alignment with the taller/shorter pylons. When using J-shaped RSPs, the components and alignment were the same at each height per model, hence athletes did not typically accommodate to the additional heights. Four athletes used their personal competition sockets for the trials with the J-shaped RSPs, and they used their everyday/walking sockets when equipped with the C-shaped RSPs. For the other athlete, a prosthetist fabricated custom sockets that replicated the participant's competition sockets (suspension, internal dimensions, etc.) for use with the C- and J-shaped RSPs.

On subsequent days, participants performed a session of one to three sets of treadmill running trials [5]. Each set of treadmill running trials started with the participant running at 3 m/s and following successful trials, treadmill speed was incremented 1 m/s for the next trial. A successful trial was determined if the participant was able to maintain forward position on the treadmill while taking 20 consecutive steps [5, 12, 52]. If the participant was unable to maintain forward position on the treadmill for 20 consecutive steps, the trial was deemed unsuccessful. *Ad libitum* rest followed each trial. Following unsuccessful trials and rest periods, participants were given the option to retry the preceding trial's speed, or deem the last successful trial as their top speed with the given prosthetic configuration.

Participants were given two options to commence each treadmill running trial. The first option began with the participant straddling the treadmill belt while it sped up to the desired

speed. Once the treadmill was up to speed, the participant lowered himself onto the moving treadmill belt using the handrails. The participant then took a few steps on the belt and, when comfortable, began to run without handrail assistance, initiating the step count. The second option allowed each participant to begin by standing on the static treadmill belt. The participant then accelerated with the treadmill belt until the target speed was achieved. Once the treadmill achieved the desired speed, we began to count steps as the participant continued to run on the treadmill. For each trial, participants were allowed to choose either starting technique.

Each participant ran using 15 different combinations of prosthetic model, stiffness category, and height. At first, participants ran using each model at three different stiffness categories (recommended and ±1) at the IPC maximum competition height. The stiffness category for each prosthetic model that elicited the fastest top speed was considered optimal. Subsequently, participants ran using the optimal stiffness category of each prosthetic model at two additional heights (±2 cm). We randomized the trial order beginning with the nine prosthetic model and stiffness category combinations at the maximum IPC competition height. Once a participant completed trials at all three stiffness categories with a certain prosthetic model, we randomly inserted the altered height trials for a respective model at the optimal stiffness category into the trial order.

6.3.3 Prosthetic Stiffness

Prosthetic stiffness categories are recommended to athletes by the respective manufacturers based on user body mass, with larger athletes being recommended numerically greater stiffness categories [45, 97, 130]; numerically greater stiffness categories indicate mechanically stiffer (kN/m) prostheses [30]. Since recommended stiffness (kN/m) differs between prosthetic models [30], we calculated prosthetic stiffness using the peak vertical GRFs

measured from each leg during each trial (present study) and the force-displacement equations from Beck et al. [30] to estimate displacement. Next, we divided the measured peak GRF magnitude by the estimated prosthetic displacement to yield stiffness. Prosthetic stiffness values were previously only recorded from participants with transtibial amputations running at 3 and 6 m/s [30]. Thus, we calculated prosthetic stiffness for trials at 3 and 6 m/s and then derived prosthetic stiffness at 4, 5, and 7 m/s assuming a linear relationship between prosthetic stiffness and running speed. We did not estimate prosthetic stiffness beyond 7 m/s.

6.3.4 Data collection and stride count

We measured GRFs throughout the duration of each running trial. We collected GRFs at 1000 Hz, filtered them using a 4th order low-pass Butterworth filter with a 30 Hz cutoff [9, 29, 131], and then used the filtered data to calculate mean GRF parameters, stride kinematics, and leg stiffness values with a custom MATLAB script (Mathworks Inc., Natick, MA, USA). We set the vertical GRF threshold at 20 N to detect periods of ground contact. For each trial, participants ran with a reflective marker on the distal end of one of their RSPs, and we tracked its position at 200 Hz (Vicon Nexus, Oxford, UK). We filtered the position data using a 4th order low-pass Butterworth filter with a 7 Hz cutoff to determine the running speed during ground contact of the respective RSP using a custom MATLAB script.

6.3.5 Data Analyses

We calculated overall leg stiffness (k_{leg}) as the quotient of peak vertical GRF (F_{peak}) and peak leg spring compression (ΔL) during ground contact (Fig. 6.1).

$$k_{leg} = \frac{F_{peak}}{\Delta L} \tag{6.1}$$

Peak leg spring compression (ΔL) was calculated using initial leg length (L_0), the distance from the greater trochanter to the distal end of the unloaded RSP [5, 9], theta (θ), the angle of the leg spring at initial ground contact relative to vertical (Fig. 6.1), running speed (v), and ground contact time (t_c).

$$\theta = sin^{-1}(\frac{v\ t_c}{2\ L_0}) \tag{6.2}$$

Next, peak leg spring compression (ΔL) was determined using peak vertical displacement of the CoM during ground contact (Δy), calculated by twice integrating the vertical acceleration of the center of mass with respect to time [72].

$$\Delta L = \Delta y + L_0(1 - \cos\theta) \tag{6.3}$$

Moreover, because biological legs and RSPs have relatively linear force-displacement profiles [2, 30], we modeled participant leg stiffness (k_{leg}) as two in-series linear springs (Fig. 6.1). We incorporated established measurements of prosthetic stiffness (k_{RSP}) [30], and current measurements of leg stiffness to determine residual limb stiffness (k_{res}) using equation 6.4.

$$\frac{1}{k_{leg}} = \frac{1}{k_{res}} + \frac{1}{k_{RSP}} \tag{6.4}$$

As aforementioned, running speed (v) is the product of step length (L_{step}) and step frequency (F_{step}).

$$v = L_{step} \cdot F_{step} \tag{6.5}$$

Steps lengthen by increasing the horizontal distance traveled by the runner's CoM during stance (contact length) (L_c), and by producing greater stance average vertical GRFs (F_{avg}) relative to body weight (BW) [12, 13]. Therefore, step length can be calculated using equation 6.6.

$$L_{step} = L_c \cdot F_{avg}/BW \tag{6.6}$$

We used equation 6 because it enables us to further investigate the biomechanical variables that govern step length (i.e. L_c and F_{avg}/BW) and therefore running speed. Step frequency is calculated from the reciprocal of the sum of ground contact time (t_c) and aerial time (t_a) [12, 13].

$$F_{Step} = \frac{1}{t_c + t_a} \tag{6.7}$$

Thus, by combining equations 6.5, 6.6, and 6.7, running speed (v) is calculated using equation 6.8.

$$v = L_c \cdot F_{avg}/BW \cdot \frac{1}{t_c + t_a} \tag{6.8}$$

For the complete derivation of equation 6.8, refer to citations [12, 13].

6.3.6 Statistical Analyses

We used a linear mixed model to evaluate the influence of prosthetic stiffness (kN/m), height, and running speed (3 to 9 m/s) on the biomechanical variables that comprise the spring-mass model and running speed (variables from equations 6.1 through 6.8). We report the fixed effect (β) from each statistically significant association (dependent variable = β independent variable + constant). We tested for all potential stiffness/speed and height/speed interactions. Additionally, prosthetic stiffness depends on the magnitude and orientation of the applied force [30], thus we performed a one-way ANOVA to determine whether running speed statistically influenced prosthetic stiffness. We set the level of significance at p=0.05 and performed statistical analyses using R-studio (Boston, MA, USA).

6.4 Results

Due to the difficulties of determining running speed during the acceleration phase, some trials contained fewer than 20 steps at the desired speed. Consequently, we used the motion

capture data to determine instantaneous running speed and only analyzed steps that were taken at the desired speed. We excluded data from the last two steps of each trial to remove any potential biomechanical alterations that occurred while participants prepared to dismount the treadmill. We also excluded data from trials that had fewer than four consecutive steps at the desired speed. Additionally, due to saturation in the force signal, we removed 16 trials from the analysis. In the end, we analyzed 73 trials at speeds of 3, 5, and 6 m/s, 74 trials at 4 m/s, 72 trials at 7 m/s, 65 trials at 8 m/s, and 37 trials at 9 m/s.

6.4.1 Prosthetic stiffness

Prosthetic stiffness increased with faster running speeds ($p<0.001$) (Table 6.2). From 3 to 7 m/s, overall prosthetic stiffness averaged (±SD) 25.4 ± 3.0, 26.1 ± 3.4, 27.1 ± 4.0, 28.0 ± 4.8, and 28.6 ± 5.6 kN/m at each successive speed (Fig. 6.3). Unless otherwise specified, all results were interpreted while controlling for covariates (e.g. interpreting the effect of prosthetic stiffness on biomechanics while controlling for prosthetic height, running speed, and interactions between prosthetic height and running speed). For every 1 kN/m increase in prosthetic stiffness, overall leg stiffness increased 0.21 kN/m ($p<0.001$), residual limb stiffness decreased 2.09 kN/m ($p<0.001$) (Fig. 6.3), contact length decreased 1.7 cm ($p<0.001$), and step frequency increased 0.042 Hz ($p<0.001$) (Fig. 6.4). Regarding the other spring-mass model variables, for every 1 kN/m increase in prosthetic stiffness, theta increased 0.004 radians ($p=0.012$), Δy decreased 0.19 cm ($p<0.001$) (Fig. 6.5), peak vertical GRF increased 0.03 times body weight ($p<0.001$), and ΔL decreased 0.07 cm ($p<0.001$). Concerning the rest of the biomechanics that govern running speed, for every 1 kN/m increase in prosthetic stiffness, stance average vertical GRF increased 0.03 times body weight ($p<0.001$), and contact time decreased 0.007 seconds ($p<0.001$) (Fig. 6.5).

Stiffness Category	Running Speed (m/s) 3	4	5	6	7
-1	22.6 ± 1.7	23.4 ± 2.2	24.3 ± 3.1	25.2 ± 4.2	26.0 ± 5.3
Rec	25.3 ± 1.6	26.0 ± 2.1	26.8 ± 3.0	27.4 ± 3.8	28.4 ± 5.0
+1	27.5 ± 2.1	28.4 ± 2.5	29.4 ± 3.2	30.3 ± 4.1	31.5 ± 5.4

Table 6.2. Average (±s.d.) recommended (Rec) prosthetic stiffness values (kN m^{-1}) for a 70 kg athlete across running speeds and prosthetic stiffness values (kN m^{-1}) from ±1 stiffness categories across speeds. We averaged prosthetic stiffness values at each category for each model, and then averaged stiffness values across models for the respective recommended category (i.e. Rec, or ±1). Prosthetic stiffness was related to running speed ($p < 0.001$).

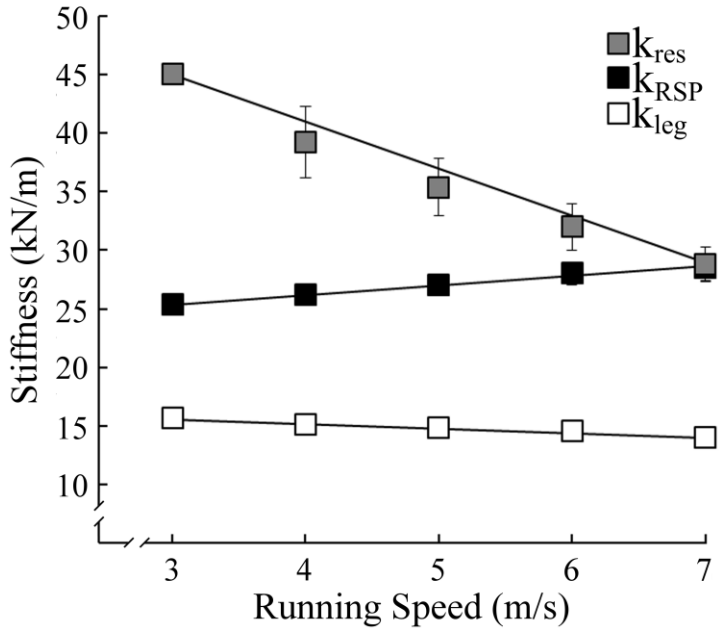

Figure 6.3. The average (±s.e.) stiffness of the overall leg (k_{leg}), the prosthesis (RSP; k_{RSP}) and the residual limb (k_{res}) across 3 through 7 m s^{-1} and across all prosthetic configurations. Across all conditions, simple linear regression equations follow as: $k_{leg} = -0.30$ Speed + 16.4, $R^2 = 0.05$, $p < 0.001$; $k_{res} = -4.0$ Speed + 56.0, $R^2 = 0.16$, $p < 0.001$; k_{RSP} (kN m^{-1}) = 0.82 Speed + 22.9, $R^2 = 0.07$, $p < 0.001$. Error bars indicate inter-subject variability and may be hidden behind the symbols.

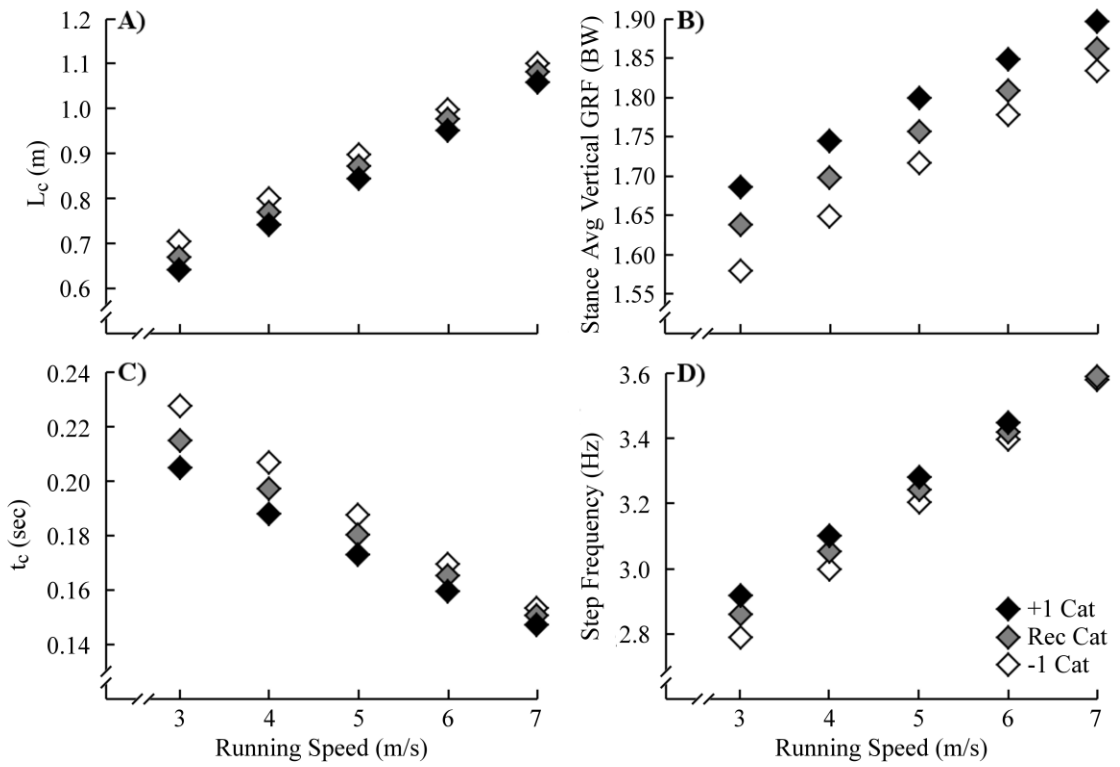

Figure 6.4. (*a*) Contact length (L_c), (*b*) stance average vertical GRF, (*c*) contact time (t_c) and (*d*) step frequency, while using RSPs averaged from three different models at one stiffness category below recommended (−1 Cat), at recommended (Rec Cat) and at one stiffness category greater than recommended (+1 Cat) across running speeds. Prosthetic stiffness categories correspond to a 70 kg athlete. See table 6.2 for prosthetic stiffness values (k_{RSP} in kN m^{-1}) used at each speed (v) and stiffness category recommendation. Biomechanical data are derived from statistical linear mixed models. The linear mixed model regression equations follow as: (*a*) $L_c = 0.08\ v - 0.02\ k_{RSP} + 0.001\ v \cdot k_{RSP} + 0.76$; (*b*) avg vertical GRF = $0.11\ v + 0.03\ k_{RSP} - 0.003\ v \cdot k_{RSP} + 0.75$; (*c*) $t_c = -0.038\ v - 0.007\ k_{RSP} + 0.001\ v \cdot k_{RSP} + 0.446$; (*d*) step frequency = $0.315\ v + 0.042\ k_{RSP} - 0.005\ v \cdot k_{RSP} + 1.258$.

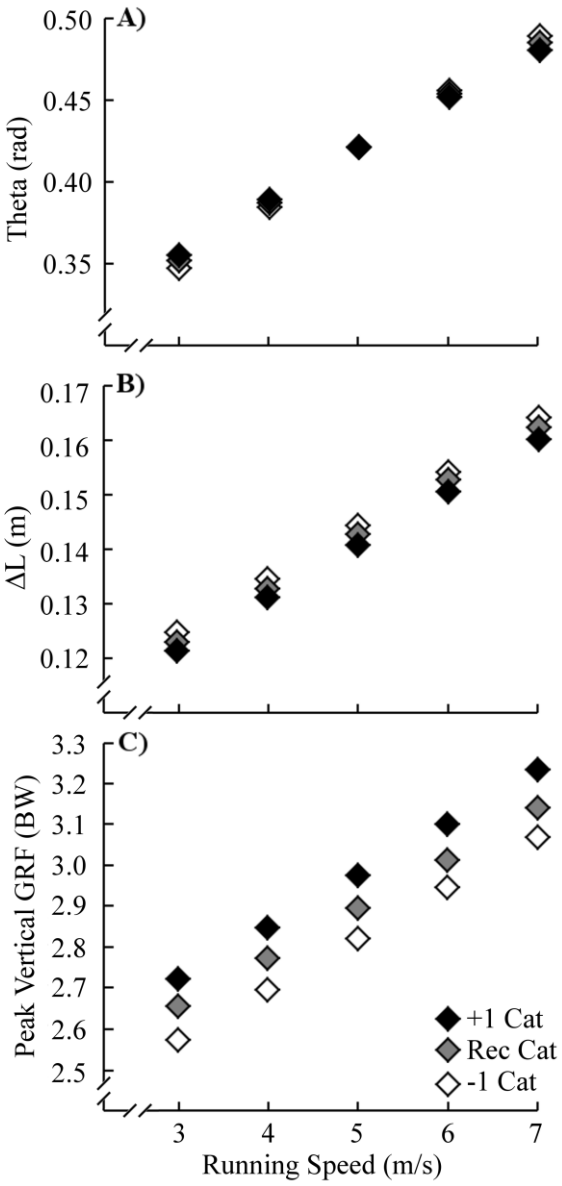

Figure 6.5. (*a*) Touch-down angle (θ), (*b*) leg spring compression (ΔL) and (*c*) peak vertical GRF averaged from three different running-specific prosthetic models at one stiffness category below recommended (−1 Cat), at recommended (Rec Cat) and at one stiffness category greater than recommended (+1 Cat) across running speeds. Prosthetic stiffness categories correspond to a 70 kg athlete. See table 2 for prosthetic stiffness values (k_{RSP} in kN m^{-1}) used at each speed (v) and stiffness category recommendation. Biomechanical data are derived from statistical linear mixed models. The regression equations follow as: (*a*) $\theta = 0.055\ v + 0.004\ k_{RSP} - 0.001$ Speed $\cdot\ k_{RSP} + 0.145$; (*b*) $\Delta L = 0.010\ v - 0.001\ k_{RSP} + 0.109$; (*c*) peak vertical GRF $= 0.10\ v + 0.03\ k_{RSP} + 1.59$.

6.4.2 Prosthetic height

Increasing prosthetic height by 2 cm resulted in no significant changes in overall leg stiffness ($p=0.756$) or residual limb stiffness ($p=0.668$), but did correlate with a 2.3 cm increased contact length ($p<0.001$) and 0.021 Hz decreased step frequency ($p=0.009$) (Fig. 6.4). For every 2 cm increase in prosthetic height, theta decreased 0.012 radians ($p<0.001$), Δy increased 0.16 cm ($p<0.001$), and peak vertical GRF decreased by 0.02 times body weight ($p=0.047$) (Fig. 6.5). Furthermore, for every 2 cm increase in prosthetic height, stance average vertical GRF decreased 0.25 times body weight ($p<0.001$), and contact time increased 0.003 seconds ($p<0.001$). Prosthetic height did not influence ΔL ($p=0.130$).

6.4.3 Running speed

Each participant was able to achieve a running speed of 9 m/s with at least one prosthetic configuration. For every 1 m/s increase in running speed, overall leg stiffness decreased 0.58 kN/m ($p<0.001$), residual limb stiffness decreased 9.42 kN/m ($p<0.001$) (Fig. 6.3), contact length increased 7.8 cm ($p<0.001$) and step frequency increased 0.32 Hz ($p<0.001$) (Fig. 6.4). For every 1 m/s increase in running speed, theta increased 0.055 radians ($p<0.001$), Δy decreased 1.15 cm ($p<0.001$), peak vertical GRF increased 0.01 times body weight ($p<0.001$), and ΔL increased 1.00 cm ($p<0.001$) (Fig. 6.5). Moreover, for every 1 m/s increase in running speed, stance average vertical GRF increased 0.12 times body weight ($p<0.001$), and contact time decreased 0.038 seconds ($p<0.001$) (Fig. 6.4). Independently, running speed did not change peak vertical GRF magnitude ($p=0.743$).

6.4.4 Prosthetic stiffness/height and speed interaction effects

At faster running speeds, the influence of prosthetic stiffness on residual limb stiffness ($\beta=0.23$; $p=0.020$), contact length ($\beta=0.13$; $p=0.019$), and step frequency ($\beta=-0.005$; $p=0.004$) (Fig.

6.5) were all diminished. Furthermore, for every 1 m/s increase in running speed, the effect of increasing prosthetic stiffness 1 kN/m was associated with a 0.001 radian decreased theta ($p=0.001$) (Fig. 6.4), and 0.03 cm increased Δy ($p<0.001$). For every 1 m/s increase in running speed, every 1 kN/m increase in prosthetic stiffness was related with a 0.003 times body weight decreased stance average vertical GRF ($p<0.001$), and a 0.001 second increase in contact time ($p<0.001$) (Fig. 6.5). No other prosthetic stiffness/height and speed interactions achieved statistical significance ($p>0.05$).

6.5 Discussion

The purpose of this study was to quantify how altered prosthetic stiffness, height, and running speed affect the biomechanics of athletes with bilateral transtibial amputations. We accepted our initial hypothesis that the use of stiffer RSPs would result in increased overall leg stiffness and step frequency (Fig. 6.3). This extends the previous research, which concluded that at a single, slow running speed, athletes with bilateral transtibial amputations increase overall leg stiffness and step frequency with the use of stiffer RSPs [9]. However, the previous study's athletes demonstrated an extremely weak positive correlation between prosthetic stiffness and residual limb stiffness [9], contrasting the present study's finding of an inverse relationship between prosthetic stiffness and residual limb stiffness (Fig. 6.3). The present study's finding corresponds with the established observation that non-amputees inversely alter overall leg stiffness with changed in-series surface stiffness to maintain nearly constant leg stiffness during running [60, 61]. Furthermore, we report an inverse relationship between leg stiffness and running speed despite a positive association between prosthetic stiffness and running speed (Fig. 6.3). This occurs because leg stiffness only increases 0.21 kN/m with each integer increase in prosthetic stiffness whereas it decreases 0.58 kN/m with every 1 m/s increase in running speed.

For example, the 3.2 kN/m average increase in prosthetic stiffness from 3 to 7 m/s, coupled with the influence of faster running speed yields a 1.65 kN/m reduction in leg stiffness (Fig. 6.3).

The leg joint mechanics that govern overall leg spring behaviour may differ between athletes with and without transtibial amputations. A previous study indicated that the affected leg knee joints of athletes with unilateral transtibial amputations do not act like sagittal plane torsional springs during running [10], which is dissimilar to that of non-amputees [39, 104] whose knee joint mechanics greatly influence leg stiffness [83]. We confirmed that at each speed, the overall leg mechanics of athletes with bilateral transtibial amputations follow the main assumptions of the spring-mass model [1-5], where the vertical GRFs and displacement of the runner's CoM gradually increase then decrease with both maximums occurring at ~50% of the stance phase (Fig. 6.6). Future analyses of residual limb joint mechanics (e.g. hip, knee, residual limb/socket interface, etc.) are necessary to determine if leg joints and the limb-socket interface of athletes with bilateral transtibial amputations perform like springs (linear and torsional springs) during running and how they contribute to the spring-like behaviour of the overall leg.

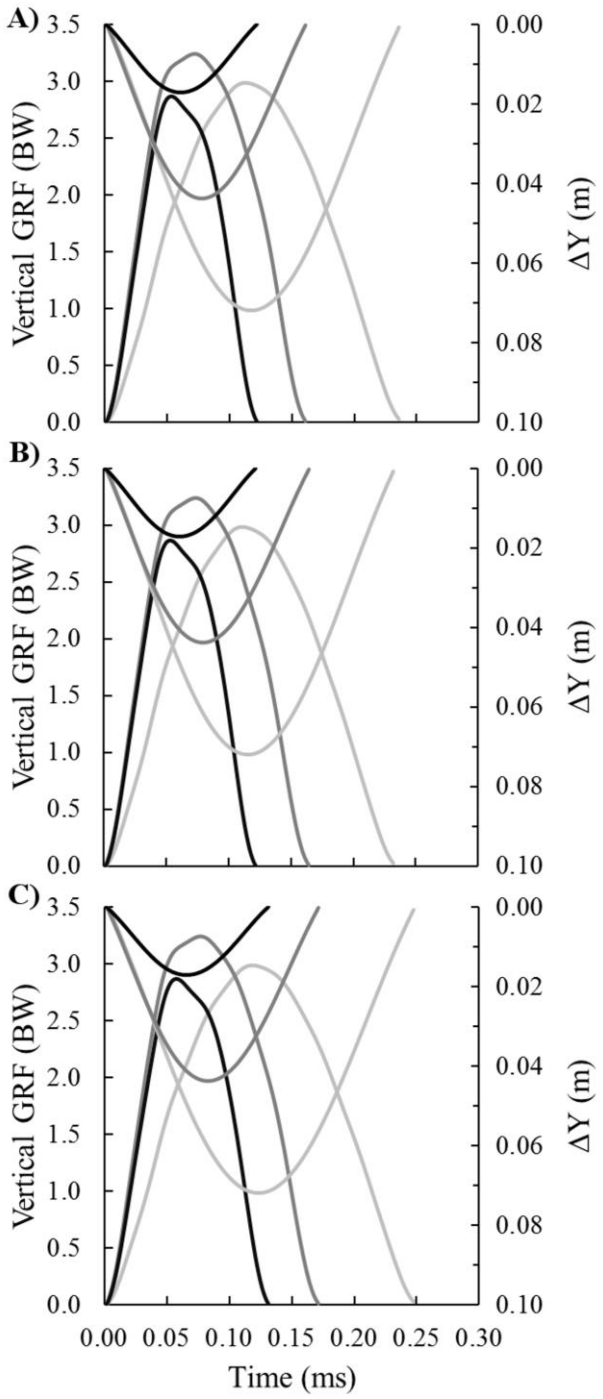

Figure 6.6. Representative vertical GRF traces (left axis), and CoM vertical displacements (ΔY; right axis) as a function of time for a participant using Össur Cheetah Xtend prostheses at (*a*) −1 prosthetic stiffness category, (*b*) recommended prosthetic stiffness category and (*c*) + 1 prosthetic stiffness category. Light grey lines represent running at 3 m s^{-1}, medium grey lines represent running at 6 m s^{-1} and black lines represent running at 9 m s^{-1}. On average, peak and stance average vertical GRFs increased with speed (v) ($p < 0.001$). Linear regressions for all participant and prosthetic combinations that achieved speeds 3 through 9 m s^{-1} were peak

vertical GRF = 0.115 v + 2.439, R^2 = 0.48, p < 0.001; stance average GRF = 0.047 v + 1.513, R^2 = 0.38, p < 0.001. However, some participant and prosthetic combinations (e.g. this figure) increased running speed despite decreasing vertical GRFs from 6 to 9 m s^{-1}.

We rejected our second hypothesis that prosthetic height would be independent of the biomechanical variables that comprise the spring-mass model and govern running speed. Notably, increased prosthetic height was associated with longer contact lengths, ground contact times, and step lengths. Intuitively, athletes with longer legs take longer steps during running, yet non-amputees exhibit a very weak association between leg length and step length during running [132]. Thus, leg length may have a stronger influence on step length in athletes with bilateral transtibial amputations compared to non-amputees.

Regarding distance running performance, the metabolic cost of running for athletes with bilateral transtibial amputations is independent of prosthetic height, but is reduced with lower leg stiffness, step frequency, and peak braking horizontal GRFs [9]. In the present study, increased prosthetic height was independent of leg stiffness, but it did reduce step frequency. Perhaps, taller RSPs increase lower-limb mass and/or inertia, counteracting the potentially beneficial effects of running with slower step frequencies [122, 133]. Moreover, many surmise that increased prosthetic height augments sprinting performance for athletes with bilateral transtibial amputations [64, 65]. Overall sprinting performance is beyond the scope of this study. Nonetheless, increased prosthetic height resulted in diminished stance average vertical GRFs and prolonged ground contact durations, both of which suggest slower running speeds [12, 13]. Assuming that leg segment geometry is unchanged, perhaps the vertical GRF impairment with taller RSPs is related to worse hip and knee joint effective mechanical advantages [13, 27]. Alternatively, achieving the same running speed with lower stance average vertical GRFs may be beneficial for sprinting performance. Thus, future research is warranted to better understand leg

segment geometry and the effective mechanical advantage of the leg joints with changes in prosthetic height.

The influence of prosthetic stiffness on biomechanics was mitigated at faster running speeds (Fig. 6.4 and Fig. 6.5), leading us to accept our third hypothesis. The stiffness of a system encompassing two in-series springs is primarily influenced by the softer spring (equation 6.4). Since the residual limb stiffness of athletes with bilateral transtibial amputations is roughly twice that of the RSP at 3 m/s, and approximately equal to that of the RSP at 7 m/s, prosthetic stiffness has a greater influence on running biomechanics at slower speeds than at faster speeds (Fig. 6.3).

It has yet to be established whether athletes with and without bilateral transtibial amputations take similar step lengths at matched running speeds. In the present study, from 3 to 5 m/s participants exhibited greater overall leg stiffness [4], decreased contact lengths and durations, and lower stance average vertical GRFs, leading to 7-11% shorter steps compared to non-amputees [132, 134]. From 5 to 8 m/s the leg stiffness values of athletes with and without transtibial amputations converge as running speed increases [2] (Fig. 6.3), leading to similar leg stiffness, contact length/duration, and step length values between groups. At speeds faster than 8 m/s step length comparisons made in previous studies between one athlete with bilateral transtibial amputations and non-amputees are conflicting. Initially, Brüggemann et al. [31] reported no difference in step length between the athlete with bilateral transtibial amputations and performance matched non-amputees at ~ 9 m/s during over ground running (2.26 m for the athlete with bilateral transtibial amputations). Alternatively, Weyand et al. [52] reported that the same athlete (during a subsequent test) took shorter steps at 10 m/s versus a different non-amputee control group during treadmill running (2.03 vs. 2.37 m, respectively). The athletes in the current study took step lengths that averaged 2.24 m at 9 m/s, consistent with Brüggemann et

al.'s report [31] (Fig. 6.7). Yet, different athletes and testing procedures may confound inter-study comparisons.

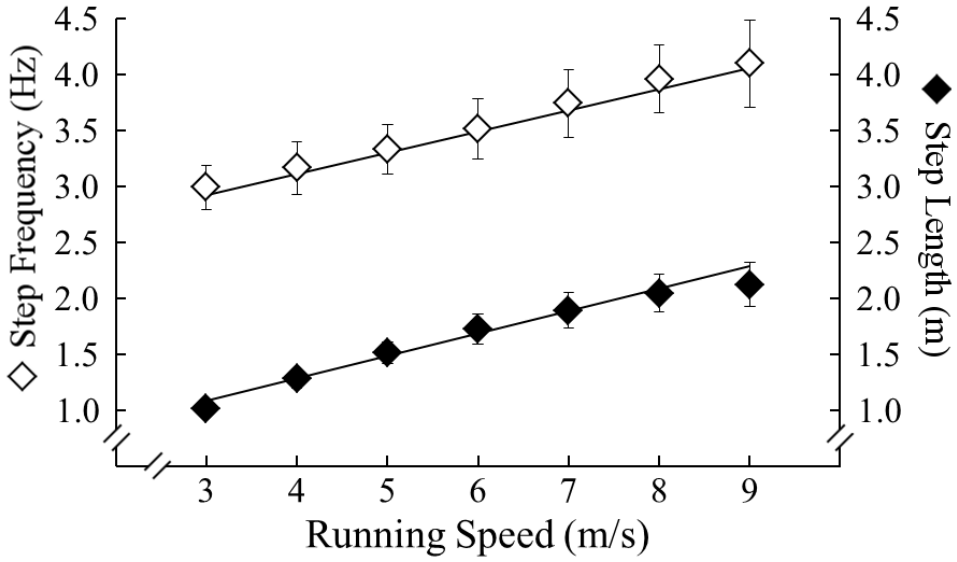

Figure 6.7. The average (±s.e.) elicited step frequency (StF) and step length (StL) at each running speed (v) across all prosthetic configurations. Linear regression equations follow as: StF = 0.20 v + 2.35, R^2 = 0.67, p < 0.001; StL = 0.20 v + 0.49, R^2 = 0.88, p < 0.001.

Regardless, because prosthetic stiffness and height affect step length for athletes with bilateral transtibial amputations, there is likely a prosthetic configuration that yields similar step lengths for athletes with and without amputations at each speed. Furthermore, during some sets of running trials, participants increased running speed beyond 7 m/s by using shorter and more rapid steps. This adaptation may explain the shorter step lengths measured by Weyand et al. at 10 m/s [52] versus that of Brüggemann et al. at 9 m/s [31]. Altogether, athletes with bilateral transtibial amputations generally increase both step length and step frequency to achieve faster running speeds (Fig. 6.7), but they can also increase running speed by decreasing step length and rapidly increasing step frequency.

We excluded the analysis of prosthetic model on running biomechanics because models, like running shoe models, are continually changing. Still, many differences exist between prosthetic

models (Fig. 6.2), including but not limited to geometry (Fig. 6.2), stiffness [30], socket attachment (Fig. 6.2), hysteresis [30], mass [9, 29], and moment of inertia [44]. Thus, a detailed analysis and simulation of RSP design on the running biomechanics of athletes with bilateral transtibial amputations may be insightful to further optimize RSPs.

A limitation of this study includes the use of different prosthetic sockets with C- versus J-shaped RSPs. This may have led to altered residual limb movement within the socket, potentially leading to altered running biomechanics. Participant fatigue may have limited our protocol. To mitigate fatigue, we limited the performed sets of running trials for each respective session to 0 (rest), 1, 2, or 3 sets, depending on athlete feedback. Due to our efforts in minimizing fatigue plus the randomisation of prosthetic configuration, we believe that participant fatigue had a negligible influence on the RSP configuration results. Yet, potential fatigue may have influenced the running speed results because of the systematic trial order. Furthermore, our relatively small sample size may have led us to falsely accept null hypotheses.

6.6 Conclusion

Athletes with bilateral transtibial amputations change their running biomechanics when using RSPs that differ in stiffness, height, and while running at different speeds. Namely, the use of stiffer RSPs increased leg stiffness, step frequency, peak and stance average vertical GRF production, and decreased ground contact time. The use of taller RSPs increased step length. Running speed was inversely associated with leg stiffness. Moreover, faster running speeds mitigate the effect of prosthetic stiffness, but not height, on running biomechanics. Therefore, prosthetic stiffness, but not height, likely has a greater influence on distance running performance than on sprinting performance for athletes with bilateral transtibial amputations.

Acknowledgements

We thank Mike Litavish CPO and Angela Montgomery CPO for their invaluable assistance throughout our study. We extend our gratitude to Dr. Rodger Kram for his support throughout this project. We also thank Freedom Innovations, Össur, and Ottobock for donating the running-specific prostheses used in this study.

7 CHAPTER 4: The biomechanics of the fastest athlete with a unilateral transtibial amputation

7.1 Abstract

People have debated whether athletes with transtibial amputations should compete with non-amputees in track events despite insufficient information regarding how the use of running-specific prostheses (RSPs) affects athletic performance. Thus, we sought to quantify the spatio-temporal variables, ground reaction forces, and spring-mass mechanics of the fastest athlete with a unilateral transtibial amputation using an RSP to reveal how he adapts his biomechanics to achieve elite running speeds. Accordingly, we measured ground reaction forces of the current male International Paralympic Committee T44 100 m and 200 m world record holder during treadmill running trials spanning 2.87 to 11.55 m/s. To achieve faster running speeds, this athlete increased his affected leg (AL) step lengths ($p<0.001$) through longer contact lengths ($p<0.001$), and his unaffected leg (UL) step lengths ($p<0.001$) through longer contact lengths ($p<0.001$) and greater stance average vertical ground reaction forces ($p<0.001$). At faster running speeds, step time was briefer for both legs ($p<0.001$) through shorter ground contact and aerial times ($p<0.001$). Unlike previously studied athletes with unilateral transtibial amputations, this athlete maintained constant AL and UL stiffness across running speeds ($p\geq0.569$). Across speeds, AL step lengths were 8% longer ($p<0.001$) despite 16% lower AL stance average vertical ground reaction forces compared to the UL ($p<0.001$). The present study's athlete exhibited biomechanics that differed from those of athletes with bilateral and without transtibial amputations. Overall, we present the biomechanics of the fastest athlete with a unilateral

transtibial amputation, providing insight into the functional abilities of athletes with transtibial amputations using running-specific prostheses.

7.2 Introduction

The fastest humans can achieve running speeds greater than 12 m/s during track competitions [135]. Running speed equals the product of stride length and stride frequency, where one stride is comprised of two steps. Humans increase step length by furthering the horizontal distance traveled by their center of mass (CoM) during ground contact (contact length) and/or by applying a greater average vertical force on the ground relative to body weight [12, 13]. Step frequency is increased by decreasing step time, which is the sum of ground contact time and subsequent aerial time [12, 13].

The running speed of athletes with leg amputations is constrained by the same spatio-temporal and vertical ground reaction force variables as non-amputees [52]. During running, athletes with leg amputations primarily use passive-elastic carbon-fiber running-specific prostheses (RSPs) on their affected leg. These devices attach in-series to carbon-fiber sockets that encompass the residual limbs, and facilitate the fundamental spring-like behavior of level-ground running [5, 9, 29]. Unlike biological lower legs, RSPs cannot generate mechanical power *de novo* or adjust stiffness neurally during running [30]. Also, the overall affected leg stiffness of athletes with unilateral transtibial amputations is inversely related to running speed, whereas their overall unaffected leg stiffness is independent of running speed [5]. Despite these differences between purely biological and RSP incorporated lower legs, RSPs have enabled many athletes with leg amputations to compete with non-amputees in track races ranging from regional competitions to the Olympic Games (9, 28).

The running performances of extraordinary athletes with transtibial amputations have been controversial because of the use of RSPs, rather than biological lower legs [33, 52]. However, in spite of the ongoing conversation regarding whether athletes with transtibial amputations should compete with non-amputees in running events [65, 84], the running biomechanics of the fastest athlete with a unilateral transtibial amputation using an RSP are unknown. Thus, to uncover the capabilities of athletes with unilateral transtibial amputations using RSPs, we sought to establish how the fastest athlete with a unilateral transtibial amputation using an RSP modulates spatio-temporal variables, ground reaction forces, and spring-mass mechanics across a wide range of running speeds including top speed.

7.3 Methods

7.3.1 Participants

One male athlete with a unilateral transtibial amputation participated (age: 23 years, height: 1.90 m, mass: 84.5 kg, unaffected leg (UL) length from the greater trochanter to the floor during standing: 1.03 m, affected leg (AL) length from the greater trochanter to the distal end of the unloaded RSP: 1.09 m, cause of amputation: trauma). We tested this athlete during the preseason of his competition cycle that concluded with two International Paralympic Committee (IPC) male T44 classification [136] world records: 10.61 s for 100 m and 21.27 s for 200 m [137]. Prior to participation, this athlete gave informed written consent according to the protocol approved by the Colorado Multiple IRB and the USAMRMC Office of Research Protection, Human Research Protection Office.

7.3.2 Experimental Protocol

Following a treadmill running warm-up, the athlete performed a set of treadmill running trials (Treadmetrix, Park City, UT, USA) using a stiffness category 7 Össur Cheetah Xtreme RSP (Össur, Reykjavík, Iceland). The running trials were performed in the following order: 2.87, 3.84, 4.60, 5.62, 6.51, 7.50, 8.35, 9.21, 10.14, 10.48, and 11.55 m/s. Each trial began with the athlete standing on the static treadmill belt. Next, he and the treadmill belt accelerated until belt speed plateaued; at that point, we began counting his steps. For each trial, the athlete maintained forward position on the treadmill while taking 18 consecutive steps [5, 12, 52]. *Ad libitum* rest preceded each trial.

7.3.3 Data Analyses

Most athletes with unilateral transtibial amputations exhibit asymmetric spatio-temporal, ground reaction force (GRF), and spring-mass model variables between legs while running [5, 29, 138]. Accordingly, we quantified the respective variables from each leg separately. We determined running speed (v) as treadmill belt speed. Biomechanically, running speed (v) is the product of step length (L_{step}) and step frequency ($Freq_{step}$).

$$v = (AL\ L_{step} \cdot AL\ Freq_{step} + UL\ L_{step} \cdot UL\ Freq_{step})/2 \tag{7.1}$$

Steps lengthen by increasing contact length (L_c) and/or stance average vertical GRF (F_{avg}) relative to body weight (BW) including running attire [12, 13].

$$L_{step} = L_c \cdot F_{avg}/BW \tag{7.2}$$

We calculated step frequency as the reciprocal of step time (t_{step}), which equals the sum of the ground contact time (t_c) and subsequent aerial time (t_a) [12, 13].

$$Freq_{step} = \frac{1}{t_{step}} = \frac{1}{t_c + t_a} \tag{7.3}$$

For our analyses, we calculated L_{step} as t_{step} multiplied by v (treadmill belt speed).

We calculated overall leg stiffness (k_{leg}) as peak vertical GRF (F_{peak}) divided by peak leg spring compression (ΔL) during ground contact in accordance with Farley et al. [2].

$$k_{leg} = \frac{F_{peak}}{\Delta L} \tag{7.4}$$

We calculated peak leg spring compression (ΔL) using the initial AL and UL lengths (L_0), theta (θ), treadmill speed (v), and ground contact time (t_c).

$$\theta = sin^{-1}(\frac{v\, t_c}{2\, L_0}) \tag{7.5}$$

Next, we determined peak leg spring compression (ΔL) using peak vertical displacement of the CoM during ground contact (Δy), calculated by twice integrating the vertical acceleration of the CoM with respect to time [72].

$$\Delta L = \Delta y + L_0(1 - \cos\theta) \tag{7.6}$$

7.3.4 Data collection

We measured vertical and horizontal GRFs (1000 Hz) throughout the duration of each trial, filtered them using a 4th order low-pass Butterworth filter (20 Hz cutoff), and then used the filtered data and a 40 N vertical GRF threshold to calculate the variables in equations 7.1 through 7.6 with a custom MATLAB script (Mathworks Inc., Natick, MA, USA).

7.3.5 Statistical Analyses

We performed linear regressions for each biomechanical variable from equations 1 through 6 across running speeds. We used paired two-tailed t-tests to assess the influence of the AL versus UL on each biomechanical variable across running speeds. We set the level of significance at p=0.05 and performed statistical analyses using R-studio (Boston, MA, USA).

7.4 Results

Some trials contained steps where the treadmill and athlete were still accelerating to the target speed. Thus, after we removed all acceleration phase running steps, some trials contained <16 consecutive steps. Nonetheless, all trials comprised ≥6 consecutive steps at a constant running speed [139]. In addition, we measured a top speed of 11.55 m/s, which to our knowledge is the fastest treadmill running trial ever recorded for a human with or without a leg amputation [12, 13].

From 2.87 to 11.55 m/s, AL and UL t_c decreased 55 and 51%, respectively ($p<0.001$) and AL and UL t_a decreased 39 and 41%, respectively ($p<0.001$) (Fig. 7.1). This led to a 47 and 46% decreased AL and UL t_{step} ($p<0.001$) and a 107 to 108% increased AL and UL L_{step}, respectively ($p<0.001$) (Fig. 7.2). Additionally, from 2.87 to 11.55 m/s, AL L_c increased 82% (AL L_c = 0.055 speed + 0.478; R^2=0.93; $p<0.001$), UL L_c increased 96% (UL L_c = 0.052 speed + 0.480; R^2=0.95; $p<0.001$), and UL F_{avg} increased 10% ($p=0.001$) (Fig. 7.3 and Table 7.1). Over the speed range, AL peak braking GRF increased 230% ($y = -0.025 x + 0.014$; R^2=0.90; $p<0.001$), UL peak braking GRF increased 466% ($y = -0.082 x - 0.021$; R^2=0.83; $p<0.001$), and AL peak propulsive GRF increased 183% ($y = 0.044 x + 0.166$; R^2=0.82; $p<0.001$) (Table 7.1). Running speed did not affect AL F_{avg} ($p=0.676$) (Fig. 7.3 and Table 7.1) or UL peak propulsive GRF ($p=0.943$) (Table 7.1).

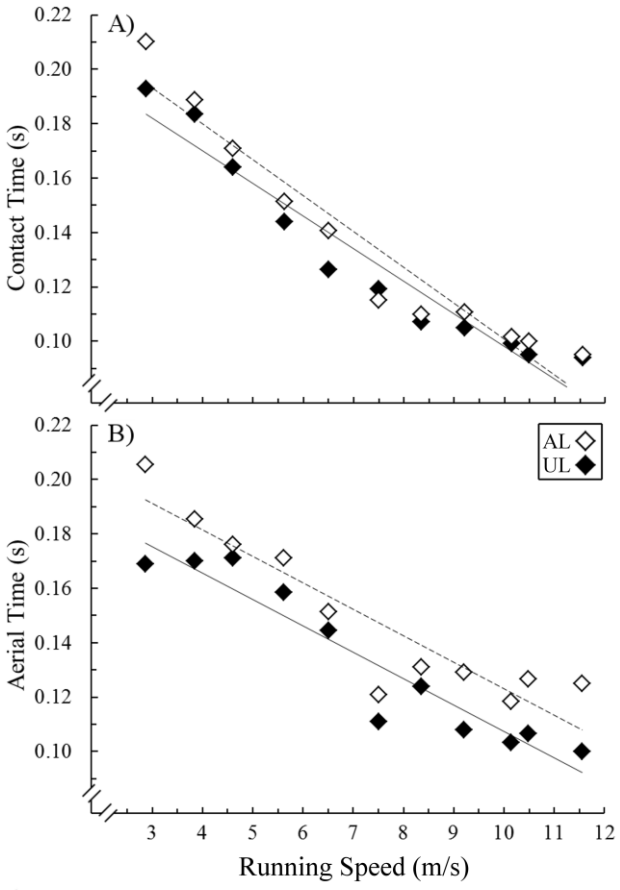

Figure 7.1. A) Ground contact time (t_c) and B) aerial time (t_a) for the affected leg (AL) and unaffected leg (UL) across running speeds (v). Dashed lines represent AL regression lines and solid lines represent UL regression lines. The following are the respective regression equations: AL t_c = -0.013 v + 0.233; R^2=0.93; p<0.001. UL t_c = -0.012 v + 0.218; R^2=0.93; p<0.001. AL t_a = -0.010 v + 0.220; R^2=0.85; p<0.001. UL t_a = -0.010 v + 0.205; R^2=0.90; p<0.001.

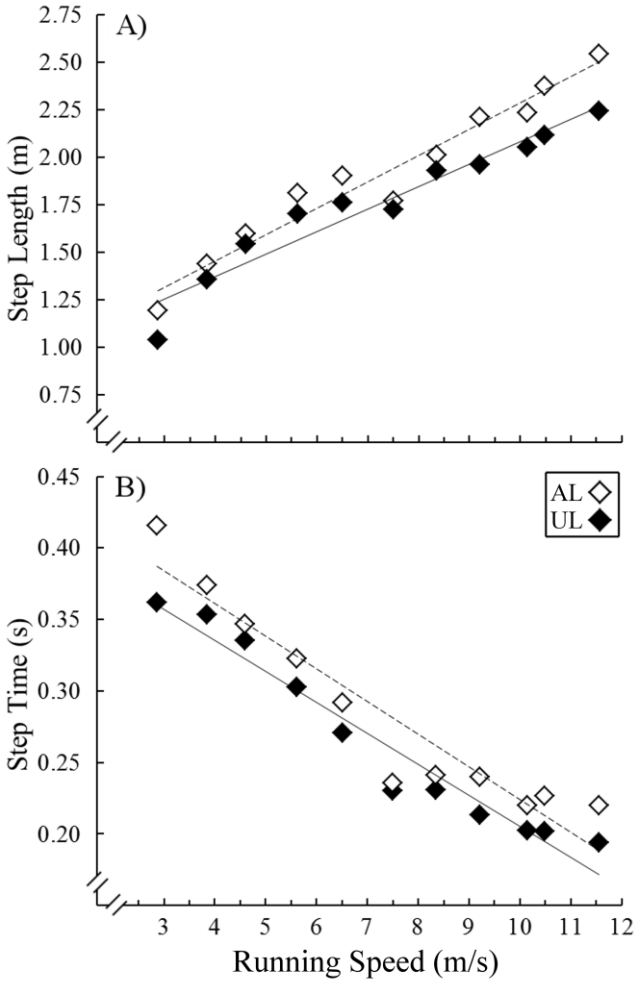

Figure 7.2. A) Step length (L_{step}) and B) step time (t_{step}) for the affected leg (AL) and unaffected leg (UL) over the range of running speeds (v). Dashed lines represent AL regression lines and solid lines represent UL regression lines. The following are the respective regression equations: AL L_{step} = 0.14 v + 0.90; R^2=0.95; p<0.001. UL L_{step} = 0.12 v + 0.90; R^2=0.93; p<0.001. AL t_{step} = -0.023 v + 0.453, R^2=0.90; p<0.001. UL t_{step} = -0.022 v + 0.423; R^2=0.95; p<0.001.

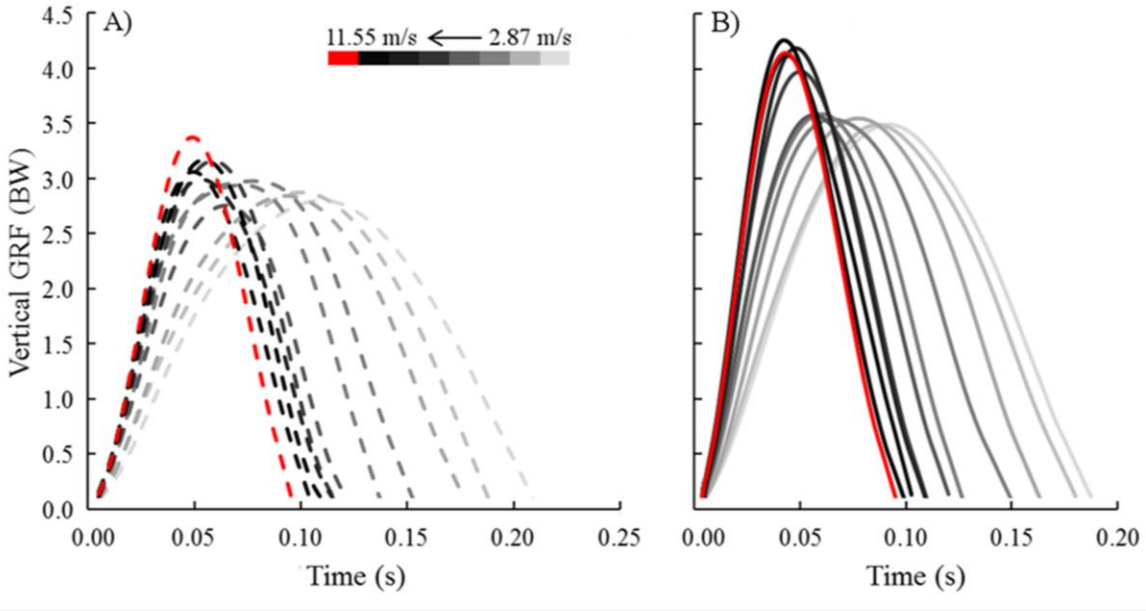

Figure 7.3. Mean vertical ground reaction force (vGRF) traces from the A) AL (dashed lines) and B) UL (solid lines) across running speeds (v) (2.87 to 11.55 m/s). Light to dark vGRF lines indicate slower to faster running trials, with the fastest running trial in red. AL F_{avg} was not statistically different across running speed (p=0.676). The following is the regression equation: UL F_{avg} = 0.03 v + 1.88; R^2=0.72; p=0.001.

Running Speed (m/s)	Peak vGRF		Stance Avg vGRF		Peak Braking hGRF		Peak Propulsive hGRF		Leg Stiffness (kN/m)	
	UL	AL	UL	AL	UL	AL	UL	AL	UL	AL
2.87	3.52	2.82	1.98	1.72	0.14	0.09	0.39	0.25	24.0	19.9
3.84	3.53	2.85	1.96	1.76	0.27	0.08	0.43	0.36	21.0	18.5
4.60	3.62	2.94	2.07	1.81	0.38	0.10	0.48	0.42	20.6	17.4
5.62	3.61	3.09	2.07	1.92	0.53	0.11	0.49	0.47	21.1	18.1
6.51	3.56	3.06	2.10	1.89	0.56	0.15	0.50	0.47	21.6	17.0
7.50	3.56	2.81	2.03	1.64	0.86	0.18	0.50	0.36	20.1	19.0
8.35	3.98	3.22	2.21	1.80	0.81	0.17	0.37	0.46	22.0	19.5
9.21	4.22	3.04	2.29	1.67	0.86	0.23	0.41	0.59	20.1	14.8
10.14	4.14	3.07	2.27	1.73	0.80	0.21	0.44	0.62	22.7	18.2
10.48	4.27	3.29	2.25	1.83	0.83	0.30	0.43	0.65	23.4	18.4
11.55	4.18	3.39	2.17	1.76	0.82	0.28	0.46	0.70	21.2	18.6

Table 7.1. The mean elicited vertical ground reaction forces (vGRFs) and horizontal ground reaction forces (hGRFs) across running speeds for the unaffected leg (UL) and affected leg (AL). All forces are presented in units of body weight. UL and AL peak vGRF ($p \leq 0.005$), UL stance average (Avg) vGRF ($p < 0.001$), AL and UL peak braking hGRF ($p < 0.001$), and AL peak propulsive hGRF ($p < 0.001$) correlated with running speed. AL stance Avg vGRF (p=0.676) and UL peak propulsive hGRF (p=0.943) were independent of running speed.

From 2.87 to 11.55 m/s, the AL peak vertical GRF increased 17% ($y = 0.05 x + 2.68$; R^2=0.60; p=0.005) and the UL peak vertical GRF increased 16% ($y = 0.10 x + 3.11$; R^2=0.79; p<0.001) (Table 7.1). Across running speeds, peak AL ($y = -0.006 x + 0.081$; R^2=0.90, p<0.001) and UL ($y = -0.007 x + 0.091$; R^2=0.89, p<0.001) Δy decreased 76 and 69%, respectively, due in part to a 110% increased AL θ ($y = 0.027 x + 0.217$; R^2=0.94, p<0.001) and 96% increased UL θ ($y = 0.026 x + 0.239$; R^2=0.91, p<0.001). Furthermore, from 2.87 to 11.55 m/s, AL ($y = 0.003 x + 0.107$; R^2=0.42, p=0.030) and UL ($y = 0.004 x + 0.116$; R^2=0.65, p=0.003) ΔL increased 28 and 38%, respectively. k_{AL} (p=0.569) and k_{UL} (p=0.941) were independent of running speed (Table 7.1). Moreover, the only variables that were similar between the AL and UL across running speeds were peak propulsive GRF (p=0.345) and θ (p=0.224).

7.5 Discussion

The purpose of this case study was to quantify the spatio-temporal, GRF, and spring-mass model parameters of the fastest athlete with a unilateral transtibial amputation across running speeds. From 2.87 to 11.55 m/s, this athlete increased his AL and UL step lengths from 1.19 to 2.54 m and 1.03 to 2.24 m, respectively (Fig. 7.2). The longer AL steps at each speed coincide with previous research suggesting that athletes with unilateral transtibial amputations exhibit similar or longer steps with their AL compared to their UL [11]. Also, at similar speeds, the present study's athlete exhibited AL and UL step lengths that were both within one standard deviation of those elicited by six athletes with unilateral transtibial amputations at their top running speeds (8.75 ± 0.97 m/s). Additionally, an Olympic athlete with bilateral transtibial amputations exhibited mean step lengths of 2.03 m at 10.0 m/s, which is similar to the mean UL

step length (2.05 m) and shorter than the mean AL step length (2.23 m) of the present study's athlete at 10.14 m/s [52]. For further comparison, non-amputees run with mean (± SD) step lengths of 2.04 m at 9.20 ± 0.59 m/s [13], 2.11 m at 9.25 ± 0.37 m/s [12], and 2.37 m at 10.0 ± 0.0 m/s [52]. Therefore, athletes with unilateral, bilateral, and without transtibial amputations generally achieve fast running speeds using different spatio-temporal variable magnitudes.

Stance average vertical GRF relative to body weight, a key determinant of step length, generally increases at faster running speeds [12, 13, 139, 140]. However, this study and others have presented representative data showing that at certain speed increments athletes with and without amputations naturally increase running speed (e.g. 6.51 to 7.50 m/s; Fig. 7.2) by *decreasing* their stance average vertical GRFs and considerably reducing their step times [139, 140] (Fig. 7.3). Thus, at these speed increments, athletes run faster by using shorter step lengths and much briefer step durations than those of the preceding, slower speed. This can happen because running speed is determined from the combination of contact length, stance average vertical GRF relative to body weight, and step time [13].

The present study's athlete's AL stance average vertical GRFs and AL step lengths were lower and longer than those of his UL at each speed, respectively. Even though he exhibited longer AL contact lengths, based on equation 7.2 we would predict this athlete to exhibit shorter, not longer, AL versus UL step lengths. Perhaps this phenomenon is related to the athlete's leg length discrepancy (the AL was 6 cm taller than the UL). For instance, AL CoM height was 5.9 ± 1.3 cm taller at initial ground contact compared to UL height across speeds (paired two-tailed t-test; $p<0.001$). Conceivably, his AL stance average vertical GRFs were lower and AL step lengths were longer than those of his UL because of the net lowering of the CoM through the AL step and the net raising of the CoM through the UL step. This notion is supported by the longer

aerial times following the AL versus UL steps (Fig. 7.1), and by our previous study [29], which found that decreased prosthetic height elicited more symmetric stance average vertical GRFs during running at 2.5 and 3.0 m/s for athletes with unilateral transtibial amputations.

The results of the present study indicate that athletes with unilateral transtibial amputations can achieve elite top speeds (i.e. >10 m/s) while utilizing different spatio-temporal, GRF, and spring-mass model characteristics than those of athletes with bilateral and without transtibial amputations. The present study's dataset may be implemented in future studies that compare the sprinting abilities of athletes with unilateral transtibial amputations to those of athletes with different amputation levels. Furthermore, this investigation may be used for the development of future RSP and socket designs by providing insight into the demands placed on these devices during running. Typically, k_{AL} of athletes with transtibial amputations decreases with faster running speeds [5, 139], which contrasts the results of the present study's athlete who maintained constant k_{AL} across running speeds. Perhaps, athletes with unilateral transtibial amputations need to maintain and not decrease k_{AL} to achieve faster top speeds. Athletes with transtibial amputations may be able to maintain constant k_{AL} by using different RSP configurations [30] or altering RSP/leg segment geometry during running. Additionally, the present study's athlete exhibited more asymmetric spatio-temporal and GRFs than those of non-amputees at matched running speeds. For example, at 9.5 ± 0.42 m/s, non-amputees exhibit average step length and stance average vertical GRF asymmetries of 1.7 ± 3.2 and 2.0 ± 4.5% (± SD), respectively [141]. Whereas at 9.21 m/s, the present study's athlete exhibited step length and stance average vertical GRF asymmetries of 12 and 31%, respectively. Currently, it is unknown whether biomechanical asymmetries limit top speed of athletes with unilateral transtibial amputations. Moreover, though treadmill and over ground running are

biomechanically similar [75], athletes only need to overcome minimal air resistance during treadmill running due to arm and leg swing [142]. Hence, athletes can theoretically attain faster running speeds on a treadmill than over ground.

7.6 Conclusion

We present spatio-temporal, ground reaction force, and spring-mass model variables of the fastest athlete with a unilateral transtibial amputation while running at 2.87 to 11.55 m/s. In general, his AL spatio-temporal variables are equivalent with those of non-amputee sprinters, whereas his AL stance average vertical GRFs better match those from of an athlete with bilateral transtibial amputations. In contrast, the UL spatio-temporal variables of the athlete in the present study coincide with those elicited by an athlete with bilateral transtibial amputations, whereas his UL stance average vertical GRFs better match those exhibited by non-amputees. Furthermore, the present study's athlete maintained constant k_{leg} in both legs across running speeds, which is like that of non-amputees and dissimilar to that of athletes with transtibial amputations. In addition to these comparisons, this study provides insight regarding how the fastest athlete with a unilateral transtibial amputation using an RSP adapts his biomechanics to achieve elite running speeds.

Acknowledgements

We thank Paolo Taboga PhD and Angela Montgomery CPO for their contributions to this study.

8 Conclusions

Prior to my dissertation, the influence of RSP configuration on running biomechanics and metabolic cost of transport for athletes with transtibial amputations were unknown. Previous studies measured the running biomechanics or metabolic costs of athletes with transtibial amputations using the athlete's personal RSP(s). Through a series of six experiments, I determined how prosthetic model, stiffness, and height affect many biomechanical variables and the metabolic cost of transport for athletes with transtibial amputations during running.

For my first study, I quantified the mechanical properties of RSPs. Conventionally, researchers consider the force-displacement profile of RSPs to be perfectly linear. I found that a curvilinear force-displacement profile better described prosthetic stiffness than a linear profile. Thus, prosthetic stiffness changes based on the magnitude and geometry of the applied force. Furthermore, we quantified actual prosthetic stiffness and hysteresis values for RSPs across multiple models and heights. These results indicate that manufacturer recommended stiffness values vary across prosthetic models, which likely affects performance.

For my second study, I quantified the influence of prosthetic model, stiffness, and height on running biomechanics and metabolic cost of transport for athletes with bilateral transtibial amputations running at 2.5 and 3.0 m/s. The main findings of this study were that prosthetic model and stiffness, but not height affected the metabolic cost of transport. Specifically, running economy was improved when athletes used 1) the Össur Flex-Run and Ottobock 1E90 Sprinter RSPs compared to the Freedom Innovations Catapult FX6 RSPs, and 2) more compliant RSPs than manufacturer recommended. Thus, athletes with bilateral transtibial amputations who seek to improve their metabolic cost of transport, and thus performance, should use certain RSP models and prosthetic stiffness that is lower than manufacturer recommended at any height.

For my third study, I quantified how prosthetic model, stiffness, and height affect the running biomechanics and metabolic cost of transport of athletes with unilateral transtibial amputations while running at 2.5 and 3.0 m/s. The main findings of this study were that prosthetic model, but not stiffness or height affects the metabolic cost of transport during running. Specifically, the metabolic cost of transport was improved when athletes used the J-shaped Ottobock 1E90 Sprinter RSP compared to the use of the C-shaped Össur Flex-Run and Freedom Innovations Catapult FX6 RSPs. Moreover, prosthetists are advised to prescribe RSP configurations to athletes with unilateral transtibial amputations that minimize stride kinematic asymmetries. We confirmed that altering RSP configuration changed the elicited stride kinematic asymmetries. However, stride kinematic asymmetries were independent of the metabolic cost of running. Hence, the current method of prescribing prosthetic configuration, to minimize stride kinematic asymmetries, does not necessarily optimize the metabolic cost of running for athletes with unilateral transtibial amputations.

For my fourth study, I compared all of the metabolic cost of transport values ever reported for athletes with transtibial amputations during running and compared them to non-amputee values. The metabolic cost of transport values for athletes with transtibial amputations are within the range of those for non-amputee runners. Thus, despite differences in lower leg architecture and biomechanics, the metabolic cost of running is similar between athletes with transtibial amputations using RSPs and non-amputees.

For my fifth study, I quantified how prosthetic stiffness and height affect biomechanics for athletes with bilateral transtibial amputations across running speeds. Overall, the influence of prosthetic stiffness on biomechanics is mitigated at faster running speeds. Alternatively, the influence of prosthetic height on biomechanics was independent of running speed. Therefore,

prosthetic stiffness likely influences distance-running performance more than sprinting performance.

For my sixth study, I quantified the biomechanics of the fastest athlete with a unilateral transtibial amputation across running speeds. In general, his affected leg spatio-temporal variables coincided with those of non-amputee sprinters, whereas his affected leg stance average vertical ground reaction forces better matched those from of an athlete with bilateral transtibial amputations. In contrast, the unaffected leg spatio-temporal variables of this athlete coincided with those elicited by an athlete with bilateral transtibial amputations, whereas his unaffected leg stance average vertical ground reaction forces better matched those exhibited by non-amputees. Additionally, he maintained overall affected leg stiffness across running speeds, which is atypical for athletes with unilateral transtibial amputations.

In conclusion, the research I have conducted for my dissertation has shown how prosthetic configuration affects the running biomechanics and economy for athletes with transtibial amputations. The results of my dissertation highlight the importance of prosthetic model, stiffness, and height on running performance. Notably, current RSP prescription methods are not ideal for optimizing the metabolic cost of running, and consequently distance running performance. I hope that the results of my research will be used to augment distance running and sprinting performances for athletes with transtibial amputations.

REFERENCES

1. Blickhan, R., *The spring-mass model for running and hopping.* J Biomech, 1989. **22**(11): p. 1217-1227.
2. Farley, C.T., J. Glasheen, and T.A. McMahon, *Running springs: speed and animal size.* J Exp Biol, 1993. **185**: p. 71-86.
3. McMahon, T.A. and G.C. Cheng, *The mechanics of running: How does stiffness couple with speed?* J Biomech, 1990. **23, Supplement 1**: p. 65-78.
4. Farley, C.T. and O. González, *Leg stiffness and stride frequency in human running.* J Biomech, 1996. **29**(2): p. 181-186.
5. McGowan, C.P., et al., *Leg stiffness of sprinters using running-specific prostheses.* J R Soc Interface, 2012. **9**(73): p. 1975-82.
6. Alexander, R.M., *Energy-saving mechanisms in walking and running.* J Exp Biol, 1991. **160**: p. 55-69.
7. Cavagna, G.A. and M. Kaneko, *Mechanical work and efficiency in level walking and running.* J Physiol, 1977. **268**(2): p. 467-81.
8. Cavagna, G.A., F.P. Saibene, and R. Margaria, *Mechanical work in running.* J Appl Physiol, 1964. **19**(2): p. 249-256.
9. Beck, O.N., P. Taboga, and A.M. Grabowski, *Reduced prosthetic stiffness lowers the metabolic cost of running for athletes with bilateral transtibial amputations.* J Appl Physiol, 2017.

10. Oudenhoven, L.M., et al., *Regulation of step frequency in endurance transtibial amputee athletes using a running-specific prosthesis.* J Biomech, 2016.

11. Hobara, H., et al., *Amputee locomotion: Spring-like leg behavior and stiffness regulation using running-specific prostheses.* J Biomech, 2013. **46**(14): p. 2483-2489.

12. Weyand, P.G., et al., *Faster top running speeds are achieved with greater ground forces not more rapid leg movements.* J Appl Physiol, 2000. **89**(5): p. 1991-9.

13. Weyand, P.G., et al., *The biological limits to running speed are imposed from the ground up.* J Appl Physiol, 2010. **108**(4): p. 950-961.

14. Joyner, M.J., *Modeling: optimal marathon performance on the basis of physiological factors.* J Appl Physiol, 1991. **70**(2): p. 683-687.

15. Joyner, M.J. and E.F. Coyle, *Endurance exercise performance: the physiology of champions.* J Appl Physiol, 2008. **586**(1): p. 35-44.

16. Douglas, L. and C.S. Krahenbuhl, *Running economy and distance running performance of highly trained athletes.* Med Sci Sports Exerc, 1980. **12**(5): p. 357-360.

17. Foster, C., *VO2 max and training indices as determinants of competitive running performance.* J Sports Sci, 1983. **1**(1): p. 13-22.

18. Daniels, J. and N. Daniels, *Running economy of elite male and elite female runners.* Med Sci Sports Exerc, 1992. **24**(4): p. 483-489.

19. Brooks, G.A. and J. Mercier, *Balance of carbohydrate and lipid utilization during exercise: the" crossover" concept.* J Appl Physiol, 1994. **76**(6): p. 2253-2261.

20. Costill, D.L., H. Thomason, and E. Roberts, *Fractional utilization of the aerobic capacity during distance running.* Med Sci Sports, 1973. **5**(4): p. 248-252.

21. Daniels, J.T., *A physiologist's view of running economy.* Med Sci Sports Exerc, 1985. **17**(3): p. 332-338.

22. Morgan, D.W., et al., *Variation in the aerobic demand of running among trained and untrained subjects.* Med Sci Sports Exerc, 1995. **27**(3): p. 404-9.

23. Williams, K.R. and P.R. Cavanagh, *Relationship between distance running mechanics, running economy, and performance.* J Appl Physiol, 1985. **63**(3): p. 1236-45.

24. Arellano, C.J. and R. Kram, *Partitioning the Metabolic Cost of Human Running: A Task-by-Task Approach.* Integr Comp Biol, 2014. **54**(6): p. 1084-1098.

25. Kram, R., *Muscular force or work: what determines the metabolic energy cost of running?* Exerc Sport Sci Rev, 2000. **28**(3): p. 138-43.

26. Roberts, T.J., et al., *Energetics of bipedal running. I. Metabolic cost of generating force.* J Exp Biol, 1998. **201**(19): p. 2745-2751.

27. Biewener, A.A., et al., *Muscle mechanical advantage of human walking and running: implications for energy cost.* J Appl Physiol, 2004. **97**(6): p. 2266-2274.

28. Nolan, L., *Carbon fibre prostheses and running in amputees: a review.* Foot ank Surg, 2008. **14**(3): p. 125-129.

29. Beck, O.N., P. Taboga, and A.M. Grabowski, *Prosthetic model, but not stiffness or height, affects the metabolic cost of running for athletes with unilateral transtibial amputations.* J Appl Physiol, 2017.

30. Beck, O.N., P. Taboga, and A.M. Grabowski, *Characterizing the Mechanical Properties of Running-Specific Prostheses.* PLoS One, 2016. **11**(12): p. e0168298.

31. Brüggemann, G.P., et al., *Biomechanics of double transtibial amputee sprinting using dedicated sprinting prostheses.* Sports Technol, 2008. **1**(4-5): p. 220-227.

32. Arellano, C.J., et al., *Effect of Running Speed and Leg Prostheses on Mediolateral Foot Placement and Its Variability.* PLoS One, 2015. **10**(1): p. e0115637.

33. Grabowski, A.M., et al., *Running-specific prostheses limit ground-force during sprinting.* Biol lett, 2010. **6**(2): p. 201-204.

34. Wilson, J.R., et al., *A new methodology to measure the running biomechanics of amputees.* Prosthet Orthot Int, 2009. **33**(3): p. 218-29.

35. He, J.P., R. Kram, and T.A. McMahon, *Mechanics of running under simulated low gravity.* J Appl Physiol, 1991. **71**(3): p. 863-70.

36. Czerniecki, J.M., A. Gitter, and C. Munro, *Joint moment and muscle power output characteristics of below knee amputees during running: the influence of energy storing prosthetic feet.* J Biomech, 1991. **24**(1): p. 63-75.

37. Snyder, K.L. and C.T. Farley, *Energetically optimal stride frequency in running: the effects of incline and decline.* J Exp Biol, 2011. **214**(12): p. 2089-2095.

38. Cavanagh, P.R. and K.R. Williams, *The effect of stride length variation on oxygen uptake during distance running.* Med Sci Sports Exerc, 1981. **14**(1): p. 30-35.

39. Kuitunen, S., P.V. Komi, and H. Kyröläinen, *Knee and ankle joint stiffness in sprint running.* Med Sci Sports Exerc, 2002. **34**(1): p. 166-173.

40. Arampatzis, A., G.-P. Brüggemann, and V. Metzler, *The effect of speed on leg stiffness and joint kinetics in human running.* J Biomech, 1999. **32**(12): p. 1349-1353.

41. Dyer, B.T., P. Sewell, and S. Noroozi, *An Investigation Into the Measurement and Prediction of Mechanical Stiffness of Lower Limb Prostheses Used for Running.* Assist Technol, 2014. **26**(3): p. 157-163.

42. *Catapult Catalog Information*, F. Innovations. 2014: Gunnison, Utah. p. 2.

43. *Fitting Guide for TT Sports Prosthesis*. Ottobock: Duderstadt, Germany. p. 9.

44. Baum, B.S. and Schultz, *Amputee Locomotion: Determining the Inertial Properties of Running-Specific Prostheses.* Arch Phys Med Rehabil, 2013. **94**(9): p. 1776-1783.

45. *Instructions for Use: Flex-Run*, Össur. 2014, Ossur: Reykjavik, Iceland. p. 1-26.

46. *Ossur Americas Prosthetics Catalog*, in *Flex-Foot Cheetah Xtend with Nike spike pad*, Ossur.: Reykjavik, Iceland. p. 1-3.

47. Grabowski, A.M. and R. Kram, *Effects of velocity and weight support on ground reaction forces and metabolic power during running.* J Appl Biomech, 2008. **24**(3): p. 288-297.

48. Chang, Y.-H., C.M. Hamerski, and R. Kram, *Applied horizontal force increases impact loading in reduced-gravity running.* J Biomech, 2001. **34**(5): p. 679-685.

49. Arellano, C.J. and R. Kram, *The effects of step width and arm swing on energetic cost and lateral balance during running.* J Biomech, 2011. **44**(7): p. 1291-1295.

50. *Prosthetics - Structural testing of lower-limb prostheses - Requirements and testing methods*. 1st Edition ed. International Standards. 2006, Switzerland.

51. Pilkey, W., *Analysis and design of elastic beams.* 2002, New York, NY.: John Wiley & Sons, Inc.

52. Weyand, P.G., et al., *The fastest runner on artificial legs: different limbs, similar function?* J Appl Physiol, 2009. **107**(3): p. 903-11.

53. Ker, R.F., et al., *The spring in the arch of the human foot.* Nature, 1987. **325**(7000): p. 147-9.

54. Bennett, M., et al., *Mechanical properties of various mammalian tendons.* J Zool, 1986. **209**(4): p. 537-548.

55. Stearne, S.M., et al., *The Foot's Arch and the Energetics of Human Locomotion.* Sci Rep, 2016. **6**: p. 19403.

56. Brown, M.B., M.L. Millard-Stafford, and A.R. Allison, *Running-specific prostheses permit energy cost similar to nonamputees.* Med Sci Sports Exerc, 2009. **41**(5): p. 1080-1087.

57. Hobara, H., et al., *The fastest sprinter in 2068 has an artificial limb?* Prosthet Orthot Int, 2015. **39**(6): p. 519-520.

58. *Catapult Running Foot Instructions for Use*, F. Innovations.: Irvine, California, USA.

59. Kerdok, A.E., et al., *Energetics and mechanics of human running on surfaces of different stiffnesses.* J Appl Physio, 2002. **92**(2): p. 469-478.

60. Ferris, D.P., K. Liang, and C.T. Farley, *Runners adjust leg stiffness for their first step on a new running surface.* J Biomech, 1999. **32**(8): p. 787-794.

61. Ferris, D.P., M. Louie, and C.T. Farley, *Running in the real world: adjusting leg stiffness for different surfaces.* Proc R Soc Long [Biol], 1998. **265**(1400): p. 989-994.

62. Biewener, A.A., *Scaling body support in mammals: limb posture and muscle mechanics.* Science, 1989. **245**(4913): p. 45-8.

63. Kram, R., *Bouncing to conclusions: clear evidence for the metabolic cost of generating muscular force.* J Appl Physiol, 2011. **110**(4): p. 865-866.

64. *Athletics Classification Rules and Regulations*. 2014; Available from: http://www.paralympic.org/sites/default/files/document/131218171256693_2013_11+ipc+athletics+classification+rules+and+regulations_digital_v4_0.pdf.

65. Weyand, P.G. and M.W. Bundle, *Point: Artificial limbs do make artificially fast running speeds possible.* J Appl Physiol, 2010. **108**(4): p. 1011-1012.

66. Storen, O., J. Helgerud, and J. Hoff, *Running stride peak forces inversely determine running economy in elite runners.* J Strength Cond Res, 2011. **25**(1): p. 117-23.

67. Chang, Y.-H. and R. Kram, *Metabolic cost of generating horizontal forces during human running.* J Appl Physiol, 1999. **86**(5): p. 1657-1662.

68. Kram, R. and C.R. Taylor, *Energetics of running: a new perspective.* Nature, 1990. **346**(6281): p. 265-7.

69. Högberg, P., *How do stride length and stride frequency influence the energy-output during running?* Eur J Appl Physiol Occup Physiol., 1952. **14**(6): p. 437-441.

70. Grabowski, A., C.T. Farley, and R. Kram, *Independent metabolic costs of supporting body weight and accelerating body mass during walking.* J Appl Physiol, 2005. **98**(2): p. 579-583.

71. Brockway, J., *Derivation of formulae used to calculate energy expenditure in man.* Hum Nutr Clin Nutr, 1987. **41**(6): p. 463-471.

72. Cavagna, G.A., *Force platforms as ergometers.* J Appl Physiol, 1975. **39**(1): p. 174-179.

73. Arellano, C.J. and R. Kram, *The energetic cost of maintaining lateral balance during human running.* J Appl Physiol, 2012. **112**(3): p. 427-434.

74. Arellano, C.J. and R. Kram, *The metabolic cost of human running: is swinging the arms worth it?* J Exp Biol, 2014. **217**(14): p. 2456-2461.

75. Cavanagh, P.R., *Biomechanics of Distance Running*. 1990: *Human Kinetics Books, Box 5076, Champaign, IL* .

76. Martin, P.E., *Mechanical and physiological responses to lower extremity loading during running.* Med Sci Sports Exerc, 1985. **17**(4): p. 427-433.

77. Morin, J.B., et al., *Effects of altered stride frequency and contact time on leg-spring behavior in human running.* J Biomech, 2007. **40**(15): p. 3341-3348.

78. Rall, J.A., *Energetic aspects of skeletal muscle contraction: implications of fiber types.* Exerc Sport Sci Rev, 1985. **13**: p. 33-74.

79. Holt, N.C., T.J. Roberts, and G.N. Askew, *The energetic benefits of tendon springs in running: is the reduction of muscle work important?* J Exp Biol, 2014. **217**(Pt 24): p. 4365-71.

80. Farley, C.T. and D.C. Morgenroth, *Leg stiffness primarily depends on ankle stiffness during human hopping.* J Biomech, 1999. **32**(3): p. 267-273.

81. Farley, C.T., et al., *Mechanism of leg stiffness adjustment for hopping on surfaces of different stiffnesses.* J Appl Physiol, 1998. **85**(3): p. 1044-1055.

82. Tominaga, S., K. Sakuraba, and F. Usui, *The effects of changes in the sagittal plane alignment of running-specific transtibial prostheses on ground reaction forces.* J Phys Ther Sci, 2015. **27**(5): p. 1347-51.

83. Moholkar, N.M., *Determinants of leg stiffness and preferred stride frequency in bouncing gaits*, in *Department of Mechanical Engineering*. 2004, University of California, Berkeley. p. 91.

84. Kram, R., et al., *Counterpoint: Artificial legs do not make artificially fast running speeds possible.* J Appl Physiol, 2010. **108**(4): p. 1012-1014.

85. Margaria, R., et al., *Energy cost of running.* J Appl Physiol, 1963. **18**(2): p. 367-370.

86. Bennett, M.B., et al., *Mechanical properties of various mammalian tendons.* J Zool, 1986. **209**(4): p. 537-548.

87. Alexander, R.M.N., *Elastic Mechanisms in Animal Movement*. 1988: Cambridge University Press.

88. Lichtwark, G.A., K. Bougoulias, and A.M. Wilson, *Muscle fascicle and series elastic element length changes along the length of the human gastrocnemius during walking and running.* J Biomech, 2007. **40**(1): p. 157-164.

89. Roberts, T.J., *Contribution of elastic tissues to the mechanics and energetics of muscle function during movement.* J Exp Biol, 2016. **219**(2): p. 266-275.

90. Daniels, J. and J. Gilbert, *Oxygen power: Performance tables for distance runners*. 1979: J. Daniels, J. Gilbert.

91. Hsu, M.J., et al., *Physiological measurements of walking and running in people with transtibial amputations with 3 different prostheses.* J Orthop Sports Phys Ther, 1999. **29**(9): p. 526-33.

92. Smith, J.A., A.D. McKerrow, and T.A. Kohn, *Metabolic cost of running is greater on a treadmill with a stiffer running platform.* J Sports Sci, 2016: p. 1-6.

93. Prince, F., et al., *Running gait impulse asymmetries in below-knee amputees.* Prosthet Orthot Int, 1992. **16**(1): p. 19-24.

94. Hobara, H., et al., *Amputee locomotion: lower extremity loading using running-specific prostheses.* Gait Posture, 2014. **39**(1): p. 386-90.

95. Buckley, J.G., *Biomechanical adaptations of transtibial amputee sprinting in athletes using dedicated prostheses.* Clin Biomech, 2000. **15**(5): p. 352-358.

96. Sanderson, D.J. and P.E. Martin, *Joint kinetics in unilateral below-knee amputee patients during running.* Arch Phys Med Rehabil, 1996. **77**(12): p. 1279-85.

97. Winter, D.A., *Moments of force and mechanical power in jogging.* J Biomech, 1983. **16**(1): p. 91-7.

98. Finley, J.M., A.J. Bastian, and J.S. Gottschall, *Learning to be economical: the energy cost of walking tracks motor adaptation.* J Physiol, 2013. **591**(4): p. 1081-95.

99. Ellis, R.G., K.C. Howard, and R. Kram, *The metabolic and mechanical costs of step time asymmetry in walking.* Proc Roy Soc [Biol], 2013. **280**(1756).

100. Herr, H.M. and A.M. Grabowski, *Bionic ankle–foot prosthesis normalizes walking gait for persons with leg amputation.* Proc Roy Soc [Biol], 2012. **279**(1728): p. 457-464.

101. Mattes, S.J., P.E. Martin, and T.D. Royer, *Walking symmetry and energy cost in persons with unilateral transtibial amputations: matching prosthetic and intact limb inertial properties.* Arch Phys Med Rehabil, 2000. **81**(5): p. 561-8.

102. Seminati, E., et al., *Anatomically asymmetrical runners move more asymmetrically at the same metabolic cost.* PLoS One, 2013. **8**(9).

103. Farley, C.T., et al., *Hopping frequency in humans: a test of how springs set stride frequency in bouncing gaits.*J Appl Physiol, 1991. **71**(6): p. 2127-2132.

104. Günther, M. and R. Blickhan, *Joint stiffness of the ankle and the knee in running.* J Biomech, 2002. **35**(11): p. 1459-1474.

105. Herzog, W., et al., *Asymmetries in ground reaction force patterns in normal human gait.* Med Sci Sports Exerc, 1989. **21**(1): p. 110-4.

106. Robinson, R.O., W. Herzog, and B.M. Nigg, *Use of force platform variables to quantify the effects of chiropractic manipulation on gait symmetry.* J Manipulative Physiol Ther, 1987. **10**(4): p. 172-6.

107. Baum, B.S., et al., *Amputee Locomotion: Ground Reaction Forces During Submaximal Running With Running-Specific Prostheses.* J Appl Biomech, 2016. **8**: p. 8.

108. Ortega, J.D. and C.T. Farley, *Effects of aging on mechanical efficiency and muscle activation during level and uphill walking.* J Electromyogr Kinesiol, 2015. **25**(1): p. 193-198.

109. Morgan, D.W., et al., *Ten kilometer performance and predicted velocity at VO2max among well-trained male runners.* Med Sci Sports Exerc, 1989. **21**(1): p. 78-83.

110. Conley, D.L. and G.S. Krahenbuhl, *Running economy and distance running performance of highly trained athletes.* Med Sci Sports Exerc, 1980. **12**(5): p. 357-60.

111. *Records World Para Athletics*. [cited 2017; Available from: https://www.paralympic.org/world-records/athletics.

112. *International Association of Athletics Federation (IAAF) Statistics*. [cited 2017 March]; Available from: https://www.iaaf.org/records/.

113. Helgerud, J., Ø. Støren, and J. Hoff, *Are there differences in running economy at different velocities for well-trained distance runners?* Euro J Appl Physiol, 2010. **108**(6): p. 1099-1105.

114. Mayhew, J.L., *Oxygen cost and energy expenditure of running in trained runners.* British J Sports Med, 1977. **11**(3): p. 116-121.

115. Menier, D.R. and L.G.C.E. Pugh, *The relation of oxygen intake and velocity of walking and running, in competition walkers.* J Physiol, 1968. **197**(3): p. 717-721.

116. Black, M.I., et al., *Is There an Optimum Speed for Economical Running?* Int J Sports Physiol Perform, 2017: p. 1-23.

117. Poole, D.C. and A.M. Jones, *Oxygen uptake kinetics.* Compr Physiol, 2012.

118. Jones, A.M., et al., *Slow component of VO2 kinetics: mechanistic bases and practical applications.* Med Sci Sports Exerc, 2011. **43**(11): p. 2046-62.

119. Mengelkoch, L.J., J.T. Kahle, and M.J. Highsmith, *Energy Costs & Performance of Transtibial Amputees & Non-amputees during Walking & Running.* Int J Sports Med, 2014. **35**(14): p. 1223-1228.

120. Lucia, A., et al., *The key to top-level endurance running performance: a unique example.* Br J Sports Med, 2008. **42**(3): p. 172-4.

121. Beck, O.N., et al., *Older runners retain youthful running economy despite biomechanical differences.* Med Sci Sports Exerc, 2016. **48**(4): p. 697.

122. Hoogkamer, W., et al., *Altered Running Economy Directly Translates to Altered Distance-Running Performance.* Med Sci Sports Exerc, 2016. **48**(11): p. 2175-2180.

123. Jones, A.M., *The physiology of the world record holder for the women's marathon.* Int J Sports Sci Coach, 2006. **1**(2): p. 101-116.

124. Marsh, R.L., et al., *Partitioning the Energetics of Walking and Running: Swinging the Limbs Is Expensive.* Science, 2004. **303**(5654): p. 80-83.

125. Browne, M.G. and J.R. Franz, *The independent effects of speed and propulsive force on joint power generation in walking.* J Biomech, 2017. **55**: p. 48-55.

126. Sawicki, G.S., C.L. Lewis, and D.P. Ferris, *It pays to have a spring in your step.* Exerc Sport Sci Rev, 2009. **37**(3): p. 130.

127. Look, N., et al., *Dynamic stability of running: the effects of speed and leg amputations on the maximal Lyapunov exponent.* Chaos, 2013. **23**(4): p. 043131.

128. Peronnet, F., G. Thibault, and D.L. Cousineau, *A theoretical analysis of the effect of altitude on running performance.* J Appl Physiol, 1985. **70**(1): p. 399-404.

129. Bassett, D.R., Jr. and E.T. Howley, *Limiting factors for maximum oxygen uptake and determinants of endurance performance.* Med Sci Sports Exerc, 2000. **32**(1): p. 70-84.

130. WILLIAMS, K.R., *Biomechanics of Running.* Exerc Sport Sci Rev, 1985. **13**(1): p. 389-442.

131. Antonsson, E.K. and R.W. Mann, *The frequency content of gait.* J Biomech, 1985. **18**(1): p. 39-47.

132. Cavanagh, P.R. and R. Kram, *Stride length in distance running: velocity, body dimensions, and added mass effects.* Med Sci Sports Exerc, 1989. **21**(4): p. 467-79.

133. Franz, J.R., C.M. Wierzbinski, and R. Kram, *Metabolic cost of running barefoot versus shod: is lighter better.* Med Sci Sports Exerc, 2012. **44**(8): p. 1519-1525.

134. Munro, C.F., D.I. Miller, and A.J. Fuglevand, *Ground reaction forces in running: a reexamination.* J Biomech, 1987. **20**(2): p. 147-55.

135. Krzysztof, M. and A. Mero, *A kinematics analysis of three best 100 m performances ever.* J Hum Kinet, 2013. **36**(1): p. 149-160.

136. *Classification Rules and Regulations*. 2017. 1-136.

137. *World Records*. 2017; Available from: https://www.paralympic.org/world-records/athletics.

138. Prince, F., et al., *Running gait impulse asymmetries in below-knee amputees.* Prosthet Orthot Int, 1992. **16**(1): p. 19-24.

139. Beck, O.N., P. Taboga, and A.M. Grabowski, *How do prosthetic stiffness, height and running speed affect the biomechanics of athletes with bilateral transtibial amputations?* J Royal Soc Interface, 2017. **14**(131).

140. Clark, K.P. and P.G. Weyand, *Are running speeds maximized with simple-spring stance mechanics?* J Appl Physiol, 2014. **117**(6): p. 604-615.

141. Korhonen, M.T., et al., *Variability and symmetry of force platform variables in maximum-speed running in young and older athletes.* J Appl Biomech, 2010. **26**(3): p. 357-66.

142. Davies, C.T., *Effects of wind assistance and resistance on the forward motion of a runner.* J Appl Physiol Respir Environ Exerc Physiol, 1980. **48**(4): p. 702-9.